CHARACTERIZATION AND SOURCE APPORTIONMENT OF PM2.5 IN THE SOUTHEASTERN UNITED STATES

A Dissertation
Presented to
The Academic Faculty

by

Sangil Lee

In Partial Fulfillment
of the Requirements for the Degree
Doctor of Philosophy in the
School of Civil and Environmental Engineering

Georgia Institute of Technology
December 2006

CHARACTERIZATION AND SOURCE APPORTIONMENT OF PM2.5 IN THE SOUTHEASTERN UNITED STATES

Approved by:

Dr. Armistead G. Russell, Advisor
School of Civil and Environmental Engineering
Georgia Institute of Technology

Dr. Michael H. Bergin
School of Civil and Environmental Engineering
Georgia Institute of Technology

Dr. James A. Mulholland
School of Civil and Environmental Engineering
Georgia Institute of Technology

Dr. Michael E. Chang
School of Earth and Atmospheric *Science*s
Georgia Institute of Technology

Dr. Yuhang Wang
School of School of Earth and Atmospheric *Science*s
Georgia Institute of Technology

Date Approved: Sept. 28, 2006

To my wife, daughter, and family

ACKNOWLEDGEMENTS

I deeply appreciate many people for their support during my Ph.D. studies at Georgia Tech. My advisor, Dr. Armistead Russell, has provided me not only an enormous research opportunity with insightful guidance and knowledge, but also a great personal interaction. His mentorship has helped me extend my knowledge about air pollution. Dr. Karsten Baumann has been a great mentor teaching me his tremendous scientific knowledge about air pollution measurements. I also thank my committee members, Drs. Michael Chang, Michael Bergin, James Mulholland, and Yuhang Wang for their time to serve on my thesis committee and helpful suggestions. I appreciate all my research group members for their interaction, help and, friendship. I really appreciate my family back in Korea for their support. My utmost appreciation goes to my wife, Eunhee Kim, for her love and being my lifetime friend.

TABLE OF CONTENTS

LIST OF TABLES

LIST OF FIGURES

Page

SUMMARY

Fine particulate matter ($PM_{2.5}$) is a complex mixture of chemical species originating from primary emission sources and secondary formation via photochemical reactions in the atmosphere. Acute and chronic human exposure to $PM_{2.5}$ can cause adverse respiratory health outcomes leading to increased morbidity and mortality rates (Burnett *et al.*, 1995; Schwartz *et al.*, 1996). The U.S. EPA designated 208 counties as non-attainment areas in 2006 as ambient $PM_{2.5}$ levels in those counties were above its National Ambient Air Quality Standards (NAAQS). Regulatory agencies in the non-attainment areas are tasked with developing effective implementation plans which can reduce $PM_{2.5}$ concentrations to meet the standards. In addition to health effects, $PM_{2.5}$ affects global climate change by disturbing the earth's radiation balance and reduces local/regional visibility due to its radiative properties.

Prescribed burning is an important source of primary and secondary $PM_{2.5}$ as its emissions can elevate ambient $PM_{2.5}$ concentrations and impair visibility in the southeastern U.S. However, lack of information about emissions from prescribed burning limits our understanding of its air quality impacts in the Southeast. In this thesis, emissions from active prescribed burning were characterized to improve our scientific knowledge of its emissions and ultimately air quality impacts.

Receptor models have been developed and applied to ambient $PM_{2.5}$ chemical composition data in order to identify emission sources and quantify their contributions to ambient concentrations. However, little information is available to provide regional perspectives of $PM_{2.5}$ sources and impacts in the Southeast. $PM_{2.5}$ source apportionment

conducted using CMB receptor modeling provides such information. This can provide new insights about whether regionally or more locally targeted control strategies should be developed and applied for $PM_{2.5}$ emission sources in the region.

Associating CMB $PM_{2.5}$ source apportionment results with adverse health outcomes has been suggested as a complementary method instead of associating $PM_{2.5}$ mass or its chemical components. However, there are issues that should be addressed before the application of source apportionment results in PM epidemiologic studies. Associating source apportionment results from a single receptor site with adverse health outcomes averaged for an entire city or metropolitan area may make PM health study results uncertain if source apportionment results are not representative for an entire study area. Spatial representativeness of source apportionment results was examined.

Uncertainties of source apportionment results are important for not only health studies but also policy analysis and decision making as they can affect confidence in the final results. They should be investigated for an appropriate application of source apportionment results. Thus, uncertainty and its contributors were estimated by propagating uncertainties in input data using Monte Carlo analysis.

In addition to conducting fundamental studies to better understand $PM_{2.5}$ sources and impacts in the southeast, it is also recognized that more issues are to be addressed. Future research is identified to continue along the path, including more emission characterization of primary sources to get representative source profiles, reduction of incongruities between source apportionment results and emission inventories, extended spatial representative studies, and application of optimized source apportionment methods.

CHAPTER 1

INTRODUCTION

Particulate matter (PM) is emitted directly from primary emission sources and formed from photochemical reactions of its precursors in the atmosphere. PM is a physically and chemically complex pollutant in the atmosphere affecting the environment and human health (U.S. EPA, 2004). Its radiative properties, such as light scattering and absorbing, play a significant role in visibility impairment (Malm, 1999; Watson, 2002) and climate change (Charlson *et al.*, 1992; Ramaswamy *et al.*, 2001), and its deposition affects vegetation, water and structures (U.S. EPA, 2002). Acute and chronic exposures to PM (especially $PM_{2.5}$, particles less than 2.5 μm in aerodynamic diameter) are suspected to cause adverse respiratory health outcomes leading to increased morbidity and mortality rates (Dockery *et al.*, 1993, 1996; Pope *et al.*, 1993, 1996; Schwartz *et al.*, 1993, 1994). PM epidemiologic studies led the United States Environmental Protection Agency (U.S. EPA) to promulgate more stringent National Ambient Air Quality Standards (NAAQS) for PM in 1997. Current $PM_{2.5}$ NAAQS are 15 and 65 $\mu g/m^3$ for annual and 24-hr standards, respectively, and a more stringent 24-hr standard of 35 $\mu g/m^3$ have been proposed (U.S. EPA, 2006). $PM_{2.5}$ is one of primary concern for regulatory agencies, which have made efforts to meet the NAAQS since the U.S. EPA designated 208 counties as non-attainment areas for $PM_{2.5}$ in March, 2006 (www.epa.gov/air/data). Agencies with $PM_{2.5}$ non-attainment counties must develop their own plans that demonstrate how they will achieve attainment status.

$PM_{2.5}$, unlike other criteria air pollutants, is a mixture of many different chemical species such as ionic species, trace metals, soot, and organic compounds. These chemical species come from a variety of primary source emissions and photochemical reactions of their precursors. Different primary sources emit chemically or physically different $PM_{2.5}$ and precursor gases producing $PM_{2.5}$ with highly variable characteristics. This makes it difficult not only for scientists to understand its chemical and physical properties but also for regulatory and policy makers to develop effective control strategies. Scientists have made significant progress in understanding $PM_{2.5}$ by developing theories and cutting-edge measurement instruments, although there is still lack of complete knowledge about $PM_{2.5}$, especially secondary organic aerosol formation. Such techniques have been used to characterize $PM_{2.5}$ both in the atmosphere and primary emissions. For example, utilizing chemical composition data in developing receptor models, such as positive factorization matrix (PMF; Paatero, 1997, 1999), UNMIX (Henry *et al.*, 1990; Kim *et al.*, 1999, 2000), iterated confirmatory factor analysis (ICFA; Christensen *et al.*, 2006), and chemical mass balance (CMB; Miller *et al.*, 1972; Watson *et al.*, 1984, Schauer *et al.*, 1996; Marmur *et al.*, 2005) has helped identify and quantify $PM_{2.5}$ sources.

$PM_{2.5}$ is regulated by NAAQS in terms of its mass, not specific components or groups. Epidemiologic studies have focused on understanding associations between adverse health outcomes and $PM_{2.5}$ mass and species, and thinking that it is more likely that the associated health outcomes may result from some toxic components of $PM_{2.5}$ rather than its mass itself. In addition, different $PM_{2.5}$ components may cause different degrees of adverse health outcomes. The specific components causing adverse health outcomes may be emitted from specific sources. Knowing which sources are of greatest

concern can help in developing control strategies in order to decrease adverse health effects. Therefore, source apportionment models can play a significant role in planning effective $PM_{2.5}$ control strategies.

There are two different types of source apportionment models. Receptor models such as CMB, PMF, UNMIX, and ICFA, identify source impacts to a receptor site based on ambient measurement data, while source-based models, such as CAMx (ENVIRON inc., 2006), RADM (Boylan *et al.*, 2002, 2006), and CMAQ (Murmur *et al.* 2006; Park *et al.*, 2005) quantify source impacts forward from emission sources based on emission data. Both types of source apportionment models have their own strengths and weaknesses. Receptor models capture more of the temporal variability of source impacts and their results are highly tied with ambient measurement data (Murmur *et al.* 2006; Park *et al.*, 2005). However, their source apportionment results are very sensitive to source profiles, not linked to emission sources directly, and estimated only where ambient measurement data is available. Source-based models provide spatial and temporal coverage of source impacts and source impacts are directly linked with emission sources (Park *et al.*, 2005; Russell *et al.*, 2005). However, the accuracy of their results highly depends on their input data, especially emission inventories which are typically the most uncertain input data (Park *et al.*, 2005; Russell *et al.*, 2004).

The CMB receptor model apportions ambient $PM_{2.5}$ to its sources by incorporating both ambient measurement and source profile data. The basic equation of the CMB model is a species mass balance, noting that the ambient concentration of a species is made up of the linear combination of total mass off $PM_{2.5}$ from individual sources times the fraction of that species in the $PM_{2.5}$ emissions from that source.

$$C_i = \sum_{i=1}^{n} f_{i,j} S_j, \quad i = 1,.....n, \tag{1}$$

where C_i is the ambient concentration of species i, f_i is the fraction of species i in source j, and S_j is the source contribution of source j. There are several assumptions in the CMB receptor model: 1) compositions of source emissions are constant over the period of ambient and source sampling; 2) chemical species do not react with each other; 3) all sources with a potential for contributing to the receptor have been identified and have had their emissions characterized; 4) the number of sources or source categories is less than or equal to the number of species; 5) the source profiles are linearly independent of each other; and 6) measurement uncertainties are random, uncorrelated, and normally distributed (Watson *et al.*, 2001).

Miller et al. (1972) has applied a chemical element balance to the Pasadena (California) particulate matter to estimate contributions of primary PM sources. The chemical element balance has been further developed and extended for understanding of primary PM emission sources in Pasadena, CA (Friedlander, 1973). A similar approach has been applied for Chicago area (Winchester and Nifong, 1971). The equation (1) is usually overdetermined since the number of chemical species is larger than that of sources. An appropriate solution of the equation (1) is a least-square fit. The ordinary weighted least squares method, which propagates only uncertainties in ambient measurement data, has been applied by Friedlander (1973). Watson *et al.* (1984) has applied an effective variance method, which is incorporated into the current version of the CMB receptor model, in order to propagate uncertainties in both ambient measurement and source profile data. The equation (1) is solved by the effective variance method, which finds a set of source impacts to minimize χ^2 (chi-square):

$$\chi^2 = \sum_{i=1}^{n} \left[\frac{\left(C_i - \sum_{j=1}^{m} f_{ij} S_j \right)^2}{\sigma_{C_i}^2 + \sum_{j=1}^{m} \sigma_{f_{ij}}^2 S_j^2} \right] \quad (2)$$

Advanced chemical speciation techniques have been developed to measure the concentrations of hundreds of particulate organic compounds emitted from various primary PM sources and collected on ambient filter samples (Rogge *et al.*, 1991; Rogge *et al.*, 1993a-d; Rogge *et al.*, 1994). The detailed organic compound speciation data extends the ability of the CMB so that source contributions of more emission sources become identifiable by overcoming collinearities among the elemental profiles of the sources (Schauer *et al.*, 1996, 2000). The CMB receptor model has also been applied to understand source impacts of volatile organic compound (VOC) emission sources (Harley *et al.*, 1992; Fujita *et al.*, 1994; Schauer *et al.*, 2000).

Prescribed burning is an important source of $PM_{2.5}$ in the U.S., emitting both primary particles and precursors of secondary particles. It has been reported that prescribed burning along with wildfires is the primary cause of elevated $PM_{2.5}$ concentrations and visibility impairment in the U.S. (Sandberg *et al.*, 2002). It is a significant PM emission source in the southeastern U.S., which has the largest forest areas subject to prescribed burning (Hardy *et al.*, 2001). Emissions from prescribed burning differ in various regions due to varying fuel and combustion conditions and are likely different in terms of chemical characteristics of $PM_{2.5}$ and volatile organic compounds (VOC). However, limited information is available about emission characteristics of active prescribed burning in the southeastern U.S. Therefore, it is essential to characterize emissions from prescribed burning to understand its air quality

impacts by providing more realistic source profiles of $PM_{2.5}$ and VOC for CMB receptor model or emission factors for emission-based air quality models.

The chemical composition of $PM_{2.5}$ varies at different regions because $PM_{2.5}$ is a complex mixture of various chemical components from different emission sources. Receptor models can be applied for ambient $PM_{2.5}$ to identify and quantify area-specific $PM_{2.5}$ emission sources. Source apportionment studies have been conducted to understand $PM_{2.5}$ sources and contributors in the southeastern U.S. (Kim *et al.*, 2003, 2004, 2005a; Liu *et al.*, 2005; Marmur *et al.*, 2005, 2006; Park *et al.*, 2005; Zheng *et al.*, 2002, 2006). The studies show the applicability of source apportionment models on more local scales. However, the studies provide little information about the regionality of $PM_{2.5}$ sources in the southeast. The U.S. EPA launched the $PM_{2.5}$ chemical Speciation Trend Network (STN) program to provide nationally consistent data for the assessments of $PM_{2.5}$ trends (U.S. EPA, 1999) as a requirement of the new NAAQS. CMB receptor modeling can incorporate the STN $PM_{2.5}$ data for source apportionment in order to give a regional perspective of $PM_{2.5}$ sources in the southeast. This can provide new insights about whether regionally or more locally-targeted control strategies should be developed and applied.

Source apportionment results from receptor models can be used for epidemiologic studies to help identify associations between adverse health outcomes and $PM_{2.5}$ emission sources (Laden *et al.*, 2000; Mar *et al.*, 2000; Tsai *et al.*, 2000; Sarnat *et al.*, 2006). However, health outcome data used for the epidemiologic studies comes from an entire city or metropolitan area, whereas source apportionment results typically are based on $PM_{2.5}$ data at a single monitoring site. This could introduce errors or uncertainties on the

results of the health studies if source apportionment results at a single monitoring site are not representative of the study area. Thus, it is important to address whether source apportionment results at a single monitoring site can represent an entire study area or not. The Assessment of Spatial Aerosol Characterization in Atlanta (ASACA) program provides data for investigating spatial representativeness of source apportionment results at a single monitoring site for an entire metropolitan area.

The ultimate objective of PM health studies incorporating $PM_{2.5}$ source apportionment is to provide useful information for policy decision making to develop effective $PM_{2.5}$ control strategies. Uncertainties of source apportionments play an important role in the policy decision since they contribute to the final uncertainties of PM health studies. Knowledge of uncertainties can help policy makers prioritize which $PM_{2.5}$ source should be further studied and controlled. For example, they may want to reduce emissions from a $PM_{2.5}$ source which is associated with a high adverse health risk with a small uncertainty rather than a high uncertainty. Therefore, it is crucial to quantify uncertainties and identify the contributors of them in the model results.

Structure and Scope of the Thesis

This thesis addresses a number of the issues confronting scientists, policy makers, and other stakeholders concerned with $PM_{2.5}$ with particular focus on the southeastern U.S.

Chapter 2, "Gaseous and particulate emissions from prescribed burning in Georgia", describes emission characteristics of prescribed burning conducted in Georgia's forested areas. Prescribed burning is an important source of air pollutants in the southeastern U.S., which has the largest forest areas subject to prescribed burning.

However, limited information is available about emission characteristics of active prescribed burning in the southeastern. Therefore, it is essential to characterize emissions from prescribed burning to understand its air quality impacts. Emission characterizations of $PM_{2.5}$ and VOC from active prescribed burning were determined by directly measuring emissions at prescribed burning sites in Georgia.

In Chapter 3, "Source apportionment of $PM_{2.5}$ in the southeastern United States", CMB receptor modeling was applied to ambient $PM_{2.5}$ data of the U.S. EPA STN program in the southeast U.S. in order to estimate regional source impacts of primary and secondary $PM_{2.5}$.

Chapter 4, "Source apportionment of $PM_{2.5}$ in Atlanta: a case study for spatial representativeness at urban scale", addresses representativeness of source apportionment results at a receptor site for an entire urban area. Source apportionment results from the CMB receptor models can be applied to PM health studies (*i.e.*, time series PM epidemiologic studies) to understand associations between adverse health outcomes and PM sources. It was investigated whether source apportionment results at a single monitoring site can represent an entire city or metropolitan area.

Chapter 5, "Estimating uncertainties and uncertainty contributors of CMB $PM_{2.5}$ source apportionment results", describes how measurement uncertainties in both ambient measurement and source profile data contribute to final uncertainties in CMB modeling. Uncertainties of CMB source apportionment results are important factors for PM health studies, and policy analysis and decision making. Monte Carlo analysis with Latin hypercube sampling (MC-LHS) was applied to quantify uncertainties and identify

their contributors in the model results due to uncertainties from both ambient measurement and source profile data.

Chapter 6 provides conclusions and recommendations for future research.

CHAPTER 2

GASEOUS AND PARTICULATE EMISSIONS FROM PRESCRIBED BURNING IN GEORGIA

(an extended version of Lee, S.; Baumann, K; Schauer, J.J.; Sheesley, R.J.; Naeher, L.P.; Meinardi, S.; Blake, D.R.; Edgerton, E.S.; Russell, A.G.; Clements, M. *Environmental Science & Technology*, 39, 9049-9056, 2005)

Abstract

Prescribed burning is a significant source of $PM_{2.5}$ in the southeastern United States. However, limited data exist on the emission characteristics from this source. Various organic and inorganic compounds both in the gas and particle phase were measured in the emissions of prescribed burnings conducted at two pine dominated forest areas in Georgia. The measurements of volatile organic compounds (VOCs) and fine particulate matter ($PM_{2.5}$) allowed the determination of emission factors for the flaming and smoldering stages of prescribed burning. The VOC emission factors from smoldering were distinctly higher than flaming except for ethene, ethyne, and organic nitrate compounds. VOC emission factors show that emissions of certain aromatic compounds and terpenes such as α and β-pinenes, which are important precursors for secondary organic aerosol (SOA), are much higher from active prescribed burnings than from fireplace wood and laboratory open burning studies. Levoglucosan is the major particulate organic compound (POC) emitted for all these studies, though its emission relative to total organic carbon (mg/g OC) differs significantly. Furthermore, cholesterol, an important fingerprint for meat cooking, was only observed in our *in situ* study indicating a significant release from the soil and soil organisms during open burning.

Source apportionment of ambient primary fine particulate OC measured at two urban receptor locations 20-25 km downwind yields 74 ±11 % (prescribed burning contribution) of measure OC during and immediately after the burns using our new *in situ* profile. In comparison with the previous source profile from laboratory simulations, however, prescribed burning source contribution is on average 27 ±5 % lower.

2.1 Introduction

Forest fires, both wildfire and prescribed burning, are important sources of primary air pollutants and precursors of secondary pollutants. In the southeastern United States, forest fires contribute about 20, 8, and 6 % of non-fugitive primary $PM_{2.5}$, CO, and volatile organic compound (VOC) emissions, respectively (Barnard *et al.*, 2003), and have been reported as the primary cause of increased $PM_{2.5}$ levels and visibility impairment in the US (Sandberg *et al.*, 2002). Primary air pollutants from forest fires can travel long distances (thousands of km). Canadian forest fires increased CO concentrations leading to elevated O_3 levels in the South-Eastern US (Wotawa *et al.*, 2000) and elevated $PM_{2.5}$ concentrations in an eastern US urban area were observed due to Canadian forest fires (Sapkota *et al.*, 2005). While emission factors for major gas-phase species, $PM_{2.5}$ mass, EC and OC have been calculated in an attempt to improve the emission inventory for forest fires in the U.S. (Battye *et al.*, 2002), they are primarily based on measurements and conditions resembling the Western US. Epidemiologic studies show an association between air pollutants emitted by forest fires (*e.g.* $PM_{2.5}$ and O_3) and adverse health effects (Samet *et al.*, 2000; Pope *et al.*, 2002; Fowler *et al.*, 2003; Bell *et al.*, 2004).

Prescribed burning is widely used (*e.g.* in Georgia >1 million acres annually) for various reasons, including controlling vegetation, enhancing biotic productivity and diversity, controlling disease and insects, reducing fuel accumulation, and habitat management for endangered species in the US, and especially in the Southeast (Hardy *et al.*, 2001). Therefore, it is important to investigate emissions from prescribed burning in order to understand its impact on air quality. Because of its mixed fuel and different combustion conditions, prescribed burning likely has a different chemical composition of $PM_{2.5}$ and VOC compared to residential wood burning emissions. Hays and colleagues (Hays *et al.*, 2002) reported source profiles of $PM_{2.5}$ and VOC from laboratory simulations of different forest fires. However, very limited data exists on emission characteristics from active prescribed burning in the US. In our study, emission characterizations of $PM_{2.5}$ and VOC from prescribed burning were determined by directly measuring emissions at prescribed burning sites, providing source profiles of $PM_{2.5}$ and VOC for future source apportionment and information for an improved emission inventory development. In addition, the newly developed source profile was applied for quantifying the primary source contributions to ambient organic carbon (OC) levels by a chemical mass balance model.

2.2 Measurement sites

Emission and ambient measurements were conducted in Georgia, U.S. during April, 2004. Emission samples were collected at two pine dominated forest areas that are managed by prescribed burning (Figure 2.1). Fort Benning and Fort Gordon are both military installations that burn approximately 32,000 and 14,000 acres, respectively,

every year mainly to maintain a healthy habitat of endangered species (*e.g.* the red-cockaded woodpecker), and to sustain military operations and training. Fort Benning is situated to the south-east of Columbus close to the Alabama border, and Fort Gordon is south-west of Augusta near the South Carolina border. Prescribed burnings were conducted on April 15 and 16, 2004 (331 and 345 acres, respectively) at Fort Gordon and on April 28 and 29, 2004 (204 and 381, respectively) at Fort Benning. During these periods, ambient samples were collected at the State's regulatory monitoring locations of both Metropolitan Statistical Areas (MSA), a residential area in Augusta, 21 km downwind, and at a residential area with a few industrial sources in Columbus, 26 km downwind from the respective prescribed burning sites.

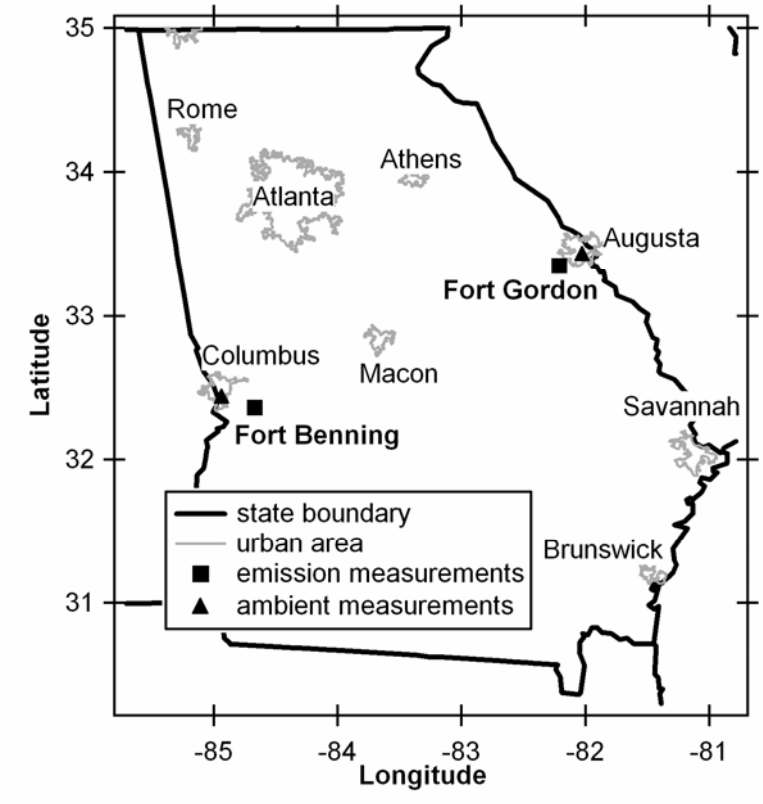

Figure 2.1. Measurement locations in Georgia with the Augusta and Columbus receptor sites being 250°N/20km and 105°N/25km downwind from the corresponding Fort's burn site, respectively

2.3 Experiment methods

2.3.1. Emission Measurements.

A total of four particle-phase emission samples, two at each site, were collected within a few m away from the downwind edge of the burning area on 4 different days in April 2004. Average ambient temperature during the measurements was 26.5 ± 2.7 °C under mostly clear skies and low to moderate winds, meeting the fundamental requirements for conducting prescribed burns in Georgia (detailed weather conditions are described in the Supporting Information). Custom-designed Particulate Composition Monitors (PCM), Federal Reference Method (FRM), and High Volume Samplers (HVS) were operated for about 3 hours simultaneously to collect particulate emissions. The PCM is for the determination of gravimetric $PM_{2.5}$ mass, water soluble ionic species, organic/elemental carbon (OC/EC), and gases (Baumann *et al.*, 2003), the FRM for gravimetric $PM_{2.5}$ mass and trace elements (U.S. EPA, 1997), and the HVS (Tisch Environmental Inc., Cleves, OH, model TE-5070 base with TE-10557 venturi, and TE-6001-2.5 $PM_{2.5}$ impactor) for OC/EC analysis and particulate organic compound (POC) speciation.

The two channel PCM was designed to measure particles less than 2.5 microns in aerodynamic diameter ($PM_{2.5}$) and gases by employing denuders (Baumann *et al.*, 2003; Perrino *et al.*, 1999) and filter packs (Figure 2.2). The $PM_{2.5}$ mass concentration was determined gravimetrically from the denuded and desiccated Teflon filter in channel 1, as well as particle phase sodium, potassium, ammonium, chloride, nitrate, sulfate, formate, acetate, and oxalate by ion chromatography (IC). In addition, 7 gaseous species, NH_3, HCl, SO_2, HNO_3, formic, acetic and oxalic acids, were measured via IC of the denuder

extracts. Channel 2 was for the determination of $PM_{2.5}$ OC and EC, employing a carbon monolith (Novacarb^{TM}, Mast Carbon Ltd., UK) to effectively remove condensable organic vapors, hence minimize semi-volatile adsorption artifact prior to particulate OC collection on a 47 mm pre-baked quartz fiber filter (Pall-Life *Science*s, Ann Arbor, MI), followed by a pre-baked back-up filter coated with XAD-4 (Gundel *et al.*, 1995, 1998; Lane, 1999). Quartz filters were analyzed by a thermal optical ECOC analyzer (Sunset Laboratory Inc., Tigard, OR) using the NIOSH protocol (Birch *et al.*, 1999; Schauer *et al.*, 2003).

A BGI PQ200 portable particulate sampler (BGI Inc., Waltham, MA) equipped with a WINS impactor (FRM) was operated to collect $PM_{2.5}$ on Teflon filters (Teflo ringed membrane, Pall-Life *Science*s, Ann Arbor, MI). After gravimetric $PM_{2.5}$ mass determination Teflon filters were analyzed for major trace elements via energy dispersive X-ray fluorescence spectroscopy (XRF).

The HVS used larger pre-baked quartz fiber filters (8 x 10 inch, Pall-Life *Science*s, Ann Arbor, MI), which were analyzed for POC via gas chromatography/mass spectrometry (GC/MS) at the University of Wisconsin, Madison. The organic analysis method has been also described previously (Sheesley *et al.*, 2000, 2004).

Precision of the IC analysis is ~7% for oxalate and better than 5% for all other ionic species, and the XRF analysis' precision is less than 10%. The precision of the GC/MS analysis is within 25% based on comparing the analysis of blank filters spiked with quantification standards composed of a mix of analytes with historical lab results (Manchester-Neesvig *et al.*, 2003). Uncertainties for $PM_{2.5}$ mass, OC, and EC were assessed by instrument inter-comparisons. Undenuded FRM mass was 5 ± 8% higher

than the denuded PCM mass at an R^2 of 0.94 based on the linear least-squares regression, indicating the FRM's susceptibility for positive artifacts from condensation and adsorption of less volatile gaseous emissions. For OC/EC inter-comparison, the same samples were analyzed by each thermal optical ECOC analyzer at Georgia Institute of Technology and University of Wisconsin, Madison. Bias between the two instruments was 7% for OC and 3% for EC. The linear least-squares regression for the OC/EC ratios between PCM (x) and HVS (y) yielded a slope of 1.40 ± 0.15 (R^2 = 0.97). This slope larger than 1 likely resulted from positive artifacts on HVS rather than small differences in the operating parameters of the analyzers (*e.g.* temperature program), considering the relatively small instrument biases.

Evacuated stainless steel canisters were used to collect gaseous species including CO, CO_2, CH_4, non-methane hydrocarbons (NMHCs), halogenated hydrocarbons, and organic nitrates. Several emission samples distinctively separating the flaming from the smoldering stage were collected in February and April, 2003 and during the above PM measurements in April 2004. The mobility of the cans allowed the sampling of emissions only a few cm away from the source, whereas the PM sampling equipment was placed a few m away from the downwind edge of the area burnt. Ambient background levels were measured prior to or upwind of every prescribed burning, and considered in the subsequent determination of the net emissions. Those samples were analyzed by gas chromatography with flame ionization detection (FID), electron capture detection (ECD), and mass spectrometry (MS). The typical analytical precision is 3% and detection limit is 5 pptv for NMHCs in accordance with the previously described analytical procedure (Colman *et al.*, 2001).

Ch	D1	D2	F1	F2
1	SC	PA	T	GSC
2	CM		Q	XQ
flow direction →				

Figure 2.2. PCM channel configurations used for emission measurements (Ch: channel number, D: denuder), F: filter, SC: sodium carbonate, PA: phosphorous acid, T: Teflon-membrane filter, GSC: SC-coated glass fiber, Q: quartz fiber, XQ: XAD-4 coated quartz fiber, CM: carbon monolith upstream of cyclone).

2.3.2. Ambient measurements.

Two 3-channel PCMs were used to alternately collect gravimetric $PM_{2.5}$ mass, water soluble ionic species, OC/EC, trace elements, and gases following the same denuded filter collection principle from above (Figure 2.3) and operational details described previously (Baumann *et al.*, 2003). Two HVSs (Thermo Electron Co., Franklin, MA, model GMW PM10-VFC with a 2.5 μm slitted pre-separator SA231) were also deployed

for POC collection and speciation following the same procedures as used for the emission samples.

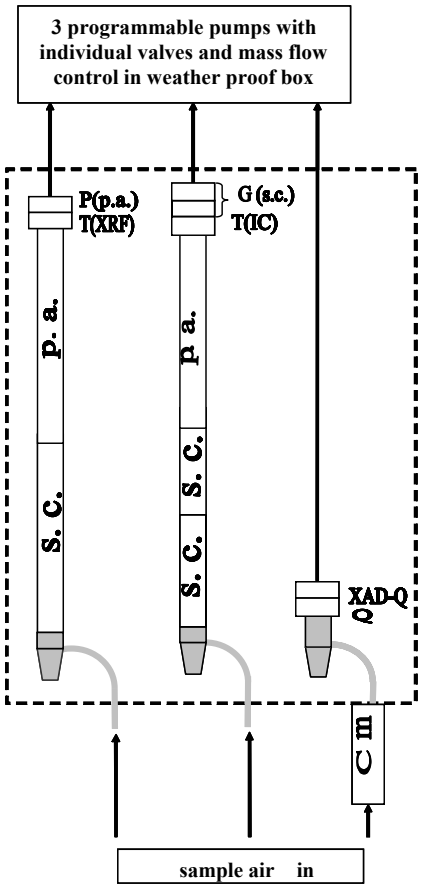

Figure 2.3. Schematic diagram of the three-channel PCM for ambient measurements (IC: ion chromatography, XRF: X-ray fluorescence spectroscopy, F: filter, SC: sodium carbonate, PA: phosphorous acid, T: Teflon-membrane filter, GSC: SC-coated glass fiber, Q: quartz fiber, XQ: XAD-4 coated quartz fiber, CM: carbon monolith upstream of cyclone).

2.3.3. CMB source apportionment.

Major primary emissions from gasoline-powered motor vehicles, medium-duty diesel trucks, meat cooking, residential wood burning, prescribed fire, and road dust were included in CMB8 in order to quantify their source contribution to ambient OC

concentrations (Schauer *et al.*, 1996; Watson *et al.*, 2001). These source profiles were obtained from previous source test studies. The gasoline-powered vehicle source profile was generated by weighted-average of catalyst-equipped gasoline-powered motor vehicles and non-catalyst gasoline-powered motor vehicles (Schauer *et al.*, 2002) based on their emissions in Georgia. The source profile for medium-duty diesel trucks was from Schauer *et al.* (1999a), meat cooking from Schauer *et al.* (1999b), prescribed burning from our study and Hays *et al.* (2002), road dust from Zheng *et al.* (2002), vegetative detritus from Rogge *et al.* (1993). The residential wood burning source profile was generated by averaging 6 source tests from Fine *et al.* (2002).

2.4 Results and Discussions

2.4.1. Chemical composition of $PM_{2.5}$ emissions.

All four $PM_{2.5}$ samples were used to calculate average chemical composition of emissions from active prescribed burnings (Table 2.1), after subtracting ambient background levels, which were determined at the corresponding burn site up to one day prior to the actual conduct of the burn. Fractions of OC and EC in $PM_{2.5}$ emissions were 60.25 ±18.5 % and 3.92 ±1.13 %, respectively. Among the water-soluble species, K^+, acetate, and Cl^- are the major ions comprising 0.65 ±0.45, 0.55 ±0.16, and 0.53 ±0.29 %, respectively. Total K and Cl are also identified by XRF (0.57 ±0.37 and 0.42 ±0.23 %, respectively). The linear regressions between total and water soluble fraction for K and Cl show that total and water soluble fractions of the two species are well correlated (R^2 = 0.97 and 0.96, respectively). Other trace elements identified by XRF were less than 0.3 %.

Table 2.1. Average and standard deviation (STD) of the chemical composition of particle-phase emissions from prescribed burning.

	AVERAGE	STD
PM 2.5 mass (mg m^{-3})	1.81	0.68
OC and EC (weight % of PM2.5 mass)		
Organic Carbon	60.25	18.52
Elemental Carbon	3.92	1.13
Ionic Species (weight % of PM2.5 mass)		
Acetate	0.548	0.156
Formate	0.447	0.114
Nitrate	0.440	0.299
Chloride	0.527	0.289
Potassium	0.649	0.435
Sulfate	0.245	0.112
Ammonium	0.107	0.108
Oxalate	0.069	0.014
Sodium	0.016	0.008
X-Ray Fluorescence (weight % of PM2.5 mass)		
Na	0.0431	0.0175
Mg	0.0001	0.0003
Al	0.0229	0.0426
Si	0.0186	0.0258
P	0.0010	0.0015
S	0.1074	0.0403
Cl	0.4217	0.2295
K	0.5707	0.3711
Ca	0.0006	0.0011
Ti	0.0004	0.0006
V	BL	BL
Cr	BL	BL
Mn	0.0011	0.0010
Fe	0.0082	0.0137
Co	BL	BL
Ni	BL	BL
Cu	0.0010	0.0010
Zn	0.0160	0.0089
Ga	BL	BL
Ge	BL	BL
As	0.0002	0.0003
Se	0.0001	0.0002
Br	0.0141	0.0091
Rb	0.0042	0.0028
Sr	0.0002	0.0003
Pb	0.0001	0.0003

*BL: below blank level

2.4.2. Organic compounds of $PM_{2.5}$ emissions.

Emissions of specific POC normalized to OC (mg/g OC) were calculated after subtracting corresponding background levels (Table A.1). The total identified POC mass is 176 ±54 mg/g OC. Levoglucosan (95 ±40 mg/g OC), a monosaccharide derivative from the pyrolysis of cellulose, is the most dominant species among the identified POC. It is followed by resin acids, alkanoic acids, and alkenoic acids, 39 ±15, 27 ±12, 5 ±4 mg/g OC, respectively. Resin acids are natural compounds that can be found in plant material, mainly conifers. Two different emission mechanisms, volatilization and

pyrolytic alteration, were suggested in a previous study (Simoneit *et al.*, 1993). Pimaric, sandaracopimaric, and abietic acid are produced by volatilization and dehydroabietic acid by pyrolytic alteration. In our study, dehydroabietic acid is the major species emitted with 33 ±14 mg/g OC. It is followed by isopimaric and pimaric acids, 3.0 ±1.2 and 2.5 ±1.0 mg/g OC, respectively. In alkanoic acids, hexadecanoic, tetracosanoic and hexacosanoic acids are the major species emitted (6.7 ±2.9, 5.0 ±2.2, 3.7 ±1.6 mg/g OC, respectively). For alkenoic acids three compounds were identified, 9-octadecenoic acid and 9,12-octadecadienoic acid being the dominant emissions (2.4 ±1.1 and 2.2 ±1.2 mg/g OC, respectively). Small amounts of alkanes were emitted (2.4 ±1.7 mg/g OC), with nonacosane being the most abundant of the identified alkanes (0.81 ±0.38 mg/g OC). Polycyclic aromatic hydrocarbons (PAH) emissions were emitted 1.5 ±0.7 mg/g OC, with retene as the major species (0.35 ±0.16 mg/g OC). Cholesterol, one of the important species identifying meat cooking smoke, was detected in our study (0.81 ±0.35 mg/g OC).

2.4.3. Gaseous Emissions.

Emission ratios were estimated for gaseous emissions from the canister measurements (Table A.2). Emission ratio relative to CO_2 is determined by dividing excess mixing ratio above ambient background level by excess mixing ratio of simultaneously measured CO_2 (Bongsan *et al.*, 1991). The canister samples were distinguished into flaming (<0.1) and smoldering (> 0.1) stages based on $\Delta CO/\Delta CO_2$ ratios. In our study, the ratio is higher for smoldering (0.234 ±0.013) than flaming (0.071 ± 0.021), indicating more incomplete combustion during the smoldering stage. The ratios listed in Table A-3 represent the

slopes (± standard error, SE) of the least squares linear correlations between the mixing ratios of the individual VOC compounds and CO_2 measured absolutely (*i.e.* non-background-corrected) in the flaming and smoldering emissions, respectively. The coefficient of determination (R^2) signifies how closely individual VOC emissions are driven by the combustion intensity and can be explained by the combustion process itself. For example, most species have higher R^2 in the smoldering than flaming phase, while biogenic compounds (terpenes) and halogenated hydrocarbons show no correlation in either stage except for the methyl chloride and methyl bromide, which are common atmospheric tracers for biomass burning. In general, emission ratios (*i.e.* slopes) are higher during smoldering than flaming except for ethene, ethyne, and organic nitrate compounds.

2.4.4. Emission factors (EF) and profiles comparisons.

EF (g-species per kg biomass burned) is estimated using the carbon mass balance method (Radke *et al.*, 1998; Sinha *et al.*, 2004) with the carbon content of biomass burned (Table A.3.a and A.3.b). In this method, it is assumed that all the burned carbon is emitted into the atmosphere as CO_2, CO, CH_4, NMHCs, and particulate carbon species (OC/EC). EF is defined by multiplying the carbon content of biomass to the relative mass ratio of a species (g) to the summation (kg) of all measured carbon mass. Hays and co-workers (2002) found that the carbon content for aged needles of loblolly pine, the main fuel here is 42.6%, which was used in our calculations. Since the discrete nature of the fine PM sample collection did not allow the distinction between flaming and smoldering,

the same particulate carbon mass was applied to the total kg biomass calculations for both flaming and smoldering.

Results from our study were compared with three other biomass burning emission estimates, two from fireplaces and one from an open burning simulation. Fine *et al.* (2002) and Schauer *et al.* (2001) measured emissions from fireplace burning of loblolly pine and pine, respectively (Fine *et al.*, 2002; Schauer *et al.*, 2001). Hays *et al.* (2002) measured emissions from open burning simulating the prescribed burning of aged loblolly pine needles. Schauer *et al.* used fuels obtained from the western US whereas in two other studies fuels from the southern US were burnt. However, similar dilution sampling systems were used by all investigators to simulate the cooling and dilution effects of the atmosphere.

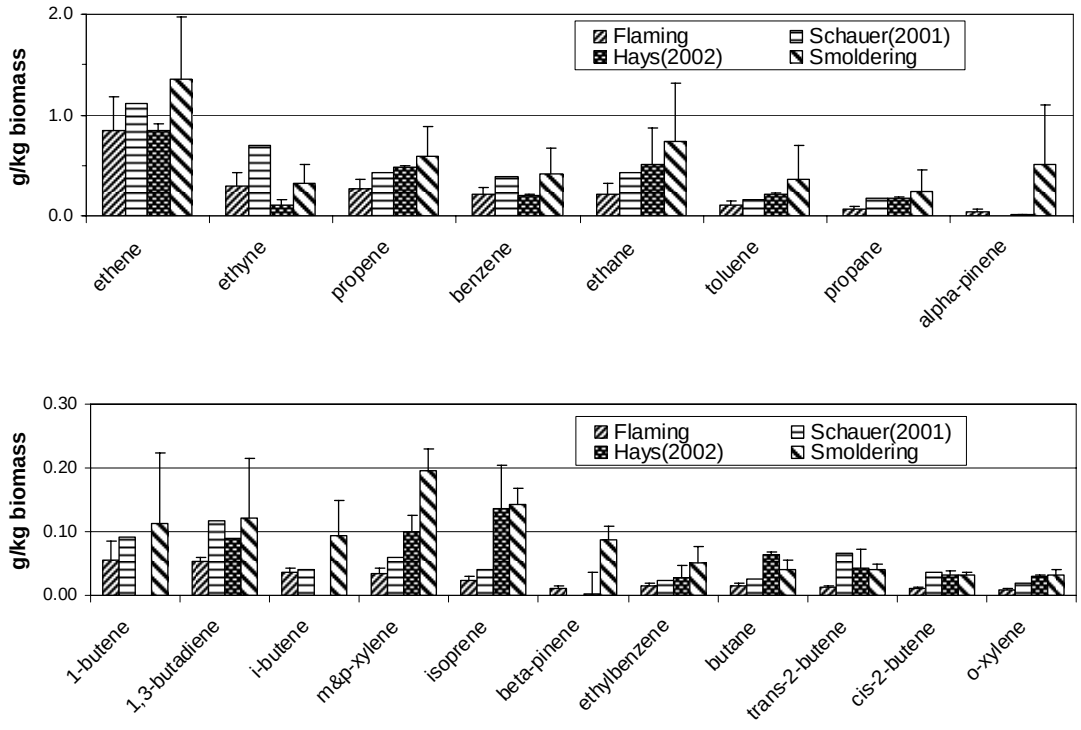

Figure 2.4. Comparisons of VOC emission factors assuming a biomass carbon content of 42.6 %; the error bars for our study represent single standard deviations of 10 flaming and 12 smoldering samples.

For the VOC species measured in our study, ethene has the highest EF for all studies (Figure 2.4). In general, emissions from laboratory burnings are in between the flaming and smoldering emissions of our study. Emissions from the smoldering stage are generally higher than from flaming and also higher than the two laboratory burnings. This trend becomes much stronger for aromatic and biogenic compounds such as benzene, toluene, xylenes, isoprene, and pinenes, which play an important role in the atmospheric formation of ozone and SOA.

OC is the dominant $PM_{2.5}$ component (more than 50 %) for all cases (Figure 2.5). K and Cl are the major trace elements (0.2~0.7 %) except for the open burning simulation, in which both were below detection limit. Water soluble potassium is often used as a tracer for biomass smoke. Note that other studies have reported only total potassium. Very similar amounts of water soluble potassium compared to total potassium was found in our study indicating that all potassium from prescribed burnings is likely water soluble. This is also the case for chlorine.

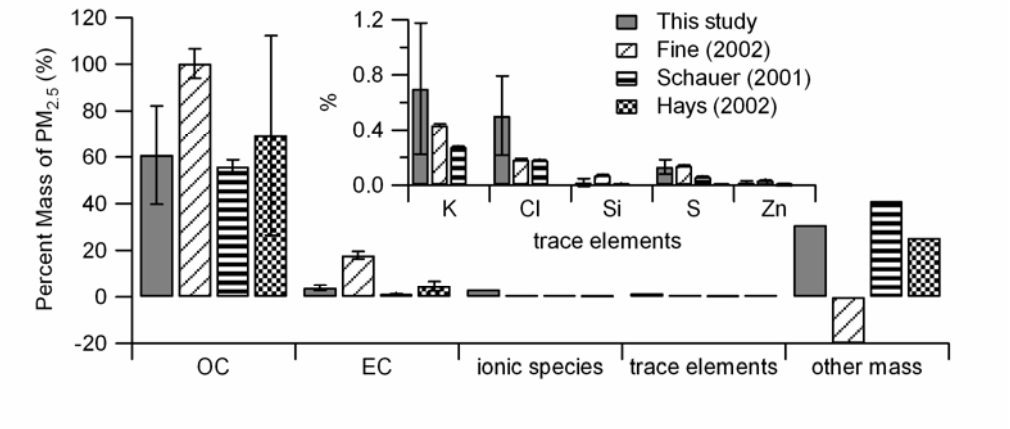

Figure 2.5. Comparison of bulk $PM_{2.5}$ chemical composition of emissions from this in situ study with different laboratory and fireplace wood burning studies; the error bars for this study represent single standard deviations of four samples.

The normalized POC emissions (mg/g OC) from those studies were calculated for the same compounds measured here (Figure 2.6). Thus, the total identified POC emissions were 307, 72, and 130 mg/g OC for Schauer *et al.* (2001), Fine *et al.* (2002), and Hays *et al.* (2002), respectively. Our POC emission of 176 mg/g OC is closer to that from Hays *et al.* (2002) than from the two fireplace wood burnings. Our distribution of major POC emissions is also most similar to Hays *et al.* (2002) (Figure 2.6a). Levoglucosan, a pyrolysis product of cellulose, is the most abundant species and is followed by resin acids for all studies. However, their normalized emissions (mg/g) are very different. While levoglucosan from our study is a factor of 2 or 3 higher than that from Fine *et al.* (2002) and Hays *et al.* (2002), it is a factor of 3 less than that from Schauer *et al.* (2001). Resin acid emissions are similar with Hays *et al.* (2002), whereas they are a factor of 2 or 3 higher than the two fireplace burnings. Dehydroabietic acid is the most dominant species for Hays *et al.* (2002) and our study, but abietic acid is the most dominant species for both fireplace burnings (Figure 2.6b). Note that abietic acid is not included for comparison of total resin acid emissions since it was not measured in our study. Unlike previous wood burning studies, the actual prescribed burning emitted cholesterol, which has been used as an important species for identifying meat cooking. Cholesterol, a common animal steroid, exists in soil due to the presence and activity of soil microorganism and higher living organisms (Puglisi *et al.*, 2003). The cholesterol emission process during prescribed burning could be similar to steam-stripping and vaporization during meat cooking (Rogge *et al.*, 1991).

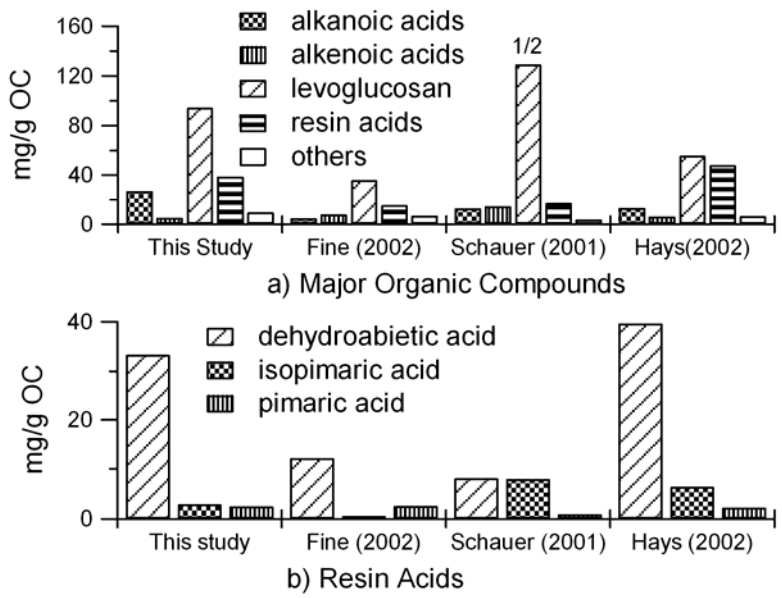

Figure 2.6. Comparisons of normalized POC emissions in mg/g OC of major organic compound groups (a, levoglucosan x ½ of Schauer (2001)), and three resin acids (b).

2.4.5. Prescribed burning source impacts

Organic mass (OM), here assumed as 1.6*OC representing a typical urban environment (Baumann *et al.*, 2003; Turpin *et al.*, 2001), and sulfate are the major species of the measured ambient $PM_{2.5}$ comprising more than 65% of its mass (Figure 2.7). Rain events associated with low pressure frontal movements occurred before and after prescribed burning at Augusta and Columbus, respectively. The CMB model was used to quantify the contributions to ambient OC concentrations of the main primary sources (motor vehicles, residential wood burning, meat cooking, road dust, and vegetative detritus) including prescribed burning. Preliminary CMB analysis showed the residential wood burning contribution being statistically equal to zero, therefore, it was excluded. The model was run two times; first with a prescribed burning source profile from our study, secondly with one from Hays *et al.* (2001). Both CMB runs used the same selection of fitting species, which is based on a previous study (Schauer *et al.*,

1996). The source apportionment results from the first CMB run are only reported here (Figure 2.8). The results show that motor vehicles and prescribed burning are the major sources contributing to the ambient [OC] at both sites during and immediately after the actual prescribed burns with 29 ±7 % and 74 ±11 % (±SE), respectively. However, before the burns and during the regional rain events, measured [OC] cannot be completely explained by the selected primary sources, leaving a relatively large fraction un-apportioned (labeled "others" in Figure 2.8). Whether this fraction can be considered SOA and to what extent it is related to the local prescribed burning emissions or more regional transport with slower atmospheric processing is highly speculative and subject to future investigation.

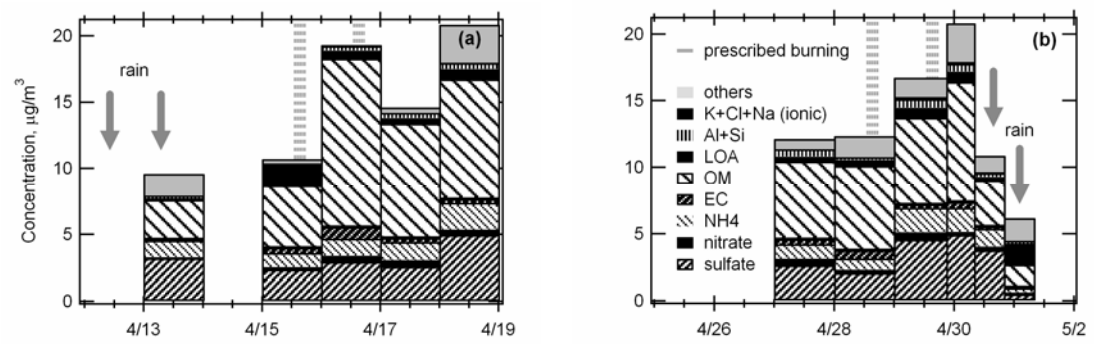

Figure 2.7. Bulk chemical composition of ambient $PM_{2.5}$ measured in April 2004 at Augusta (a), and Columbus (b); LOA is the sum of the three light organic acids.

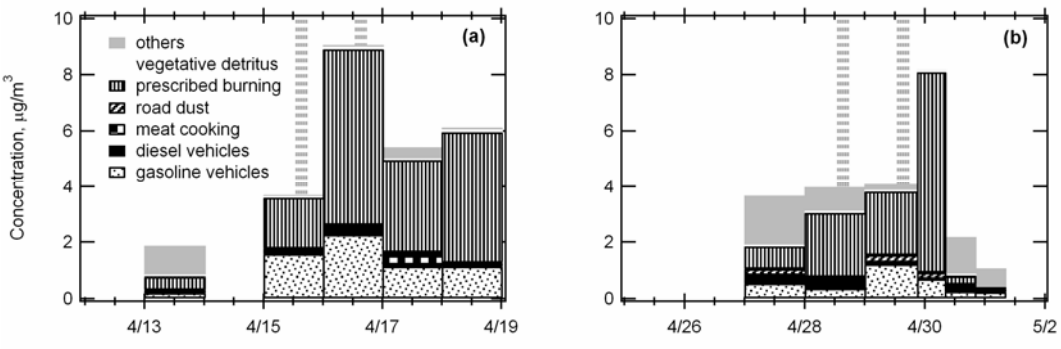

Figure 2.8. Contributions to ambient fine particulate OC concentrations measured at Augusta (a) and Columbus (b).

CMB sensitivity using different prescribed burning source profiles is evaluated by comparing the two model results via linear least-squares regression (Table 2.2). Application of the two different prescribed burning source profiles changes not only the source contribution of prescribed burning itself, but yields also significant differences for both diesel and meat cooking source impacts. Higher levoglucosan (g/g OC) from our study leads to a 27 ±5 % (±SE) lower prescribed burning contribution. A 25 ±6 % lower meat cooking contribution is largely due to a higher 9-octadecenoic acid (g/g OC) relative to Hays *et al.* (2001) The CMB result yielding lower prescribed burning contribution from our *in situ* profile apportions less EC to that source, leading to a 20 ±16 % higher diesel vehicle contribution.

Table 2.2. Linear least-square regressions between two CMB source apportionment results using two different prescribed burning emission profiles; *i.e.* our *in situ* vs. lab simulation from Hays *et al.*.

source	R^2	Slope*	Intercept*
gasoline vehicles	0.99	0.94 ± 0.02	0.02 ± 0.03
diesel vehicles	0.94	1.20 ± 0.16	0.00 ± 0.03
meat cooking	0.99	0.75 ± 0.06	-0.03 ± 0.02
road dust	1.00	1.00 ± 0.01	0.00 ± 0.00
prescribed burning	0.96	0.73 ± 0.05	-0.21 ± 0.26
vegetative detritus	0.96	0.94 ± 0.07	0.00 ± 0.01

* The regression slopes and intercepts with standard error; our study (y) vs. Hays *et al.* (x).

2.4.6. Implication of a new prescribed burning $PM_{2.5}$ source profile for CMB source apportionment

CMB receptor modeling can attribute ambient $PM_{2.5}$ to primary emission sources by using $PM_{2.5}$ bulk chemical speciation data at both a receptor and emission sources. Biomass burning activities (*i.e.*, wild fire, prescribed burning and residential wood burning *etc*) are significant primary emission sources of $PM_{2.5}$. However, Source contribution of individual biomass burning activity can not be estimated accurately at the same time in CMB receptor modeling because of similarities among their source profiles. Source profiles of biomass burning emissions can be combined to estimate source impacts of biomass burning instead of estimating inaccurate each biomass burning impacts. There are two different biomass burning source profiles which were developed by using woody material in the southeast. One is residential wood burning from Fine *et al.* (2002), and the other is prescribed burning from this study. Source contribution estimates by CMB receptor modeling are typically more sensitive to source profile than ambient measurement data. Biomass burning source impacts were estimated by using three different source profiles in order to examine sensitivity of calculated source impacts to the source profiles (Table 2.3). Ambient measurement data at Dekalb, GA were used for this purpose.

Table 2.3. Weight fraction of OC and K in three biomass burning source profiles.

	residential wood burning (Fine *et al.*, 2002)	prescribed burning (this study)	residential wood burning + prescribed burning (combined)
OC	0.883 ± 0.060	0.603 ± 0.185	0.743 ± 0.195
K	0.0070 ± 0.00008	0.0057 ± 0.0037	0.0063 ± 0.0037

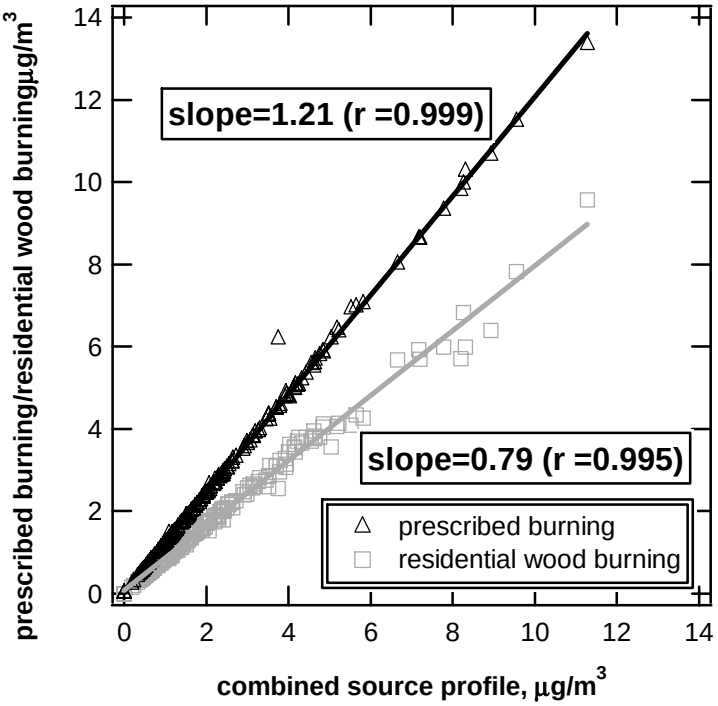

Figure 2.9. Comparison of estimates of biomass burning source contribution using different source profiles.

Results show that biomass burning source impacts estimated by using a combined source profile are 21% lower than those by using only prescribed burning source profile, but 21% higher than those by using only residential wood burning source profile (Figure 2.9). Relatively different fractions of K and OC (Table 2.3), which are main driving forces of biomass burning source contribution, result in different source impact estimates.

In CMB receptor modeling, uncertainties in both ambient measurement and source profile data are propagated by inversely weighting effective variance to estimate uncertainties of source contributions (Watson *et al.*, 1984). Therefore, using different source profiles with different uncertainties changes not only source contribution estimates, but also uncertainties in estimated source contributions. Relatively lower

uncertainties in residential wood burning source profile lead to much lower uncertainties in source contribution estimates than those in other two estimates (Figure 2.10). Residential wood burning source profile was created from laboratory emission source tests by burning different southeastern wood types in a same experiment setup (Fine *et al.*, 2002), while prescribed burning source profile was produced by directly measuring emissions from actual prescribed burning (Lee *et al.*, 2005). Woody materials were combusted in a same or very similar combustion condition, whereas mixed biomass materials (*i.e.*, woods, dead leaves, small brushes, organic materials in soils *etc*) combusted in different combustion conditions. Mixed fuels and different combustion conditions may contribute to relatively higher uncertainties in the prescribed burning source profile.

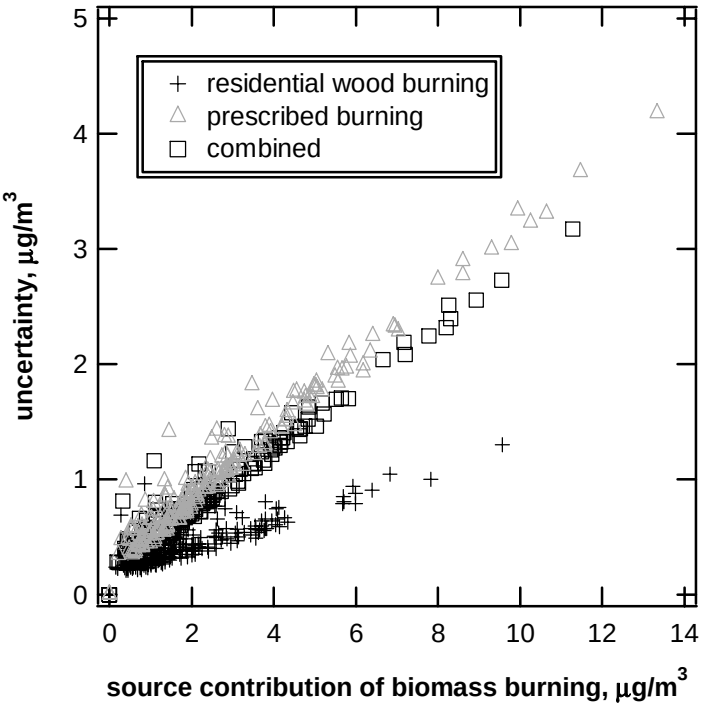

Figure 2.10. Comparison of uncertainty estimates of biomass burning source contribution using different source profiles.

CHAPTER 3

SOURCE APPORTIONMENT OF PM2.5 IN THE SOUTHEASTERN UNITED STATES

(Lee, S.; Baumann, K.; Russell, A.G. Journal of the Air and Waster Management Association, 2006, in preparation)

Abstract

$PM_{2.5}$ source apportionment by chemical mass balance receptor model was performed to understand regional perspectives of source impacts in the southeastern United States. Secondary particles, such as NH_4HSO_4, $(NH_4)_2SO_4$, NH_4NO_3, and secondary organic carbon (SOC), formed by atmospheric photochemical reactions, contribute the majority (>50%) of ambient $PM_{2.5}$ with strong seasonality. Source apportionment results indicate that motor vehicle and biomass burning are the two main primary sources in the southeast showing relatively more motor vehicle source impacts rather than biomass burning source impacts in populated urban areas and *vice versa* in less urbanized areas. Spatial distributions of primary source impacts show that each primary source has distinctively different spatial source impacts from each other. The results also illustrate possible emission impacts from ship activities along the coast. Spatial-temporal correlations indicate that secondary particles are more regionally distributed, and impacts of primary sources are more local. In order to reduce primary source impacts, the results imply that targeted control strategies should be developed for specific regions based on the most important sources identified and the relative costs of emission reductions.

3.1. Introduction

Epidemiologic studies suggest that ambient particulate matter (PM) has significant associations with adverse respiratory and cardiovascular health effects (Dockery *et al.*, 1993; Pope *et al.*, 1995; Schwartz *et al.*, 1994, 1996; Thurston *et al.*, 1994), and prompted the U.S. Environmental Protection Agency to promulgate National Ambient Air Quality Standards (NAAQS) in July, 1997. The majority of the past epidemiologic studies focused on linking human exposures to PM mass, its chemical components and size. More recent studies have been conducted to understand associations between PM emission sources and human exposure (Laden *et al.*, 2000; Mar *et al.*, 2000; Tsai *et al.*, 2000, Sarnat *et al.*, 2006).

Associated with the new NAAQS, the U.S. EPA established the $PM_{2.5}$ chemical Speciation Trend Network (STN) program to provide nationally consistent data for the assessment of trends (U.S. EPA, 1999). Twenty-four hours integrated filter based samples are collected every 3 or 6 days at each monitoring site. The samples are analyzed to determine gravimetric mass and chemical composition, including ions, trace elements and carbonaceous compounds (*i.e.*, organic and elemental carbons).

There have been $PM_{2.5}$ source apportionment studies to understand its sources and contributions in the southeast (Kim *et al.*, 2003, 2004, 2005a; Liu *et al.*, 2005; Marmur *et al.*, 2005, 2006; Park *et al.*, 2005; Zheng *et al.*, 2002, 2006). The studies also demonstrate the applicability of different source apportionment methods. However, little information about the regional perspective of $PM_{2.5}$ source impacts in the region has been provided in the studies. The main goal of this study is to conduct source apportionment of $PM_{2.5}$ and develop a regional perspective of source impacts in the southeastern U.S. 23 STN sites

from 6 southeastern states were selected (Figure 3.1). This study provides useful information for possible future epidemiologic studies that aim to improve our understanding of the association between fine PM sources and human health exposure and ultimately to help develop effective PM control strategies.

A chemical mass balance receptor model (CMB) is applied to identify primary source contributions for ambient measurement data collected at 23 STN sites between January 2002 and November 2003. Seasonal variation and spatial-temporal correlations of the identified PM sources are examined.

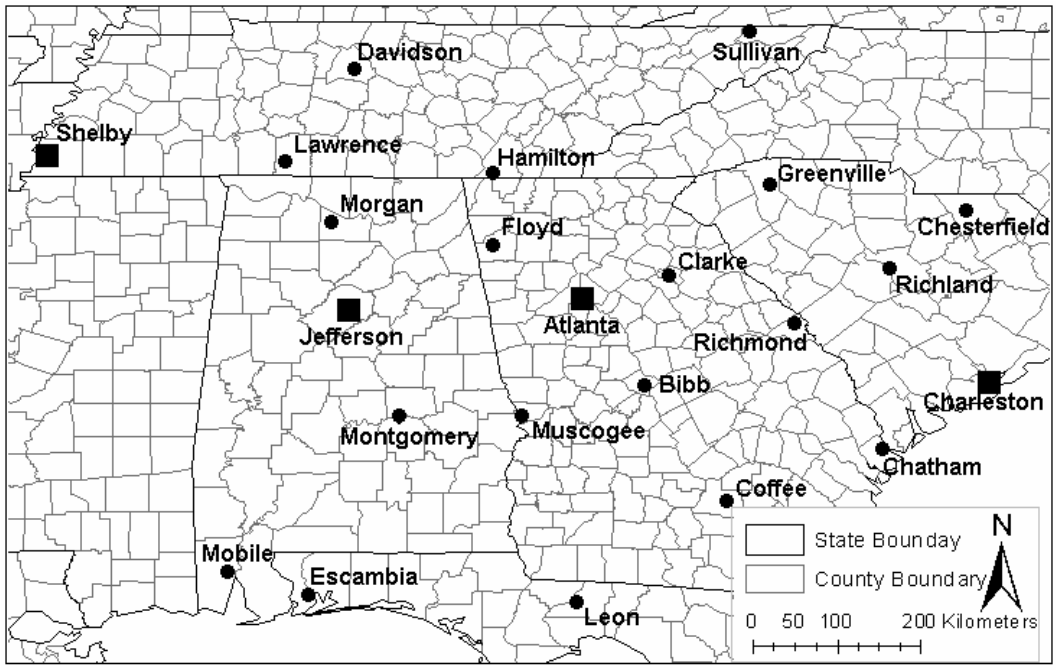

Figure 3.1. STN ambient monitoring sites in the Southeast of U.S. every 3 days (■) or 6 days (●) measurements.

3.2 Method

3.2.1. Primary Organic Carbon (OC) Estimation

The CMB receptor model is used to estimate primary source contributions by using ambient measurement and source profile data.

$$C_i = \sum_{i=1}^{n} f_{i,j} S_j, \quad i = 1,.....n, \tag{1}$$

where C_i is the ambient concentration of species i, f_i is the fraction of species i in source j, and S_j is the source contribution of source j. Chemical species used in CMB are assumed to be non-reactive (Watson *et al.*, 2001). However, organic carbon (OC) measured at a receptor site includes primary OC emitted from emission sources and secondary OC from photochemical formation. In order to apply CMB using OC information one must either add a secondary OC source, or, as done here, estimate primary OC. Simply adding a pure secondary OC source could lead to collinearity problems with OC dominant sources. Therefore, it is desirable to estimate primary OC prior to the source apportionment. Although many studies have been conducted to understand secondary OC (Altshuller, 1983; Claeys *et al.*, 2004; Glasius *et al.*, 2000; Hoffmann *et al.*, 1997; Jang and Kamens, 1999; 2001; Noziere *et al.*, 1999; Odum *et al.*, 1996; 1997; Stern *et al.*, 1987; Wangberg *et al.*, 1997; Yu *et al.*, 1999), it is problematic separating primary from secondary OC via direct chemical analysis.

The EC tracer method, an indirect method, has been used to estimate primary and secondary OC, since EC is a good tracer for carbonaceous particles from primary combustion sources (Cabada *et al.*, 2002, 2004; Castro *et al.*, 1999; Gray *et al.*, 1986; Strader *et al.*, 1999; Turpin *et al.*, 1991, 1995). In general, there are two approaches in the EC tracer method to separate primary and secondary OC. One is using ambient measurement data and the other is based on primary emission inventory data. In this study, a combined method was used to estimate monthly primary OC/EC ratios. First, a

primary OC/EC ratio was derived by using ambient OC and EC data at each site. A recent study shows that the Deming linear least-squares regression is the superior method among several ambient EC tracer methods (Chu, 2005). Deming regression was applied for daily OC and EC data in the lowest 10 % by OC/EC ratio. Second, monthly primary OC/EC ratios were obtained by compiling primary OC and EC emission data (equation 1). Based on the 2001 National Emission Inventory, annual PM emissions were calculated for various categories from counties within 25 km of each monitoring site. Monthly temporal profiles of PM emissions were applied to get monthly PM emissions at each site and then a source specific OC and EC weight fraction from source emission experiments was multiplied to obtain monthly OC and EC emissions (Table 3.1):

$$\left[\frac{OC}{EC}\right]_{primary} = \frac{\sum_{i=1}^{n} PM2.5_i \times OC_{f,i}}{\sum_{i=1}^{n} PM2.5_i \times EC_{f,i}} \quad (2)$$

where $[OC/EC]_{primary}$ is the monthly primary OC to EC ratio, $PM2.5_i$ is the monthly primary PM2.5 emission (tons/month) from a source i, and $OC_{f,i}$ is the weight fraction of PM2.5 from source i, $EC_{f,i}$ is the weight fraction of PM2.5 from a source i. The OC and EC weight fractions of $PM_{2.5}$ from the Interagency Monitoring of Protected Visual Environments (IMPROVE) method (Chow *et al.*, 1993) were used since more comprehensive emissions data are available. Ambient STN OC/EC data were obtained using the National Institute of Occupational Safety and Health (NIOSH) method (Birch *et al.*, 1996). The Deming regression does provide one primary OC/EC ratio for the entire ambient data set at each site. However, the primary OC/EC ratio varies as primary emissions change seasonally. The variability of monthly primary OC/EC ratios from a

median ratio based on emission inventory was weighted to the primary OC/EC ratio from the Deming regression (ambient data) in order to obtain monthly primary OC/EC ratios.

Table 3.1. Primary OC/EC ratio estimations by combining two different EC tracer methods. * Primary $PM_{2.5}$ source categories and references for OC and EC weight fraction of $PM_{2.5}$ were used to obtain monthly primary OC/EC ratios based on emission inventory. **On-road**: light/heavy duty gasoline and diesel vehicles (*Zielinska et al., 1998*); **Non-road**: off-highway gasoline and diesel vehicles (*Zielinska et al., 1998*); **Point non-electricity generation**: fuel combustion [coal (*Chow et al., 2004*), distilled oil (*Houck et al., 1989*), natural gas (*Watson et al., 1988*)], mineral production (*Shareef, 1987*), pulp and paper production (*Shareef, 1987*), metal production (*Shareef, 1987*); **Point electricity generation**: power plant [coal (*Chow et al., 2004*), distilled oil (*Houck et al., 1989*), natural gas (*Watson et al., 1988*)]; **Area**: wild fires (*Watson et al., 2001*), prescribed burning (*Watson et al., 2001*), agricultural burning (*Houck et al., 1989*), yard waste burning (*Chow et al., 2004*), land clearing (*Chow et al., 2004*), fuel combustion [coal (*Chow et al., 2004*), distilled oil (*Houck et al., 1989*), natural gas (*Watson et al., 1988*)], residential wood burning (*Zielinska et al., 1998*), waste incineration (*Houck et al., 1989*), meat cooking (*Zielinska et al., 1998*); **Dust**: agricultural production (*Cooper et al., 1981*), construction (*Chow et al., 1991*), paved road dust (*Chow et al., 2004*), unpaved road dust (*Chow et al., 2004*).

State	County	Primary OC/EC ratio from ambient data (95% confidence interval)	Median Primary OC/EC ratio from emission inventory* (Min-Max)	Min-Max Primary OC/EC ratio from a combined method
Georgia	Bibb	5.84 (5.13-6.56)	3.31 (2.90 – 4.70)	5.13-8.30
	Coffee	6.99 (6.14-7.85)	4.02 (2.10 – 7.11)	3.66-12.38
	Clarke	4.08 (2.95-5.20)	2.84 (2.84 – 4.00)	3.01-5.75
	Chatham	4.06 (3.04-5.08)	3.38 (2.87 – 5.19)	3.45-6.24
	Dekalb	3.02 (2.70-3.34)	2.10 (1.51 – 2.44)	2.18-3.51
	Floyd	7.33 (4.56-10.09)	5.86 (5.41 – 5.49)	6.76-8.12
	Muscogee	7.63 (5.95-9.30)	3.13 (2.10 – 4.95)	5.12-12.05
	Richmond	6.42 (5.05-7.08)	3.53 (2.65 – 4.54)	4.82-8.27
Alabama	Jefferson	2.74 (2.47-3.01)	4.05 (3.93 – 4.42)	2.66-2.99
	Mobile	4.35 (3.00-5.69)	3.67 (3.26 – 4.74)	3.86-5.60
	Montgomery	4.13 (3.13-5.14)	2.48 (1.93 – 3.77)	3.21-6.30
	Morgan	6.99 (5.35-8.63)	2.57 (2.15 – 3.35)	5.85-9.14
Florida	Escambia	5.03 (4.15-5.90)	4.46 (3.71 – 10.55)	4.18-11.89
	Leon	3.53 (3.22-3.85)	5.23 (2.78 – 12.64)	1.88-8.53
South Carolina	Charleston	3.83 (3.42-4.23)	3.40 (2.63 – 5.43)	2.96-6.11
	Chesterfield	7.88 (5.53-10.23)	3.36 (2.63 – 4.27)	6.20-10.02
	Greenville	5.86 (4.43-7.28)	2.55 (1.99 – 3.02)	4.57-6.94
	Richland	4.65 (3.74-5.56)	3.72 (3.37 – 4.06)	4.21-5.07
Tennessee	Davidson	3.11 (2.48-3.75)	2.24 (1.84 – 2.64)	2.56-3.66
	Hamilton	5.06 (4.12-5.99)	2.30 (1.64 – 3.14)	3.60-6.89
	Lawrence	4.89 (3.92-5.86)	2.78 (2.32 – 4.75)	4.08-8.34
	Shelby	3.45 (3.02-3.89)	1.72 (1.31 – 2.08)	2.63-4.16
	Sullivan	3.81 (2.82-4.80)	3.63 (3.59 – 4.39)	3.76-4.61

3.2.2. Source Apportionment

Major primary sources used in the source apportionment include motor vehicles, biomass burning, dust, coal combustion, oil combustion, mineral, metal, and pulp and paper production. Theoretical profiles based on molecular weight fraction for ammonium bisulfate, ammonium sulfate, and ammonium nitrates were also included to identify inorganic secondary particle formation. The source profile for motor vehicles was generated by weighted-average of catalyst-equipped gasoline power vehicles and diesel vehicles based on their estimated emissions (Schauer *et al.*, 1999, 2002). The biomass burning source profile was generated by averaging 6 source tests of southern woods (Fine *et al.*, 2002). The source profile used for dust was from measurements in Alabama (Cooper *et al.*, 1981). The source profile for coal combustion was from Chow *et al.* (2004). Other industrial source profiles were from Shareef (1987). When the reported ambient concentration of trace elements is below detection limit, it was replaced with a value of half of its detection limit. Uncertainty for each species in ambient data was calculated as 5 % of its concentration plus one third of its detection limit.

3.3. Results and Discussion

CMB source apportionment was done by targeting chi-square values less than 4 and r-square values larger than 0.8 over a period covering January 2002 to November 2003. In general, annual averaged $PM_{2.5}$ concentrations are relatively higher in the inland than the coastal area (Figure 3.2). Results show that most (>50%) of ambient $PM_{2.5}$ are secondary from photochemical reactions. Motor vehicles and biomass burning are two

major primary sources in the study area. Dust and industrial sources typically follow in importance.

Source contribution results averaged for three months representing each of the four seasons, winter (December-February), spring (March-May), summer (June-August), and fall (September-November) (Figure 3.3) show strong seasonality for secondary particles. Sulfate particles (NH_4HSO4 and $(NH_4)_2SO_4$) are higher in the warmer seasons whereas NH_4NO_3 is higher in the colder seasons. Like sulfate particles, secondary OC is also higher in the warmer seasons when the atmosphere is photochemically more active. Two primary sources, biomass burning and dust, have a strong seasonality. Biomass burning contributes more in the colder seasons when residential wood burning, prescribed burning, and agricultural burning are increased. In contrast, dust is higher in the drier summer season. There is no distinct seasonality for other primary sources.

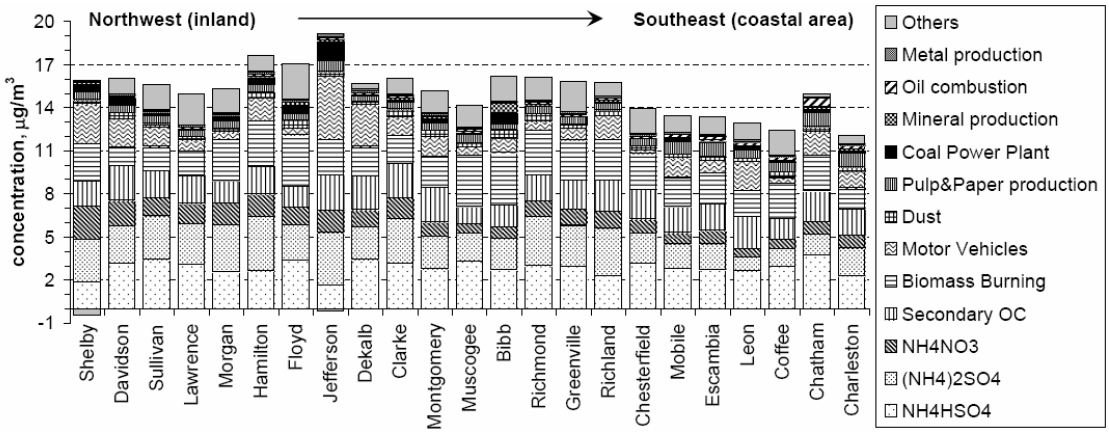

Figure 3.2. Source apportionment results-averaged from November, 2002 to November, 2003

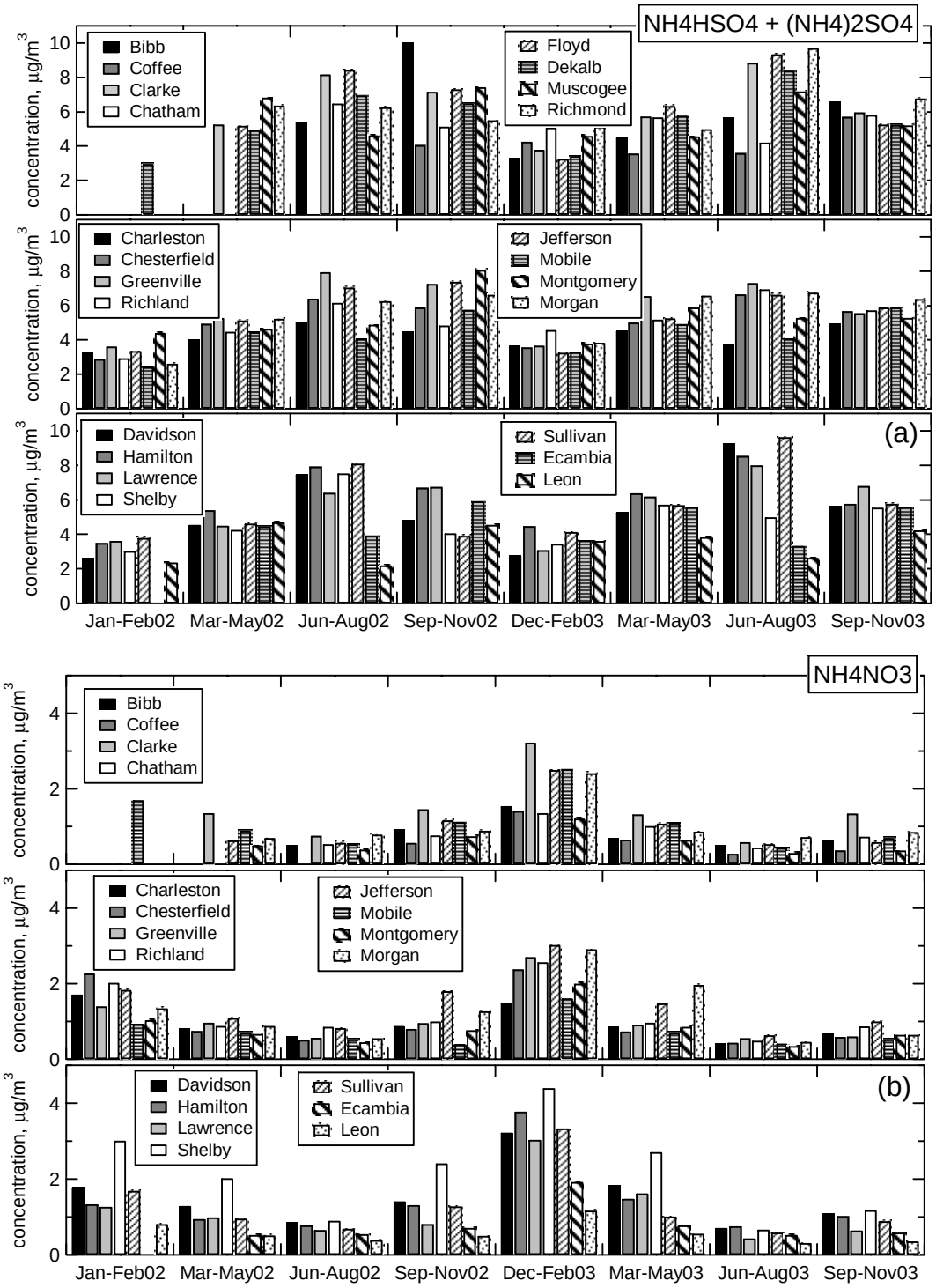

Figure 3.3. Seasonal source contributions. (a) NH_4HSO_4+$(NH_4)_2SO_4$, (b) NH_4NO_3.

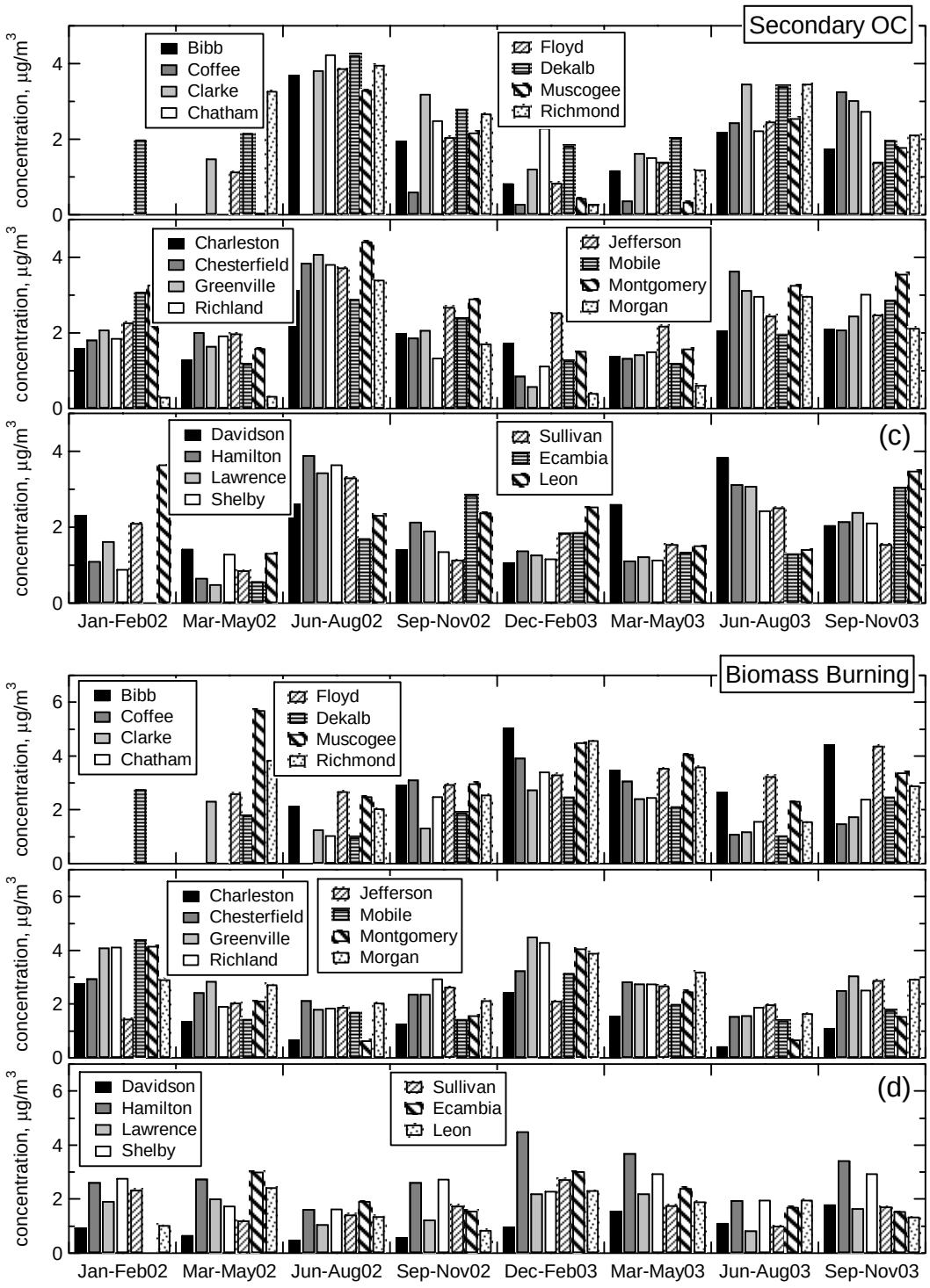

Figure 3.3. Seasonal source contributions (continued). (c) secondary OC, (d) biomass burning.

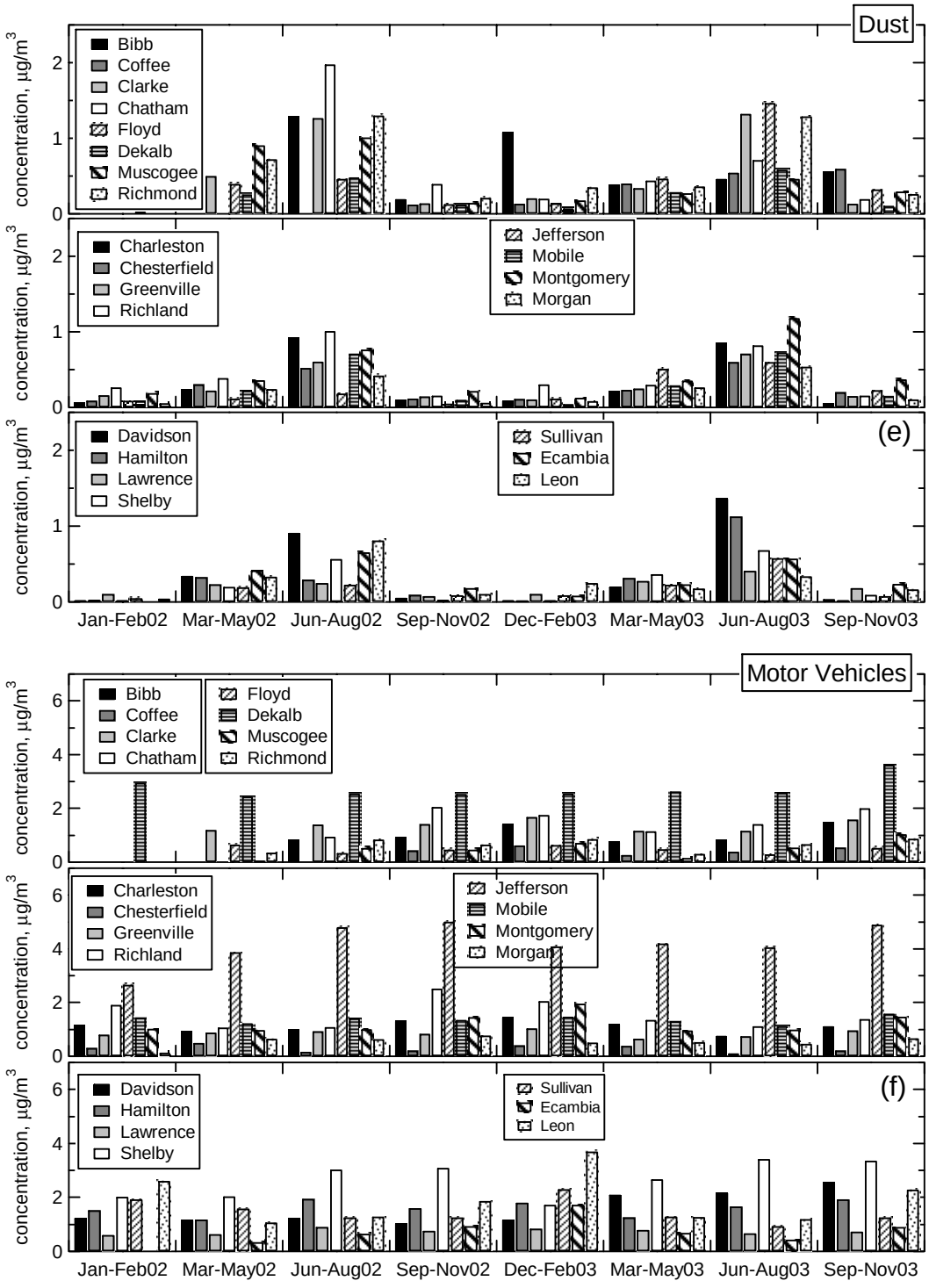

Figure 3.3. Seasonal source contributions (continued). (e) dust, (f) motor vehicles.

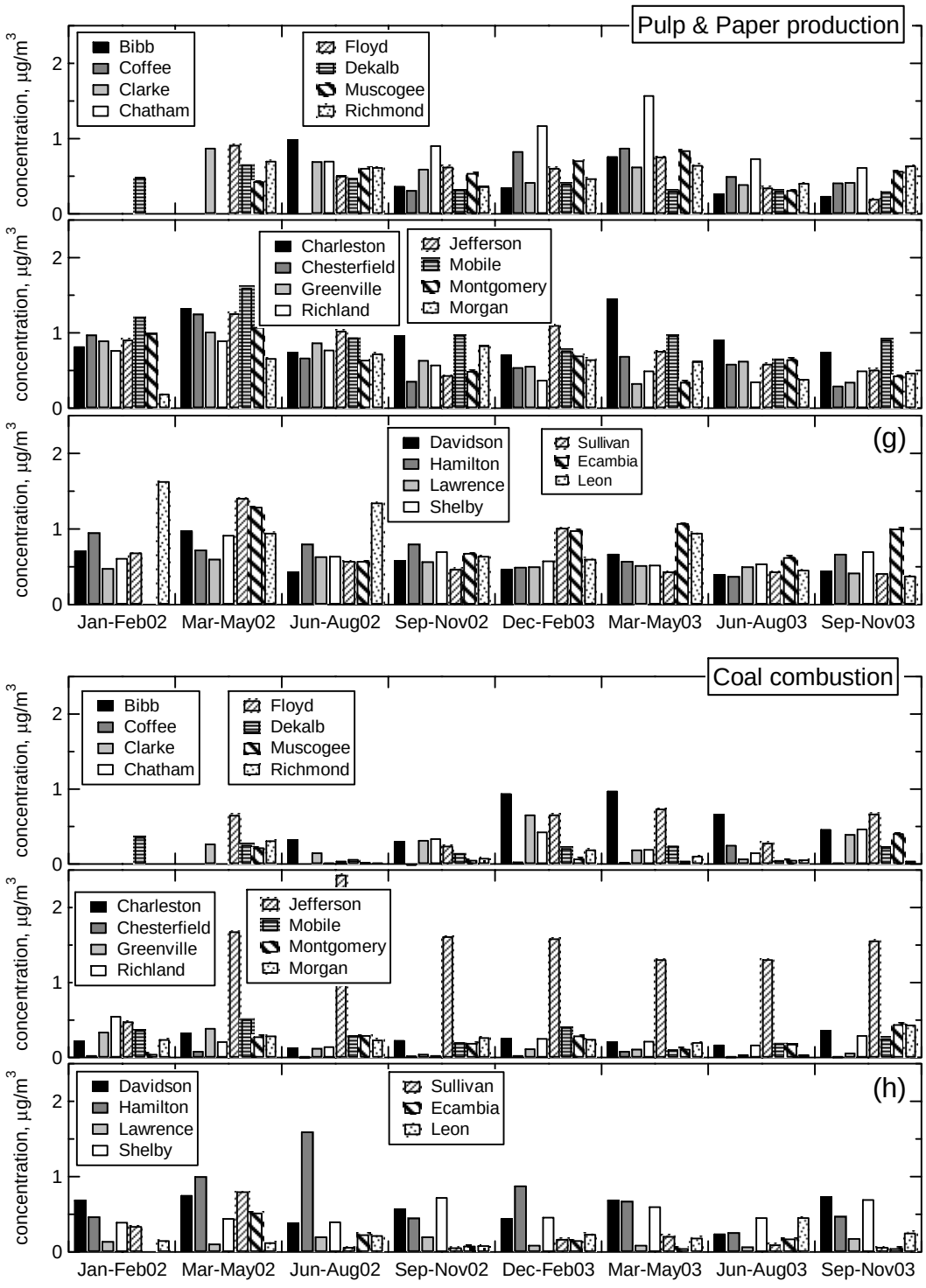

Figure 3.3. Seasonal source contributions (continued). (g) pulp/paper production, (h) coal combustion.

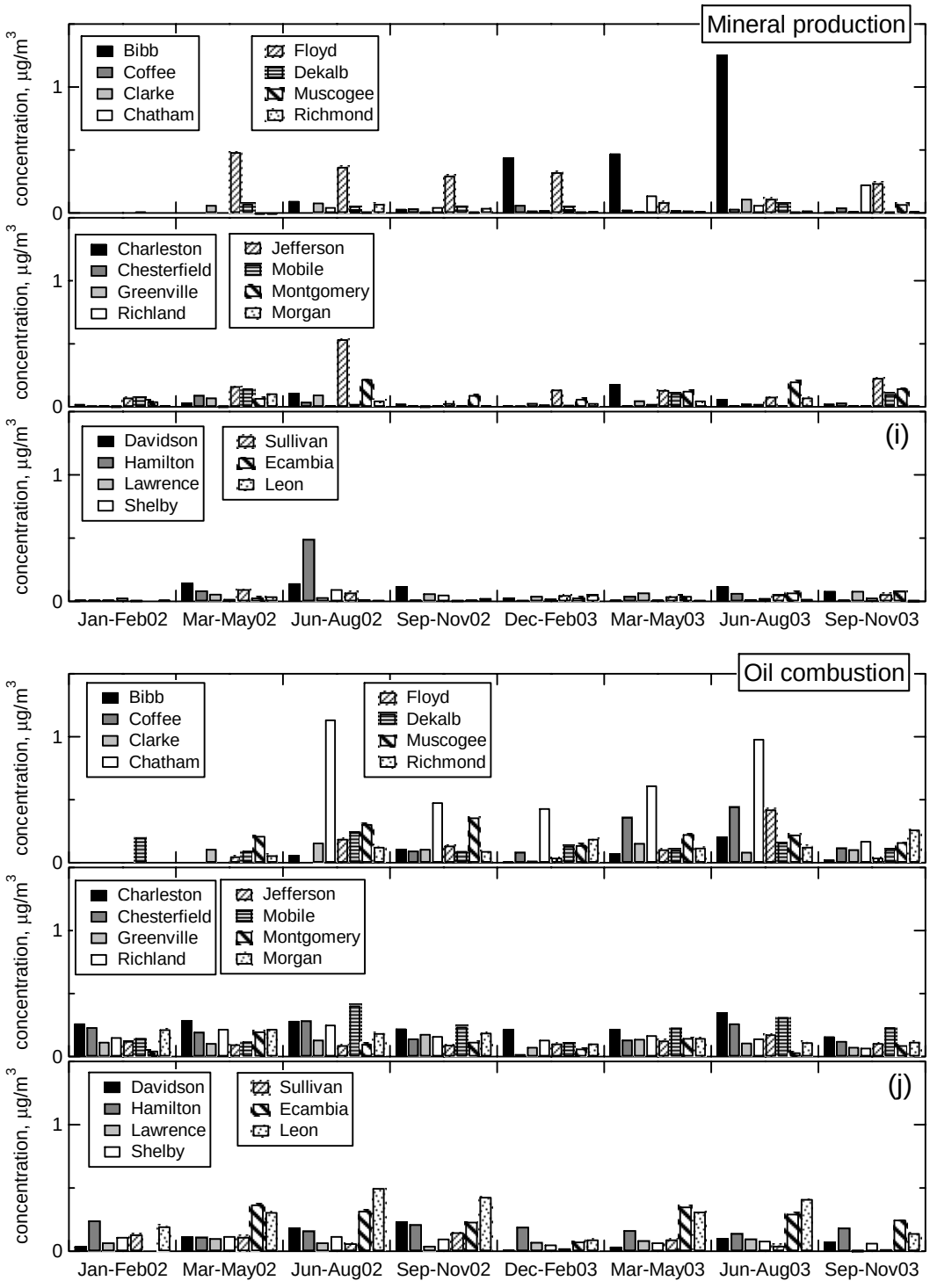

Figure 3.3. Seasonal source contributions (continued). (j) oil combustion, (k) metal production.

To address spatial distribution of each source category, surface maps were created by using one year averaged source apportionment results (Figures 3.4-3.6) and the inverse distance squared weighted method in ESRI® ArcGIS™ 9.0 (*ESRI, 2004*). In the northwestern part of the study area, NH_4HSO_4 is relatively lower than $(NH_4)_2SO_4$, but NH_4NO_3 is relatively larger than that in the southeastern area. This indicates that particles in the northwest are more neutralized by NH_3 forming $(NH_4)_2SO_4$ with excess NH_3 producing NH_4NO_3. In contrast, the southeastern area experiences relatively higher NH_4HSO_4 but lower $(NH_4)_2SO_4$ and NH_4NO_3 than the northwestern part, which is indicative of more acidic particles due to less NH_3 neutralization. This is consistent with NH_3 emissions showing relatively higher emissions in the northwest than in the southeastern area (Figure 3.7). Motor vehicle source contributions are relatively larger in the more populated areas such as Dekalb (Atlanta), Jefferson (Birmingham), and Shelby (Memphis) while biomass burning contributions are larger in the less urbanized areas where biomass burning is more prevalent and actively used in controlled applications for land management purposes (Lee *et al.*, 2005). For coal combustion, higher contributions occur in the areas close to source locations and are highest at Jefferson (Birmingham), AL where industrial facilities use coal for fuel. Relatively higher pulp and paper source contribution occurs along the coastal line where pulp and paper mills are located. Oil combustion contribution is also relatively higher along the coast especially at Chatham (Savannah), GA. This corresponds to $PM_{2.5}$ emissions from shipping activities in the coastal port areas since residual oil is used for ships (Corbett and Fischbeck, 1997). Mineral production is higher at Bibb, Floyd, and Jefferson. Jefferson County has

relatively higher metal production impacts than other sites, but its source contribution is the lowest among the included industrial sources.

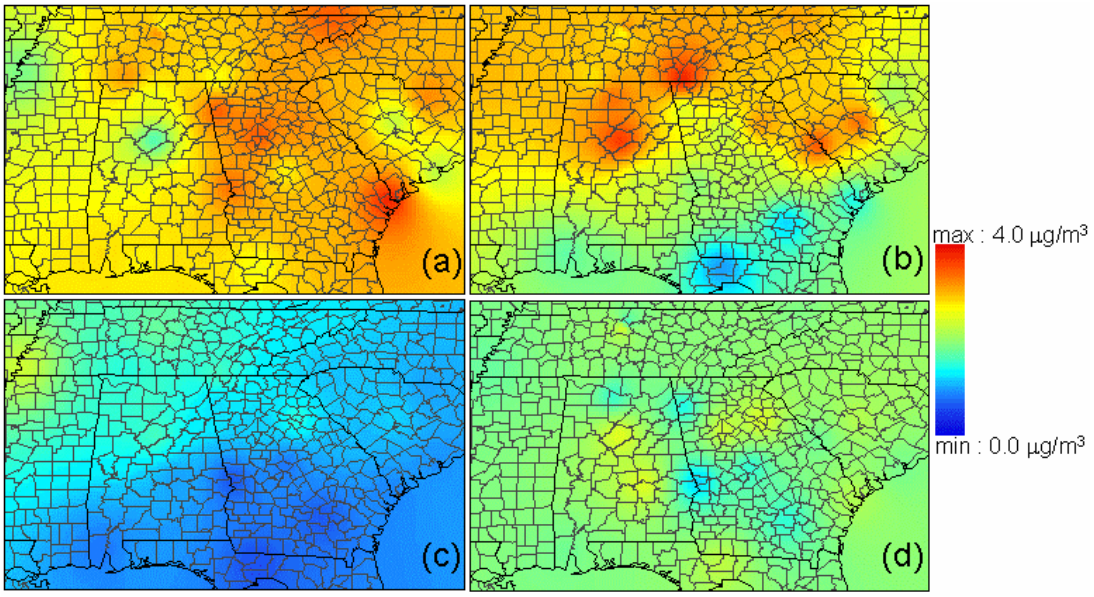

Figure 3.4. Spatial distribution of source contributions. (a) NH_4HSO_4, (b) $(NH_4)_2SO_4$, (c) NH_4NO_3, (d) SOC.

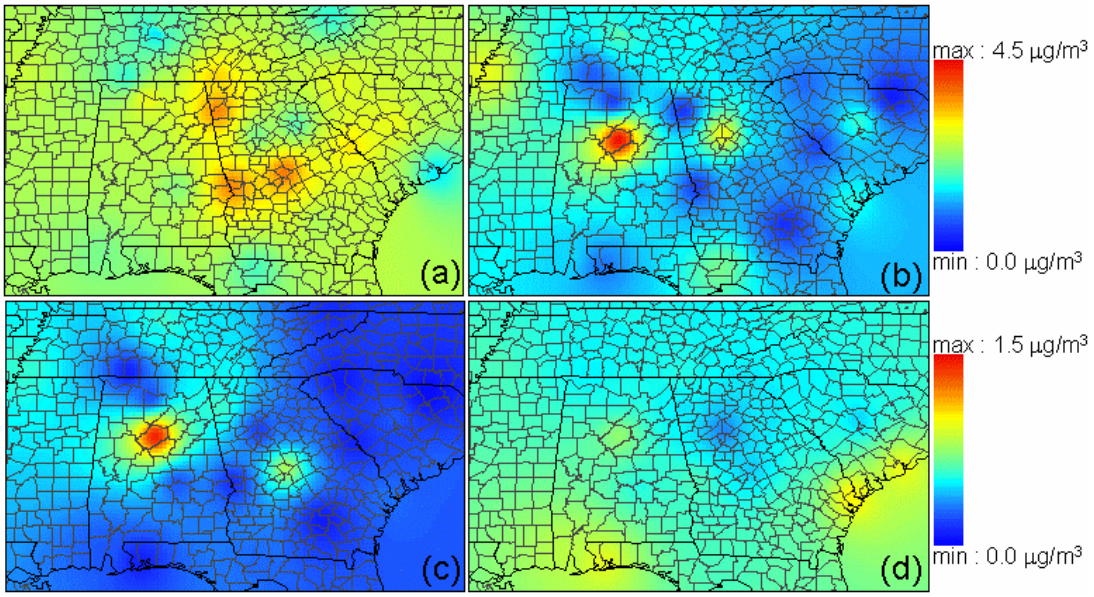

Figure 3.5. Spatial distribution of source contributions. (a) biomass burning, (b) motor vehicles, (c) coal combustion, (d) pulp and paper production.

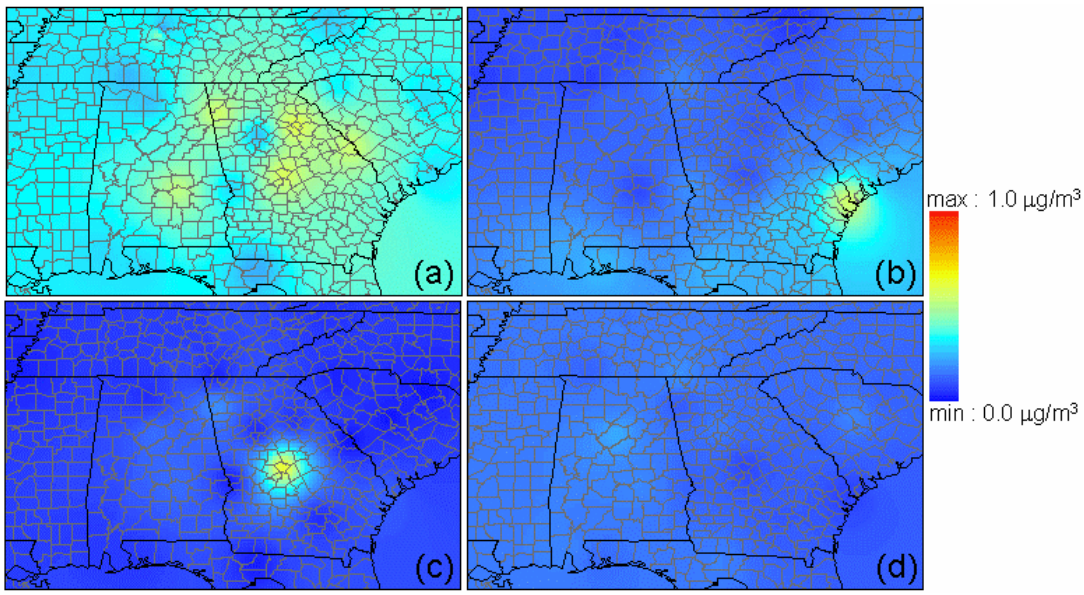

Figure 3.6. Spatial distribution of source contributions. (a) dust, (b) oil combustion, (c) mineral production, (d) metal production.

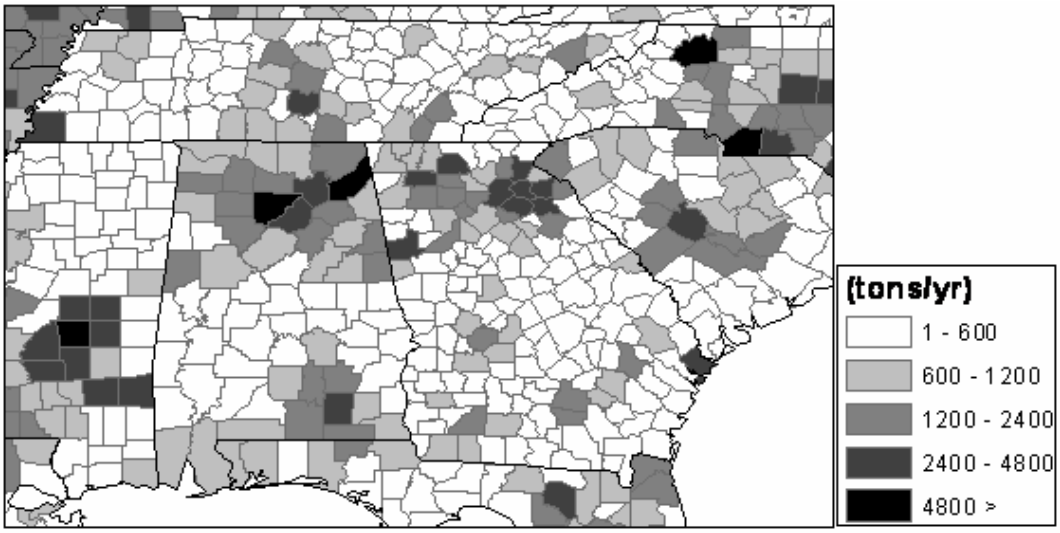

Figure 3.7. Annual NH_3 county emissions based on U.S. EPA 2001 National Emission Inventories.

Spatial-temporal correlations between all possible pairs of sites were calculated for each source category to understand which sources have more local or regional impact in the study area. In general, the correlations decrease as the distance between sites increases. This trend is distinct for the secondary origin particles (Figure 3.8), for which the correlations become insignificant once the pair is more than 300~400 km apart, thus showing the regional nature of secondary species. For the primary sources, correlations are generally poor, even for short distances, indicating a local nature of their impacts. Hence, the secondary particles formed from chemical reactions during atmospheric transport and dispersion have better correlation across larger distances than the primary source categories. It suggests that secondary particles underlying atmospheric formation have a more regional character whereas the primary sources are more local.

Source apportionment results consistently show more motor vehicle impacts relative to biomass burning in the urbanized areas but vice versa in the less urbanized areas. However, motor vehicle source impacts in Jefferson (Birmingham) are higher than in Dekalb (Atlanta), although $PM_{2.5}$ emission inventories show relatively less motor vehicle emissions in Jefferson than Dekalb (Figure 3.9a). Jefferson is located in a valley which is surrounded by long parallel mountain ridges, while Dekalb is located in more flat terrain (www.epa.gov/wed/pages/ecoregions.html). The geographical environment of Jefferson may cause much less dispersion of pollutants so that more source impact happens with less motor vehicle emissions relative to Dekalb. Source apportionment results suggest that pulp/paper produciton impacts relatively higher along the coastal area. Pulp/paper production emission inventories also show a similar pattern suggesting

relatively higher emissions along the coast (Figure 3.9b). The highest pulp/paper emission occurs in Floyd, GA based on emission inventories.

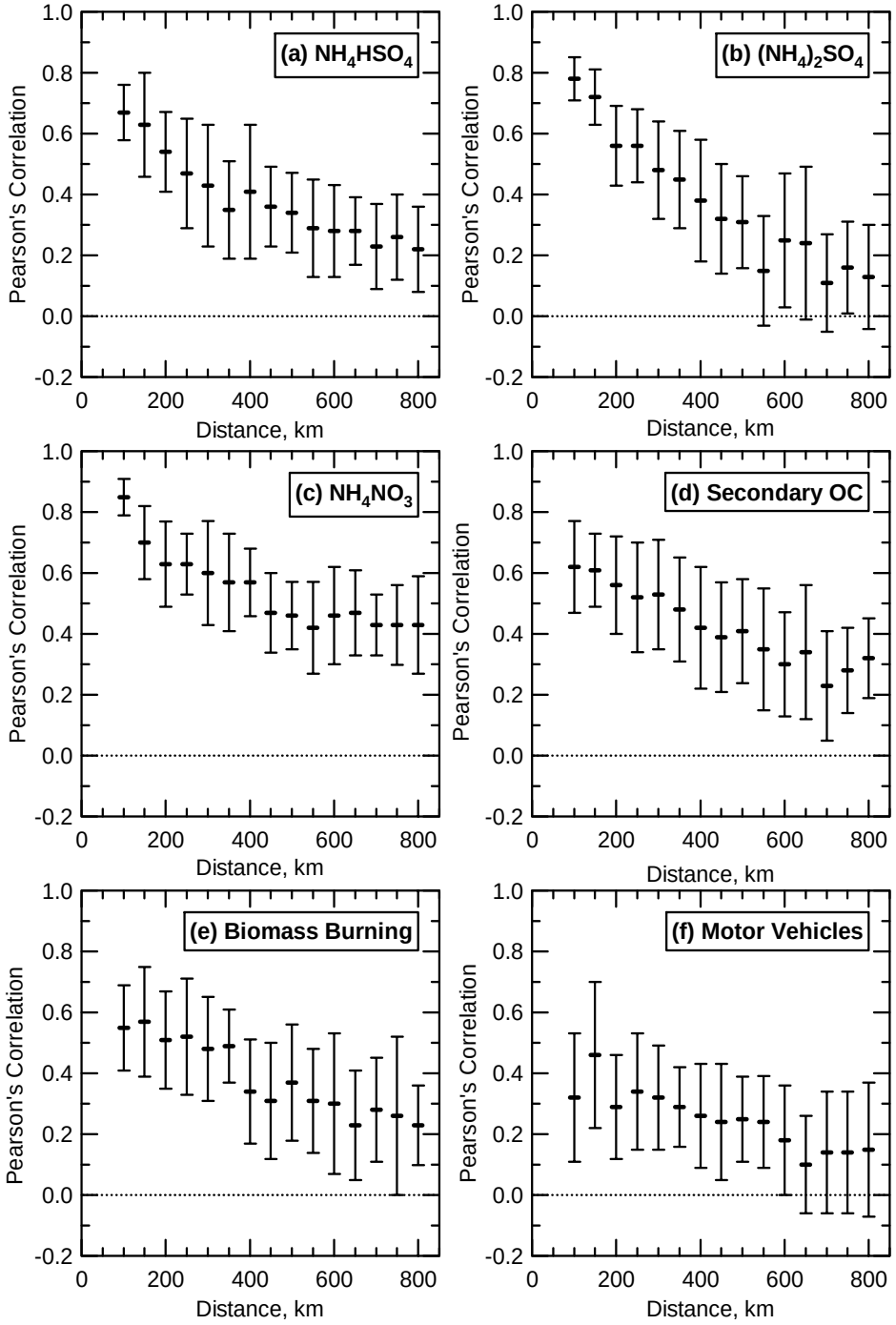

Figure 3.8. Spatial-Temporal correlations of source contributions. (a) NH_4HSO_4 (b) $(NH_4)_2SO_4$, (c) NH_4NO_3, (d) secondary OC, (e) biomass burning, (f) motor vehicle

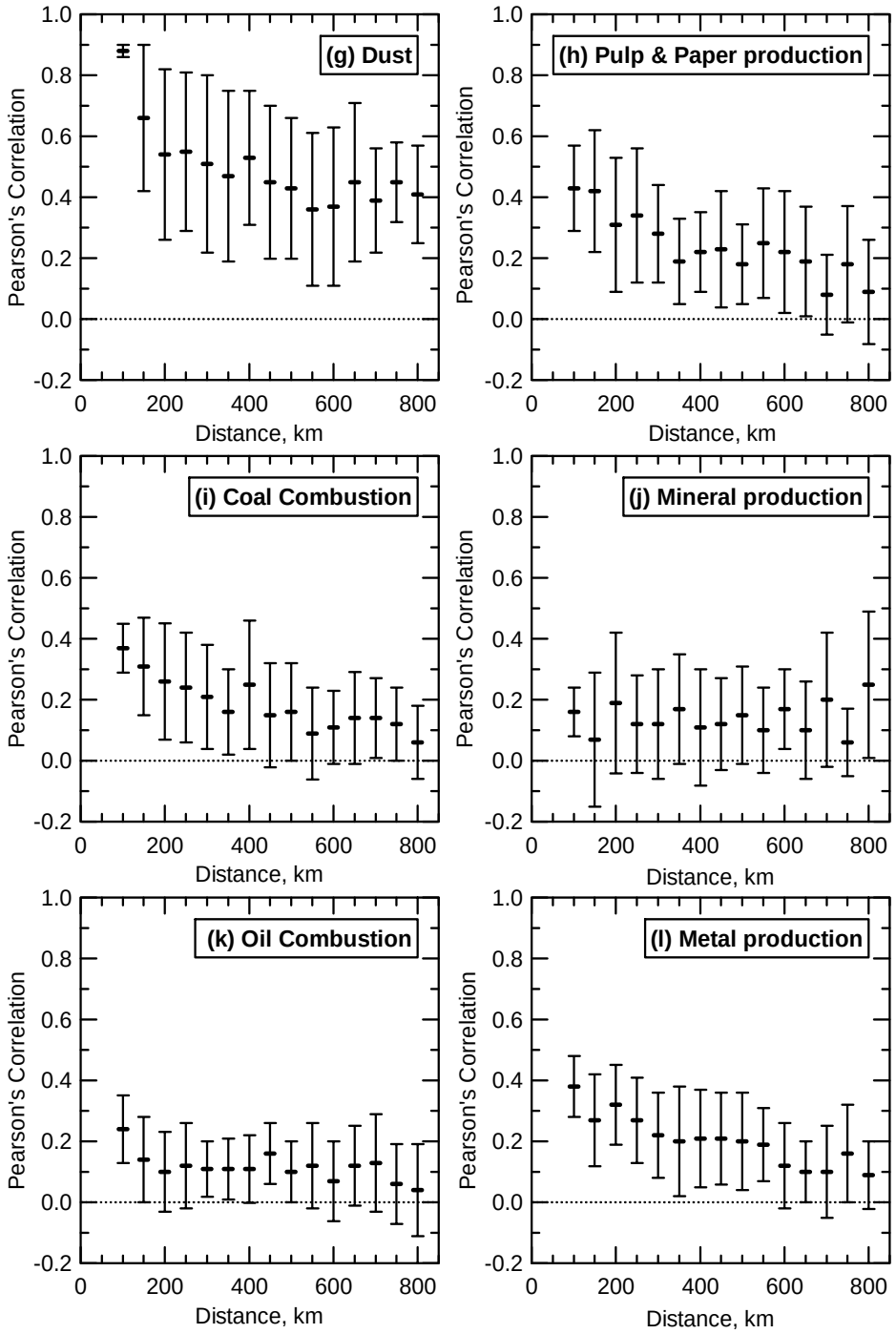

Figure 3.8. Spatial-Temporal correlations of source contributions (continued). (g) dust, (h) pulp/paper production, (i) coal combustion, (j) mineral production, (k) oil combustion, (l) metal production

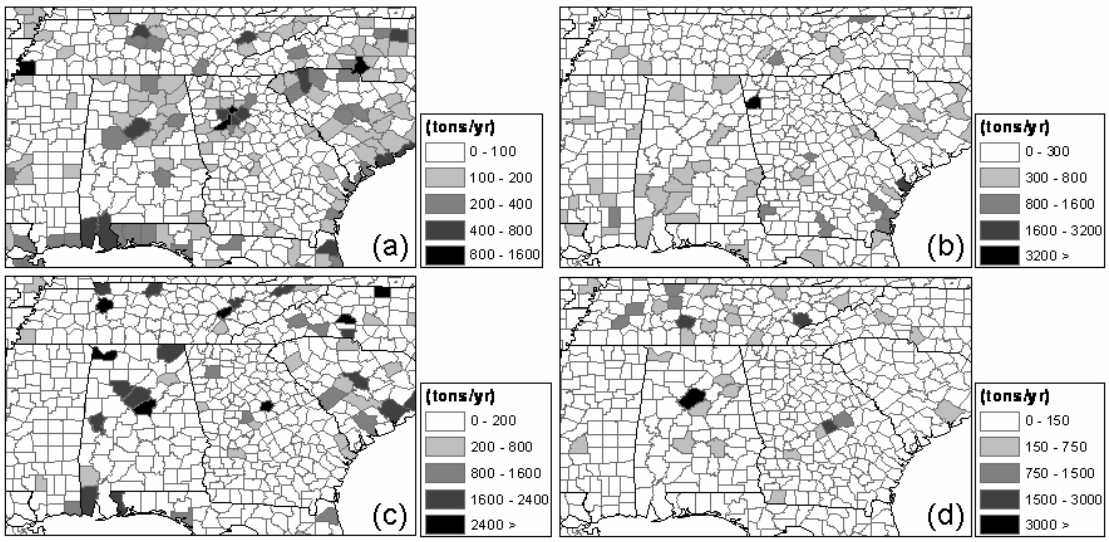

Figure 3.9. Annual primary $PM_{2.5}$ county emissions based on U.S. EPA 2001 National Emission Inventories. (a) motor vehicle, (b) pulp/paper production, (c) coal combustion, (d) metal production

However, this is not the case for the source apportionment results. For coal combustion, both source apportionment results and emission inventories show relatively higher impacts on the Tennessee and North Alabama areas (Figure 3.9c). Metal production impact is the highest at Jefferson, AL, where its emission inventories also suggest the highest emissions (Figure 3.9d). It appears that source impacts of oil combustion are relatively higher along the coast, especially at Chatham (Savannah). Most commercial ships (70~80%) use residual oils which contain more contaminants (Corbett and Fischbeck, 1997) and approximately 80% of ship emissions are concentrated mainly near the shore where the ship traffic density is the highest (Skjølsvik *et al.*, 2000). Therefore, the emissions from ships may impact the inland near ports as shown, especially, at Chatham.

3.4. Conclusions

Source apportionment using CMB receptor model was performed for 24-hr ambient $PM_{2.5}$ measurement data from U.S. EPA STN sites in the southeastern U.S. Secondary particles formed by atmospheric photochemical reactions make up the majority (>50%) of ambient $PM_{2.5}$ and have strong seasonality. Motor vehicles and biomass burning are the two main primary sources. Motor vehicles are the highest primary source contributor in urban areas, while biomass burning dominates more in less urbanized areas. Spatial-temporal correlations show that secondary particles are more regionally distributed, and primary particles are more locally distributed. It implies that targeted control strategies can be developed for specific regions based on the most important sources identified and the relative costs of emission reductions. The comparisons with primary $PM_{2.5}$ emission inventories suggest that the source apportionment results are congruous with the emission inventories in general. However, there are still incongruities between both data sets. The results might be used to compromise both emission inventory and source apportionment data to improve the congruity between both data sets.

CHAPTER 4

SOURCE APPORTIONMENT OF PM2.5 IN ATLANTA: A CASE STUDY FOR SPATIAL REPRESENTATIVENESS AT AN URBAN SCALE

(Sangil Lee and Armistead G. Russell, *Environmental Science & Technology*, in preparation)

Abstract

$PM_{2.5}$ source apportionment results from receptor models, such as chemical mass balance (CMB) are being used for epidemiologic studies by associating source impacts with adverse health outcomes. However, source apportionment results at a single monitoring site can introduce uncertainties into PM health studies when they are associated with averaged adverse health outcomes for an entire city or metropolitan area. Spatial representativeness of source apportionment results needs to be investigated to better assess their proper application in health studies. CMB source apportionment was conducted in both winter and summer, 2005 at four ambient monitoring sites operated as part of the Assessment of Spatial Aerosol Composition in Atlanta (ASACA). Comparison of source apportionment results indicate that secondary particles are spatially relatively uniform in Atlanta, while the degree of spatial representativeness of impacts of primary PM sources varies widely from one source to another. Biomass burning, dust, and motor vehicle source impacts at one site are spatially representative, whereas both coal and oil combustion sources are poorly representative. When source impacts of coal and oil

combustion at a single monitoring site are used, errors and/or uncertainties are introduced in regards to their use in PM health studies.

4.1. Introduction

Particulate matter, particularly the fraction that is less than 2.5 μm in aerodynamic diameter ($PM_{2.5}$), has been associated with adverse health effects, increasing morbidity and mortality rates due to both acute and chronic exposures (Dockery *et al.*, 1993, 1996; Pope *et al.*, 1993, 1996, 2002; Schwartz *et al.*, 1993, 1994). However, its chemical complexity makes it difficult to understand associations between specific health outcomes and $PM_{2.5}$ components. As an alternative approach, recent studies tried to understand associations between adverse health effects and $PM_{2.5}$ emission sources by incorporating source apportionment results (Laden *et al.*, 2000; Mar *et al.*, 2000; Tsai *et al.*, 2000; Sarnat *et al.*, 2006). However, health outcome data used for epidemiologic studies typically come from an entire city or metropolitan area, whereas source apportionment results are based on $PM_{2.5}$ data at a single monitoring site. As mentioned in Ito *et al.* (2004), this may introduce errors or uncertainties in the results of the health studies if source apportionment results at a single monitoring site are not representative for a study area. In previous studies, spatial variability of individual $PM_{2.5}$ components at an urban scale has been examined by estimating spatiotemporal correlation between sites (Pinto *et al.*, 1995; Ito *et al.*, 2004; Kim *et al.*, 2005b; Wade *et al.*, 2006) or by a data-withholding analysis (Park *et al.*, 2006). Those studies show that secondary origin particles (*i.e.*, sulfate) are uniformly distributed in an urban area, whereas primary

components are inhomogeneous. Thus, it is important to address whether source apportionment results at a single monitoring site can represent an entire study area.

In order to address regionality of $PM_{2.5}$ source impacts in the southeast U.S., source apportionments using a chemical mass balance (CMB) receptor model have been conducted for two years of $PM_{2.5}$ data (Lee *et al.*, 2006). That study suggests that primary $PM_{2.5}$ emission sources contribute to more local impacts, while secondary $PM_{2.5}$ sources are found to have more regionally uniform impacts.

In this study, it is investigated how well source apportionment results from a single monitor can represent local air sheds. The Assessment of Spatial Aerosol Composition in Atlanta (ASACA) project provides unique data for studying spatial representativeness (Bulter *et al.*, 2003). A case study was performed for periods in both winter and summer of 2005 in order to address spatial representativeness of source apportionment results.

4.2 Method

4.2.1. Ambient measurement data

The ASACA project was initiated to investigate $PM_{2.5}$ air pollution problems in Atlanta by understanding its sources and spatial and temporal trends (Figure 4.1). In this project there are three ambient monitoring sites [Fort McPherson (FMP), South Dekalb (SDK), and Tucker (TUK)] in Atlanta and one at Fort Yargo state park (FYG), about 50 km away from TUK. A particulate composition monitor (PCM) was operated to collect 24 hr filter-based $PM_{2.5}$ samples for every day at three Atlanta sites and every 3 days at FYG (Bulter *et al.*, 2003). The PCM has three channels to collect $PM_{2.5}$ on three different

filters. The three different filters were used for the analysis of water-soluble ionic species (nylon filter), organic/elemental carbon (quartz filter), and trace elements (Teflon filter). The collected filter samples were analyzed for ionic species, organic/elemental carbon (OC/EC), and trace elements by means of ion chromatography (IC), thermal optical transmittance (TOT), and X-ray fluorescence (XRF), respectively. Continuous $PM_{2.5}$ mass was measured by a Tapered Element Oscillating Microbalance (TEOM®, Thermo Electron Corp., NY) at the three Atlanta sites. The mean, median, and 25 and 75th percentile values for $PM_{2.5}$ mass, major ions and carbonaceous species (OC and EC) are presented here for the most recent two years, 2004-2005 (Table 4.1). The average temperature of the case study period is 11 ± 3˚C and 28 ± 2˚C for winter and summer, respectively.

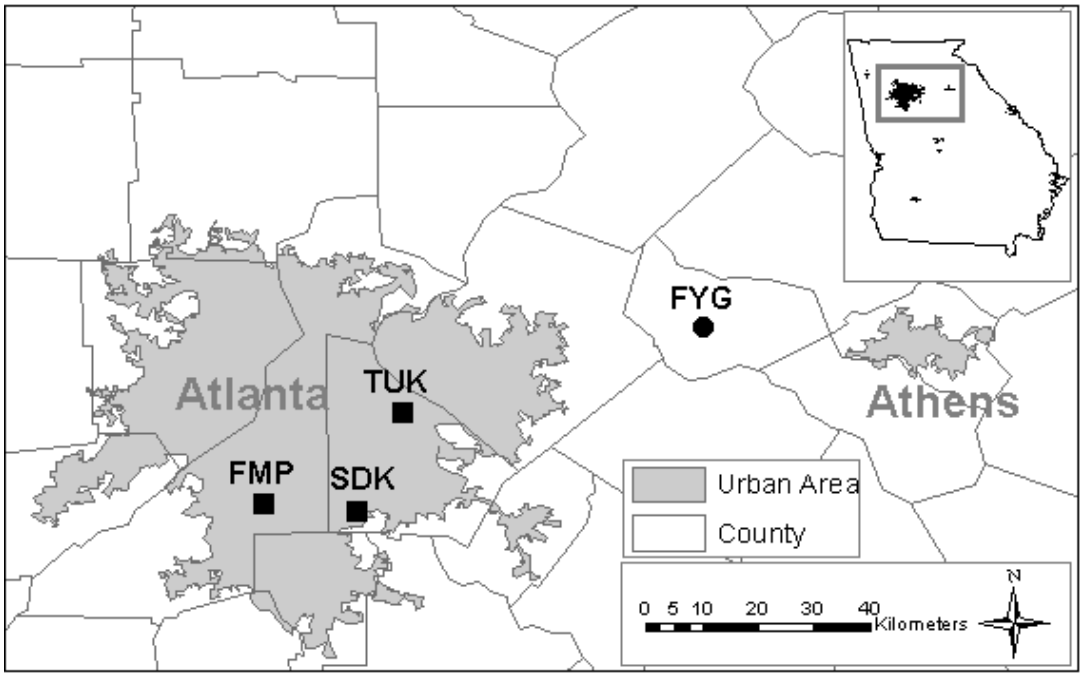

Figure 4.1. ASACA ambient monitoring sites.

Table 4.1. Mean, Median, 25th and 75th percentile for ambient concentrations (μg/m^3) of $PM_{2.5}$ mass, major ions, and OC/EC at four ASACA sites (2004-2005).

	Mean	Median	25, 75th percentiles	# of data	Mean	Median	25, 75th percentiles	# of data
			FMP				**SDK**	
$PM_{2.5}$	18.42	16.58	(12.08, 22.65)	601	19.01	16.54	(11.60, 24.34)	562
NH_4^+	1.61	1.37	(0.83, 2.06)	682	1.62	1.36	(0.93, 1.98)	691
NO_3^-	1.01	0.75	(0.48,1.20)	682	0.84	0.55	(0.39, 0.96)	691
SO_4^{2-}	4.57	3.58	(2.04, 5.79)	682	4.40	3.56	(2.26, 5.53)	691
OC	5.02	4.70	(3.12, 6.51)	690	5.05	4.55	(3.03, 6.43)	692
EC	0.51	0.42	(0.27, 0.66)	690	0.77	0.53	(0.30, 1.09)	692
			TUK				**FYG**	
$PM_{2.5}$	18.37	16.45	(11.96, 22.93)	559	-	-	-	-
NH_4^+	1.65	1.44	(0.94, 2.10)	623	1.54	1.35	(0.93, 1.93)	196
NO_3^-	1.04	0.69	(0.44, 1.36)	623	0.91	0.42	(0.24, 1.06)	196
SO_4^{2-}	4.25	3.38	(2.14, 5.32)	623	4.11	3.34	(2.24, 5.25)	196
OC	4.99	4.61	(3.14, 6.29)	628	4.49	4.18	(2.90, 5.81)	193
EC	0.48	0.40	(0.26, 0.61)	628	0.27	0.23	(0.13, 0.34)	193

4.2.2. Source apportionment

To investigate spatial representativeness of source apportionment results, we analyzed $PM_{2.5}$ data covering seven days in both winter (January, 2005) and summer (July, 2005) from three Atlanta sites (only three days for FYG site). Source apportionment was performed using CMB receptor model (Watson *et al.*, 2001) to identify and quantify primary and secondary source contributions at each site. Primary OC was estimated using EC tracer methods (Turpin *et al.*, 1991, 1995; Cabada *et al.*, 2002) as described in Lee *et al.* (2006) prior to the CMB source apportionment. Major primary sources included in the CMB analysis are motor vehicles (Schauer *et al.*, 1999; 2002), biomass burning (Fine *et al.*, 2002; Lee *et al.*, 2005), dust, coal combustion, oil combustion, and metal production. Source profiles of gasoline and diesel power vehicles are combined to generate a source profile for motor vehicles (Schauer *et al.*, 1999; 2002). Source profiles of 6 different southern wood burnings and prescribed burning were combined to create a biomass burning source profile. Dust source profile is from Cooper *et al.* (1981) and the source profiles of the other primary sources are obtained from

Shareef (1987). Theoretical profiles estimated from the molecular weight fraction of NH_4HSO_4, $(NH_4)_2SO_4$, NH_4NO_3 were included to address secondary origin particles.

4.3. Results

$PM_{2.5}$ is found to be to have a strong spatial correlation in Atlanta during the past two years (Figure 4.2). In general, similar trends are also observed in major $PM_{2.5}$ components among the four ASACA sites, except for EC (Figure 4.3). Secondary components produced from photochemical reactions in the atmosphere are found to have higher spatial correlations than primary components directly emitted from their sources. Although ambient OC contains both primary OC and secondary OC, a significant portion is secondary, especially in summer, leading to significant correlations. $PM_{2.5}$ between sites is also highly correlated since secondary components are the major fraction of $PM_{2.5}$. However, EC, a solely primary component, is spatially more poorly correlated. These are consistent with what have been found in a previous study (Wade *et al.*, 2006; Park *et al.*, 2006). Scatter plots also show that EC has the largest deviation from a 1:1 line. It suggests that primary EC impacts vary differently with the highest levels at SDK and lowest at FYG. Among the three Atlanta sites, the spatial correlations become stronger, even for primary EC (to higher than 0.5).

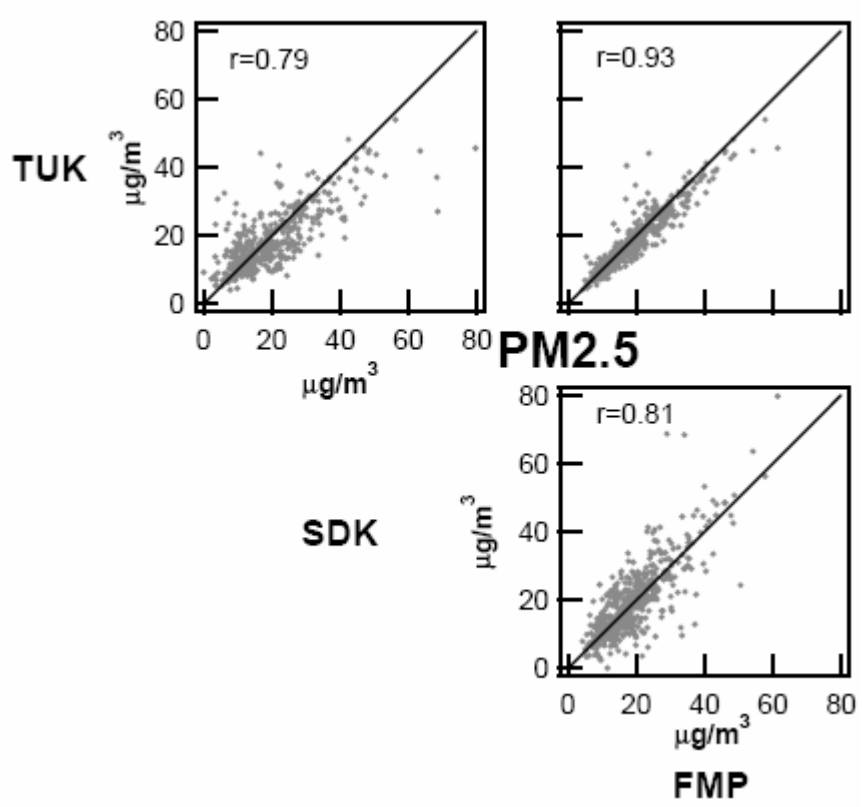

Figure 4.2. Spatial correlations of 24 hrs $PM_{2.5}$ ($\mu g/m^3$) in three Atlanta sites for two years (2004-05). The solid line is the 1:1 line.

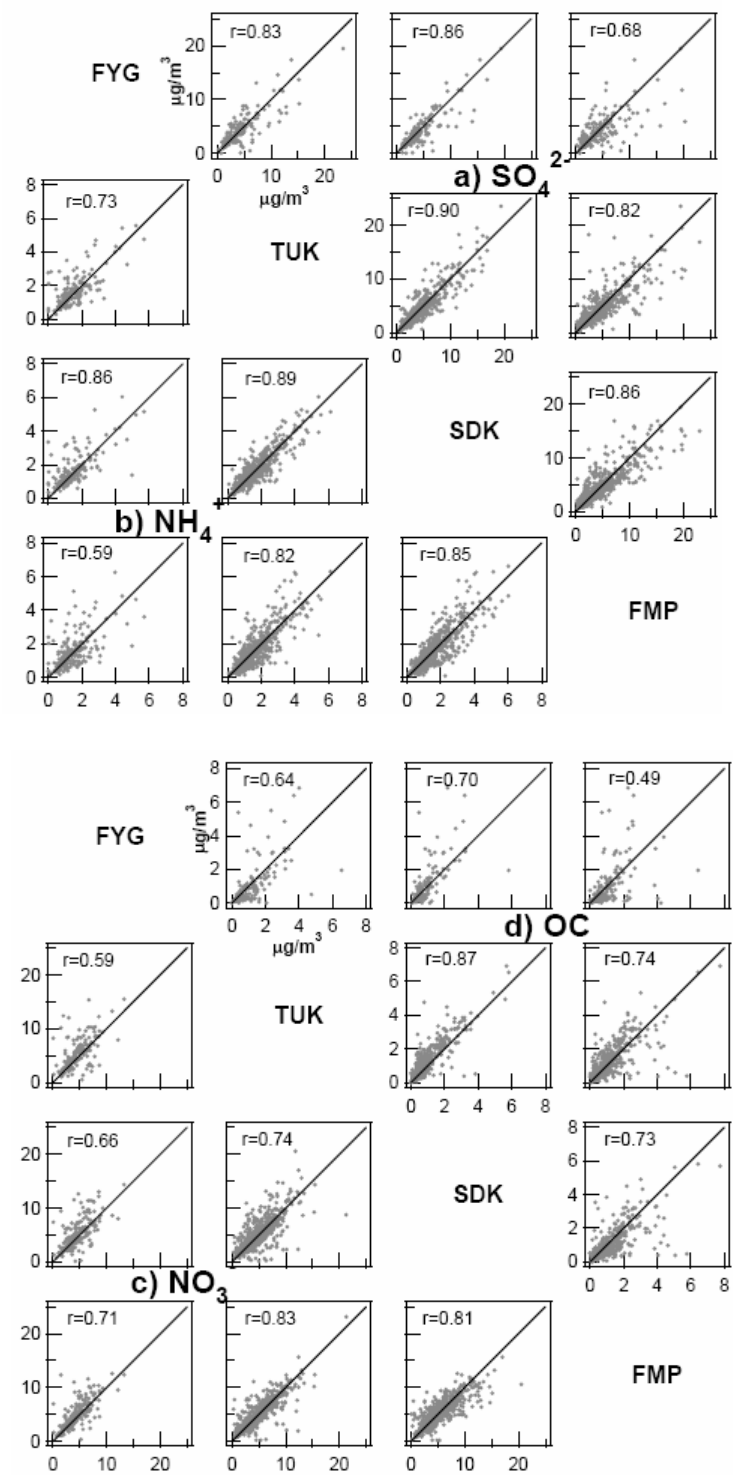

Figure 4.3. Spatial correlations of major $PM_{2.5}$ ($\mu g/m^3$) components. a) Sulfate, b) ammonium, c) nitrate, d)OC (2004-2005). The solid line is the 1:1 line.

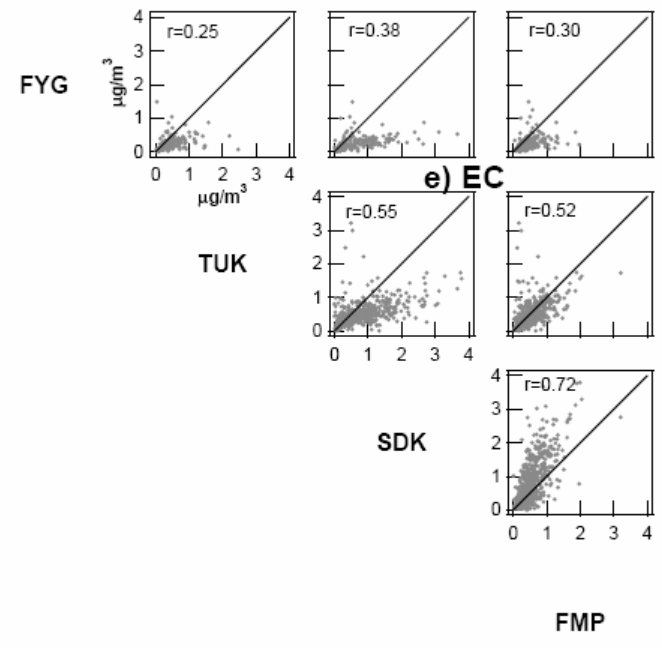

Figure 4.3. Spatial correlations of major $PM_{2.5}$ ($\mu g/m^3$) components (continued). e) EC (2004-2005). The solid line is the 1:1 line.

Source apportionment results for seven (three Atlanta sites) or three days (FYG) were averaged for both winter and summer (Figure 4.4). $PM_{2.5}$ mass was calculated by summing major components such as SO_4^{2-}, NO_3^-, NH_4^+, EC and organic matter. Organic matter mass was estimated by multiplying OC by a factor of 1.6 (Turpin and Lim, 2001). $PM_{2.5}$ mass is much higher in summer than in winter at all of the sites mainly because of increased secondary particulate matter production from photochemical reactions. There is a clear seasonal trend for secondary particles and primary sources, such as biomass burning and dust. Sulfate mass, especially NH_4HSO_4, is much higher in summer than winter, while NH_4NO_3 is higher in winter. Photochemical reactions during summer convert SO_2 to condensed-phase sulfate faster. Finding that the sulfate is only partially

neutralized by NH_3 suggests that $PM_{2.5}$ is more acidic during summer. Relatively higher NH_4NO_3 during the winter is due largely to its temperature dependence for gas/particle equilibrium and less sulfate being produced leading to more ammonia ($NH_{3(g)}$) being available to react with nitric acid ($HNO_{3(g)}$). Secondary OC (SOC) is relatively higher in the summer than in the winter, likely due to increased biogenic VOC emissions. Biomass burning shows more impacts in the winter than summer as suggested by higher potassium (K) levels during winter (Table 4.2). Dust PM is relatively higher during the summer, a drier period which leads to more resuspension. The seasonal trend of dust source impacts is also supported by relatively higher Al and Si concentrations during the summer (Table 4.2). Little seasonality was observed for the other primary sources. The results also show clearly that more motor vehicle impacts were observed at more populated Atlanta areas than at FYG. SDK has relatively higher motor vehicle impacts among the three Atlanta sites mainly due to heavy duty diesel trucks (HDDT). The HDDT is one of the main primary sources emitting EC. SDK is located near I-285 through which the HDDT detour around downtown Atlanta.

Table 4.2. Seasonal average concentrations ($\mu g/m^3$) of tracer species of dust and biomass burning for the periods of the case study.

species, $\mu g/m^3$	FMP		SDK		TUK		FYG	
	Winter	Summer	Winter	Summer	Winter	Summer	Winter	Summer
Al	0.0162	**0.0484**	0.0276	**0.0678**	0.0186	**0.0479**	0.0108	**0.0358**
Si	0.0309	**0.0604**	0.0227	**0.0985**	0.0234	**0.0350**	0.0073	**0.0506**
K	**0.0701**	0.0393	**0.0729**	0.0531	**0.0714**	0.0382	**0.0635**	0.0424

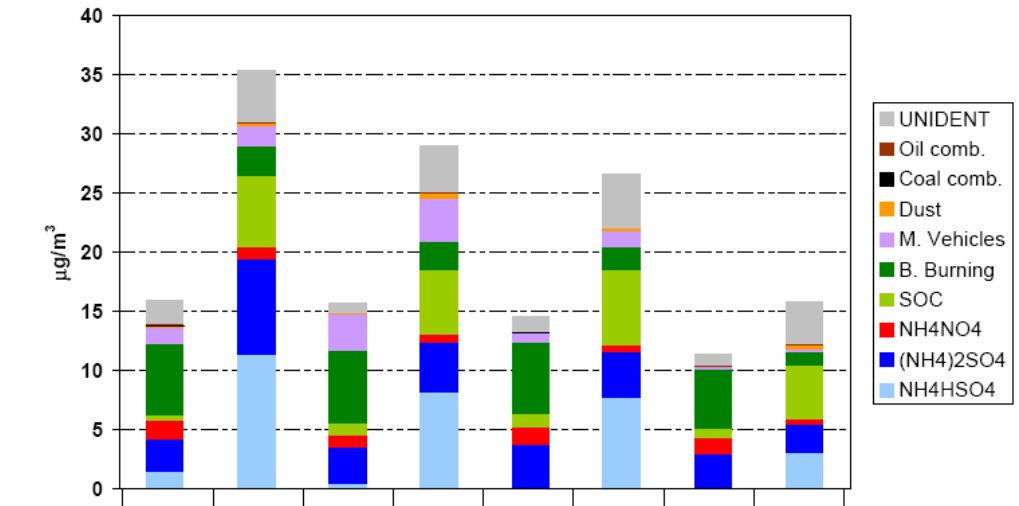

	FMP_W	FMP_S	SDK_W	SDK_S	TUK_W	TUK_S	FYG_W	FYG_S
NH4HSO4	1.54	11.43	0.53	8.18	0.12	7.82	0.00	3.10
(NH4)2SO4	2.66	8.06	2.99	4.26	3.74	3.77	2.97	2.35
NH4NO4	1.68	1.05	1.04	0.67	1.41	0.64	1.37	0.48
SOC	0.44	5.98	1.11	5.51	1.19	6.30	0.79	4.55
B. Burning	5.97	2.49	6.07	2.38	5.99	2.01	5.06	1.18
M. Vehicles	1.45	1.67	3.15	3.55	0.73	1.32	0.21	0.27
Dust	0.07	0.28	0.05	0.41	0.05	0.18	0.03	0.23
Coal comb.	0.06	0.05	0.03	0.08	0.10	0.05	0.01	0.06
Oil comb.	0.15	0.01	0.03	0.06	0.05	0.03	0.02	0.08
UNIDENT	1.90	4.37	0.76	3.87	1.15	4.51	1.00	3.50

Figure 4.4. Averaged source apportionment results for one week in both winter and summer 2005. (FMP: Fort McPherson, SDK: South Dekalb, TUK: Tucker, FYG: Fort Yargo, W: winter, S: summer).

Table 4.3. Correlations (R) of estimated source contributions

NH4HSO4 + (NH4)2SO4	FMP	TUK	SDK	FYG		**MOTOR**	FMP	TUK	SDK	FYG
FMP	1.00					FMP	1.00			
TUK	0.94	1.00				TUK	0.70	1.00		
SDK	0.98	0.95	1.00			SDK	0.83	0.72	1.00	
FYG	0.89	0.94	0.90	1.00		FYG	0.04	0.15	0.42	1.00
NH4NO3	FMP	TUK	SDK	FYG		**DUST**	FMP	TUK	SDK	FYG
FMP	1.00					FMP	1.00			
TUK	0.87	1.00				TUK	0.86	1.00		
SDK	0.70	0.76	1.00			SDK	0.92	0.88	1.00	
FYG	0.91	0.81	0.81	1.00		FYG	0.96	0.87	0.92	1.00
SOC	FMP	TUK	SDK	FYG		**COAL**	FMP	TUK	SDK	FYG
FMP	1.00					FMP	1.00			
TUK	0.98	1.00				TUK	0.48	1.00		
SDK	0.95	0.94	1.00			SDK	-0.04	0.09	1.00	
FYG	0.91	0.91	0.85	1.00		FYG	0.08	-0.43	0.54	1.00
BIOMASS	FMP	TUK	SDK	FYG		**OIL**	FMP	TUK	SDK	FYG
FMP	1.00					FMP	1.00			
TUK	0.95	1.00				TUK	0.21	1.00		
SDK	0.86	0.93	1.00			SDK	-0.09	0.51	1.00	
FYG	0.79	0.67	0.70	1.00		FYG	-0.39	0.38	0.63	1.00

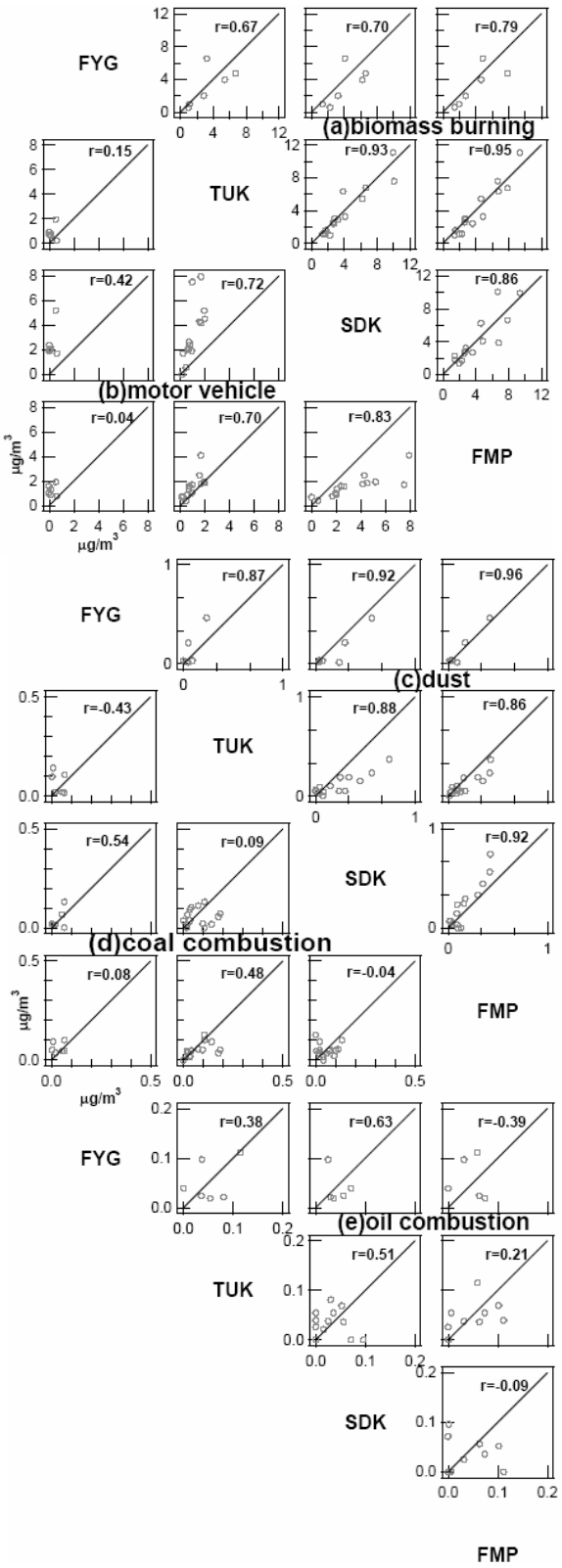

Figure 4.5. Spatial correlations of primary sources (mg/m3). (a) biomass burning, (b) motor vehicle, (c) dust, (d) coal combustion, (e) oil combustion. The solid line is the 1:1 line.

Spatial correlations between possible pair sites were estimated for each source based on source apportionment results (Figure 4.5 and Table 4.3). The results show strong spatial correlations for secondary particles produced from photochemical reactions during atmospheric transport and dispersion as is indicated by the significant correlations of secondary $PM_{2.5}$ components (Table 4.4). In general, primary source impacts directly from their emissions have weak spatial correlations except biomass burning and dust. Both biomass burning and dust impacts are correlated well, even for a non-urban site (FYG). This is also supported by significant correlations of K and Si, for biomass burning and dust, respectively (Table 4.4). Biomass burning includes wild fires, prescribed burning and residential/industrial wood burning. It looks like residential/industrial wood burning is more homogeneous in both urban and non-urban areas or distant burning activities (wild fires and prescribed burning) are the major activities of biomass burning as impacting all four sites similarly. Fugitive dust is highly affected by regional or local weather (*i.e.*, rain and wind speed). It is reasonable to assume that all four sites are influenced by a similar weather so that dust source impacts are more homogeneous. Motor vehicle impacts show moderate spatial correlations inside urban Atlanta area, but correlations with FYG are weak. This suggests that emission activities in Atlanta are similar inside the urban area, but very different from those around FYG. The other primary sources, coal combustion and oil combustion, are not well correlated even inside urban Atlanta, as indicated by poor correlations of Se and Ni, for coal and oil combustion, respectively (Table 4.4). This suggests that both sources have a very local nature of their impacts. Their source impacts likely depend on relative location of a receptor site to point sources and wind direction. However, in urban areas, emissions of

area and mobile sources are relatively more uniformly distributed than point sources leading to good spatial uniformities of their source impacts. This suggests that the degree of spatial representativeness of primary source impacts depends on how they are distributed and if the sources are local.

Table 4.4. Correlations of important species for source apportionment.

SO_4^{2-}	FMP	TUK	SDK	FYG		**OC**	FMP	TUK	SDK	FYG
FMP	1					FMP	1			
TUK	0.94	1				TUK	0.97	1		
SDK	0.99	0.96	1			SDK	0.89	0.93	1	
FYG	0.90	0.94	0.90	1		FYG	0.31	0.26	0.37	1
NH_4^+						**EC**				
FMP	1					FMP	1			
TUK	0.87	1				TUK	0.89	1		
SDK	0.93	0.92	1			SDK	0.79	0.85	1	
FYG	0.79	0.93	0.90	1		FYG	0.25	0.11	0.08	1
NO_3^-						**K**				
FMP	1					FMP	1			
TUK	0.87	1				TUK	0.96	1		
SDK	0.94	0.86	1			SDK	0.71	0.69	1	
FYG	0.91	0.80	0.91			FYG	0.94	0.96	0.41	1
Si						**Se**				
FMP	1					FMP	1			
TUK	0.77	1				TUK	0.05	1		
SDK	0.92	0.71	1			SDK	-0.05	0.69	1	
FYG	0.95	0.93	0.97	1		FYG	*	*	*	1
Ni										
FMP	1									
TUK	0.02	1								
SDK	-0.34	0.6	1							
FYG	0.03	-0.15	-0.38	1						

* below detection limit or blank level

4.4 Discussion

Epidemiologic studies have been performed to understand adverse health effects associated with PM components (Schwartz *et al.*, 1996; Mar *et al.*, 2000; Tolbert *et al.*, 2000; Metzger *et al.*, 2004; Peel *et al.*, 2005). A complementary method for the studies is associating adverse health effects with source apportionment results from receptor

models such as CMB. This provides information for developing effective PM control strategies as well. However, there are still limitations for applying source apportionment results at a single monitoring site to PM health studies. This study investigated one of the limitations, which is spatial representativeness of source apportionment results at a single monitoring site on an urban scale. Results show that each source has a different degree of spatial representativeness. Secondary particles are spatially very representative for urban Atlanta. However, primary sources have very different spatial representativeness from one source to another. Some primary sources, such as biomass burning, dust, and motor vehicle, are spatially relatively uniform in urban Atlanta, while the spatial representativeness of both coal and oil combustion source apportionment results is weak. Due to lack of spatial uniformity, associating both coal and oil combustion at one site with adverse health outcomes could give variable results depending on which results are used. For those poorly representative sources, using source apportionment results at more monitoring sites should be considered to reduce errors or uncertainties arising from assuming that results from one site are spatially representative.

CHAPTER 5

ESTIMATING UNCERTAINTIES AND UNCERTAINTY CONTRIBUTORS OF CMB PM2.5 SOURCE APPORTIONMENT RESULTS BY PROPAGATING UNCERTAINTIES

(Sangil Lee and Armistead G. Russell, *Environmental Science & Technology*, in preparation)

Abstract

The chemical mass balance (CMB) model was applied for source apportionment of $PM_{2.5}$ in Atlanta in order to explore levels and causes of uncertainties in source contributions. Monte Carlo analysis with Latin hypercube sampling (MC-LHS) was performed to estimate uncertainties and uncertainty contributors in CMB source apportionment results due to uncertainties in ambient measurement and source profile data. It was found that the most influential uncertainty contributors vary among the sources. The uncertainties in the source profile data contribute more to the final uncertainties in source apportionment results than by those in ambient measurement data. Mineral production source has the largest relative uncertainties, which is larger than twice of its source impacts. Uncertainty contribution estimations suggest that non-linear interactions and collinearities among source profiles also affect the final uncertainties although their influence is typically less than uncertainties in the source profiles.

5.1. Introduction

Particulate matter (PM) is a complex mixture of various chemical species from primary sources and secondary sources through photochemical formations in the atmosphere. The chemical mass balance (CMB) model (Watson *et al.*, 2001), which utilizes various chemical components of ambient and emission source PM, has been used to identify PM sources and quantify their contributions to ambient PM. Such information can thus be used to develop effective control strategies. Recently, results from receptor models have been being used to understand associations between PM sources and adverse health effects (Laden *et al.*, 2000; Mar *et al.*, 2000; Tsai *et al.*, 2000; Sarnat *et al.*, 2006). For both applications, it is thus important to identify, understand, and quantify uncertainties in model results.

CMB typically uses an effective variance (EV) solution approach to incorporate uncertainties from both ambient measurement and source profile data into its calculation (Watson *et al.*, 1984). In the EV solution approach, input variables with smaller uncertainty tend to have more influence on solutions and vice versa. Uncertainties in input variables are also incorporated into uncertainty estimates of source contributions. Previous studies have been conducted to evaluate CMB performance with respect to model assumptions, such as constant source emission profiles, uncorrelated source composition, and normally distributed errors for input data (Christensen and Gunst, 2004; Javitz *et al.*, 1988). Several different solution approaches along with the EV approach were applied for performance comparisons of different solution approaches in Christensen and Gunst (2004).

This study focuses on estimating CMB uncertainties due to uncertainties in input variables (*i.e.*, ambient measurement and source profile data), and linking uncertainties in input variables to uncertainties of source contributions. In this study, Monte Carlo analysis with Latin hypercube sampling (MC-LHS) was applied to quantify uncertainties in source contributions due to uncertainties from both ambient measurement and source profile data (Morgan and Henrion, 1990). Multiple linear regression was applied to the MC-LHS results to identify the important variables and quantify their contributions to the uncertainties (Morgan and Henrion, 1990).

5.2. Approach

5.2.1. Ambient measurement data

Ambient $PM_{2.5}$ (*i.e.*, particulate matter with an aerodynamic diameter less than 2.5 μm) measurement data used in this study is for Atlanta, GA. The ambient monitoring site, one from the U.S. Environmental Protection Agency's $PM_{2.5}$ Speciation Trend Network (U.S. EPA STN), is located in Dekalb County inside the Atlanta metropolitan area. 24-hr $PM_{2.5}$ filter samples were collected every 3 days and analyzed for ionic species, trace metals, and organic/elemental carbon. Data between January 2002 and November 2003 were used in this study (see Table B.1 for a summary). After removing the missing data, a total of 211 daily measurement data are included in this study.

In order to apply the CMB model using OC information, one must either add a secondary OC source, or, as done by Lee *et al.* (2006), estimate primary OC since measured OC comes from primary emissions and photochemical reactions. Simply adding a pure secondary OC source could lead to collinearity problems with OC

dominant sources. Primary OC were estimated by applying EC tracer methods and applied in the CMB source apportionment. Detailed information about the source apportionment approach is presented elsewhere (Lee *et al.*, 2006). For CMB source apportionment, a total of 11 source profiles were selected, which include ammonium bisulfate, ammonium sulfate, ammonium nitrate, biomass burning, motor vehicle, dust, coal combustion, paper and pulp production, oil combustion, mineral production, and metal production (Table B.2).

5.2.2 CMB model and uncertainty sources

The basic equation of the CMB model is a statement of species conservation (Watson *et al.*, 1984):

$$C_i = \sum_{i=1}^{n} f_{i,j} S_j, \quad i = 1,.....n, \tag{1}$$

where C_i is the ambient concentration of species i, f_i is the fraction of species i in source j, and S_j is the source contribution of source j. Equation (1) is solved for S_j by an effective variance weighted least square approach: minimizing χ^2, where

$$\chi^2 = \sum_{i=1}^{n} \left[\frac{\left(C_i - \sum_{j=1}^{m} f_{ij} S_j \right)^2}{\sigma_{C_i}^2 + \sum_{j=1}^{m} \sigma_{f_{ij}}^2 S_j^2} \right] \tag{2}$$

In the CMB model, uncertainties of the source contribution are estimated as:

$$\sigma_{s_j} = \left(\sum_{i=1}^{n} \frac{f_{ij}^2}{\sigma_{C_i}^2 + \sum_{j=1}^{m} \sigma_{f_{ij}}^2 S_j^2} \right)^{-1/2} \tag{3}$$

where σ_{s_j} (μg/m^3) is the uncertainty of source contribution S_j (μg/m^3) σ_{C_i} (μg/m^3) is the uncertainty on the ambient concentrations species *i*, and $\sigma_{f_{ij}}$ is the uncertainty in the fraction of species *i* in the source *j* profile. Uncertainties in input variables are propagated by inversely weighting the effective variance.

5.2.3. Uncertainty propagation and Regression analysis

Influences of uncertainties in input variables on uncertainties of source contributions was evaluated through MC-LHS simulations followed by multiple linear regression analysis. It is assumed that the uncertainties in input variables are log-normally distributed to sample non-negative values. For each CMB simulation, the values for each input variable were randomly paired with other values drawn from each input variable distribution by using Latin hypercube sampling (LHS). The LHS method is a stratified random sampling in which each input variable distribution is divided up into the number of samples with equally probable intervals (Morgan and Henrion, *1990*). This method produces a more uniform distribution covering a full range of each distribution for a limited number of samples. Uncertainties in input variables are characterized by probability distributions in the MC-LHS analysis. Uncertainties are propagated through the CMB model by multiple simulations with randomly drawn values from the probability distributions of input variables. For source profiles, the sampled values were normalized if the sum of the sampled values is larger than 1. In this study, 600 samplings were done for each input variable to perform 600 CMB simulations. Source profiles of secondary inorganic particles (*i.e.*, NH_4HSO_4, $(NH_4)_2SO_4$, NH_4NO_3) were kept constant since their source profiles are theoretical molecular weight ratios.

The main objective of this study is to identify important input variables in terms of their relative contribution to uncertainties in calculated source impacts. Multiple linear regression is applied to the MC-LHS results to estimate the importance of each input variable to the source contribution uncertainties:

$$S = \beta_0 + X\beta + \varepsilon \tag{4}$$

where S is an n-by-1 vector of the predicted source contributions from n simulations, β_0 is the regression intercept, X is a matrix n-by-p of p input variable values used in the n simulations, β is an p-by-1 vector of the regression coefficients of input X, ε is an n-by-1 vector of residual errors, n is the number of the simulation, and p is the number of the input variables.

Regression coefficients were determined by least squares fitting of the data. Residual errors were examined to check normality, and they were approximately normally distributed with residuals appearing randomly around zero. The variance of source contribution from simulations is approximately equal to the sum of the squares of the variance contribution from each input variable (Morgan and Henrion, 1990)

$$\sigma_s^2 \approx \sum_{i=1}^{p} \beta_i^2 \sigma_i^2 \tag{5}$$

where σ_s is the standard deviation of the source contribution from simulations and σ_i is the standard deviation of the input variable i. The β_i regression coefficients were standardized to be dimensionless, removing the dependence on input variable scales or units (Cullen and Frey, 1998; Morgan and Henrion, 1990).

$$SRC_i = \beta_i \times \frac{\sigma_i}{\sigma_s} \quad (6)$$

where SRC_i is the standardized regression coefficient of the input variable *i*. The standardized regression coefficients were used to estimate the uncertainty contributions of the input variables to the uncertainties in the source contributions.

$$UC_i(\%) = SRC_i^2 \times 100 \quad (7)$$

where UC_i is the percent contribution from the uncertainty in input variable *i* to the uncertainty in the source contribution. Uncertainty estimates from both nominal CMB (*i.e.*, calculated by the CMB model using equation 3) and MC-LHS will be compared as relative ratio of uncertainty to source contribution in scatter plots.

5.3. Results and Discussion

5.3.1 Comparison between CMB nominal and MC-LHS simulation

Six hundred MC-LHS simulations were performed for each day of total 211 measurement data. Means and standard deviations for source impacts from the 600 simulations were calculated to compare with those of the nominal CMB simulation. The mean source contributions from MC-LHS simulations were compared with those from the CMB nominal simulation (Figure 5.1). The mean source contributions are within ± 50% of the nominal contributions except for dust, coal combustion, and mineral production. In general, the mean source contributions taken from the MC-derived impacts of coal combustion are lower than the nominal contributions, while the mean source contributions of dust and mineral production are higher than the nominal contributions, especially for lower source impacts. Source contribution uncertainties typically are a factor of 2 less than the source contributions for NH_4HSO_4, $(NH_4)_2SO_4$, NH_4NO_3,

biomass burning, motor vehicle, and metal productions calculated using either approach (Figure 5.2). Other sources, which generally have smaller impacts, have uncertainties which are about equal to or larger than their source contributions using either approach. For pulp/paper production and coal combustion, uncertainties found using MC-LHS are larger than those from the nominal simulation. The MC-LHS results indicate that those two source contributions are essentially indifferent from zero, while both sources are "identifiable" in the CMB nominal simulation. For mineral production, uncertainties are larger than the source contributions in both the nominal and MC-LHS simulations, suggesting that the impact is seldom significantly different than zero.

5.3.2. Multiple regression analysis and uncertainty contribution

Uncertainty contributions of individual input variables were estimated by applying multiple linear regression to the MC-LHS simulation results. OC and OC_f represent OC in ambient measurement and source profile data, respectively. The subscript *f* indicates a fraction of species in source profiles. For both NH_4HSO_4 and $(NH_4)_2SO_4$, the only two major variables accounting for the final uncertainty are the uncertainties in the observed levels of NH_4^+ and SO_4^{2-} (Table 5.1). However, the most influential variable within each secondary source is different; for example, SO_4^{2-} is the most influential variable with for NH_4HSO_4, whereas NH_4^+ is for $(NH_4)_2SO_4$. NO_3^-, on the other hand, is the most important variable in NH_4NO_3, contributing almost all of the total uncertainty. $(NH_4)_2SO_4$ has negative SRCs to the acidic species (SO_4^{2-} and NO_3^-) but a positive SRC to NH_4^+ suggesting that more neutralization by NH_3 leads to more SO_4^{2-} in $(NH_4)_2SO_4$ rather than in NH_4HSO_4. Both OC and OC_f contribute about 64% to total

uncertainty in biomass burning source contribution, while both EC and EC_f (about 71%) are the most influential variables for motor vehicle source impacts. For dust, most (55%) of the total uncertainty is due to the uncertainties in the fractions of specific metals in the source profile (*i.e.*, Al_f, Ca_f and Si_f). 54% of the total uncertainty in pulp/paper production is contributed by both Na_f and K_f. For coal combustion, about 61% of the total uncertainty can be explained by the uncertainties in both Ca_f and Se_f. Both Ca_f and Al_f account for about 24% of the total uncertainty in mineral production impacts. Both Ni and Ni_f are the major uncertainty contributors (35%) for oil combustion, while Ca_f and Pb_f are the primary contributors (46%) for metal production. Ca_f is an important uncertainty contributor for several primary sources such as dust, coal combustion, mineral, and metal productions, but with different responses (*i.e.*, positive for dust and metal production; negative for coal combustion and mineral production). For primary sources, uncertainties in source profile data contribute more than those in ambient measurement data to total uncertainties. Although uncertainties in source profile data account for most of the total uncertainty, there are a few cases where ambient measurement data has a significant influence (*e.g.* biomass burning (OC), motor vehicle (EC), and oil combustion (Ni). However, the results of uncertainty contribution estimates show that the sum of fractions of the uncertainty explained by linear regression is significantly less than 100% for some sources. This suggests that non-linear interactions can be important, and that collinearity in source profiles is an issue. In particular, mineral production impacts are significantly affected. The two most influential variables of mineral production are Al_f and Ca_f, but both are also important variables for dust and coal combustion. In addition, there is no unique variable significantly affecting the uncertainty

of mineral production. Source profile similarities with other sources contribute significant amounts of uncertainty for collinear sources, especially for mineral production.

Uncertainties in CMB source contributions were estimated by treating uncertainties in both ambient and source profile data under a probabilistic framework instead of the EV solution approach. Uncertainties in both input data were propagated through CMB model by applying MC-LHS analysis. Multiple linear regression analysis applied to the MC-LHS results was able to provide estimates of how much uncertainty is contributed by individual input variables. The results illustrate that the uncertainties in source profile data have a more significant influence to total uncertainties of source contributions. It suggests that uncertainties in the estimates of source contributions can be reduced largely by decreasing those in source profile data. Accurate CMB source apportionment depends on how well source profiles used in CMB represent sources impacting a particular receptor site. The source profile data used in this study, especially industrial emission sources, were generated from emission source tests in the 1980s and not in the southeast. These source profiles may not be representative for current primary sources in the southeast. Thus, more emission characterization studies of major primary sources in the southeast are necessary to better estimate source impacts and also to reduce source apportionment uncertainties. Uncertainties in source profile data can be reduced by applying more sensitive analytical methods such as inductively coupled plasma mass spectrometry (ICP-MS). Very sensitive methods may also be able to detect chemical species in low abundance which were not measured in the past, but are unique to specific sources. This can reduce source collinearity and would lead to reduction of the total uncertainty. Incorporating source-indicative gas to particle ratios into the CMB model

(Marmur *et al.*, 2005) can also help differentiate between similar sources rather than only using $PM_{2.5}$ chemical speciation, again reducing the influence of source collinearity on results and uncertainties.

This study shows how uncertainties of input data, especially source profile data, significantly affect CMB source apportionment results and uncertainties. High uncertainties in source profile data result source impacts estimated by the CMB model in being not significantly different from zero. Uncertainty estimates identified significant uncertainty contributors to identify key data needed to provide more accurate source apportionment. In particular, source profile data has to be updated for representative emission sources in specific regions, *e.g.*, by conducting more source emission tests.

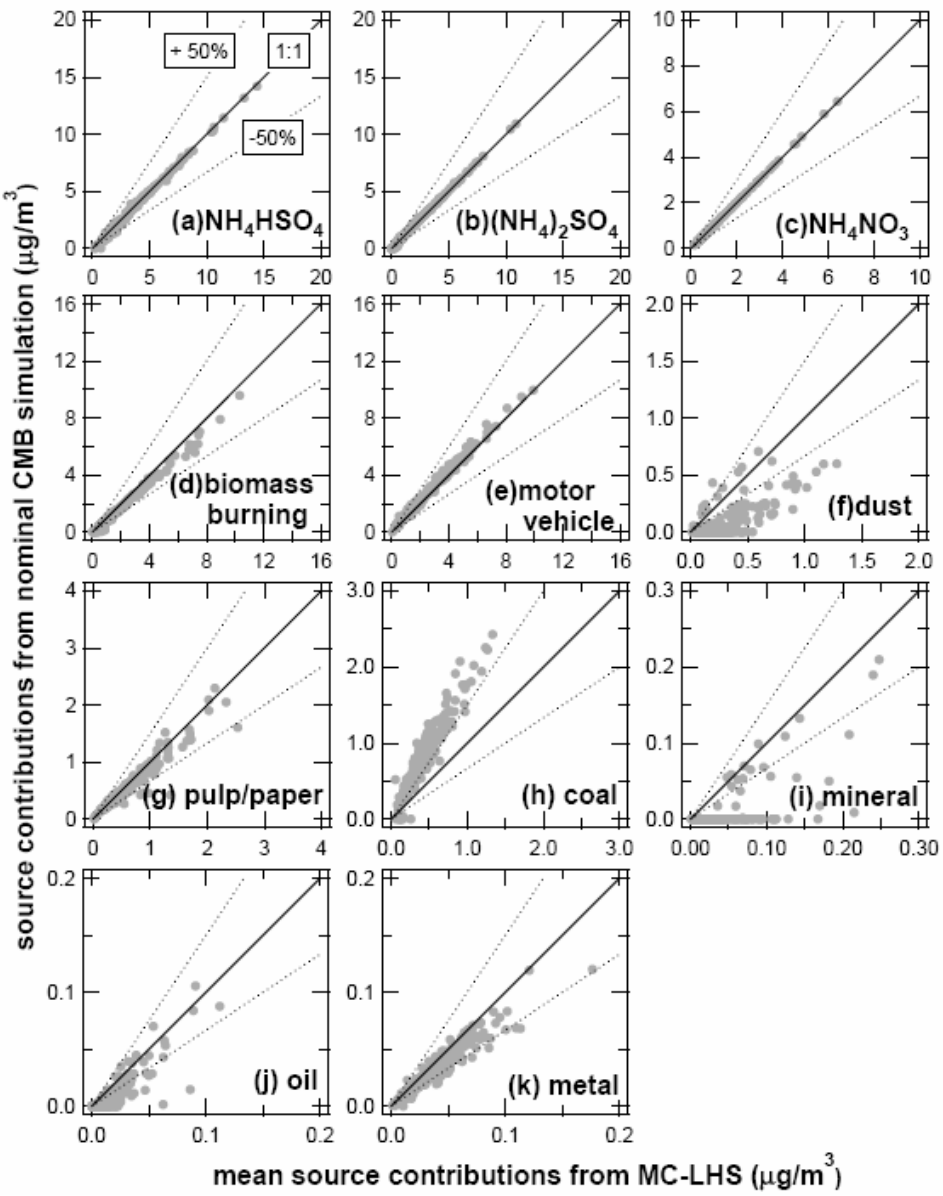

Figure 5.1. Mean source contributions from MC-LHS simulations (x, μg/m^3) compared with source contributions from nominal CMB simulations (y, μg/m^3). (a) NH_4HSO_4, (b) $(NH_4)_2SO_4$, (c) NH_4NO_3, (d) biomass burning, (e) motor vehicle, (f) dust, (g) pulp/paper production, (h) coal combustion, (i) mineral production, (j) oil combustion, (k) metal production. The solid (–) line is the 1:1 line, bracketed by the two dashed (···) 1:2, 2:1 lines.

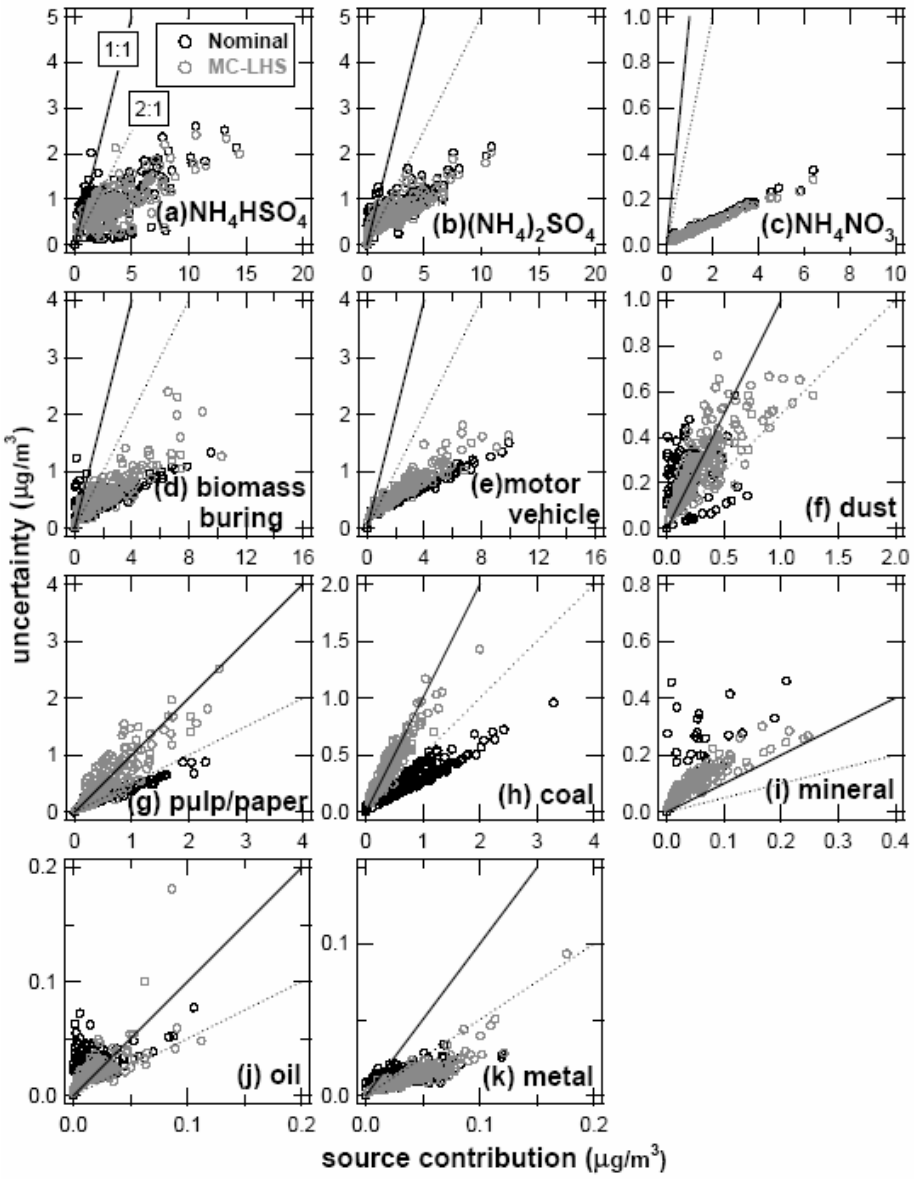

Figure 5.2. Source contribution (x, μg/m^3) vs. uncertainty (y, μg/m^3). (a) NH_4HSO_4, (b) $(NH_4)_2SO_4$, (c) NH_4NO_3, (d) biomass burning, (e) motor vehicle, (f) dust, (g) pulp/paper production, (h) coal combustion, (i) mineral production, (j) oil combustion, (k) metal production. The solid (–) line is the 1:1 line, and the dashed (···) line is 2:1 (the source impact ("signal") is twice the uncertainty (noise)).

Table 5.1. Averaged standardized regression coefficients and uncertainty contributions of input variables contributing the most uncertainty.
(* subscript $_f$ means variables from source profiles)

variable*	UC (%) mean	UC (%) STD	SRC mean	SRC STD
NH_4HSO_4 ($R^2 = 0.68 \pm 0.20$)				
SO_4^{2-}	43.21	18.46	0.64	0.15
NH_4^+	29.66	11.89	-0.51	0.20
NO_3^-	2.09	3.56	0.10	0.10
Sum	**76.18**	**23.82**		
$(NH_4)_2SO_4$ ($R^2 = 0.80 \pm 0.15$)				
NH_4^+	64.11	13.52	0.80	0.09
SO_4^{2-}	22.00	9.98	-0.45	0.12
NO_3^-	3.97	5.83	-0.16	0.12
Sum	**90.76**	**17.44**		
NH_4NO_3 ($R^2 = 0.89 \pm 0.09$)				
NO_3^-	102.30	11.15	1.01	0.06
Sum	**102.94**	**10.69**		
biomass burning ($R^2 = 0.60 \pm 0.10$)				
OC_f	37.41	10.80	-0.60	0.09
OC	26.16	8.70	0.50	0.09
EC	7.85	3.62	-0.27	0.06
EC_f	3.11	1.75	0.17	0.06
Zn_f	1.96	1.30	0.13	0.05
Na_f	0.95	1.07	-0.08	0.05
K_f	0.81	0.77	-0.05	0.07
Sum	**78.26**	**14.14**		
motor vehicle ($R^2 = 0.82 \pm 0.05$)				
EC	49.58	14.33	0.70	0.10
EC_f	21.12	9.38	-0.45	0.11
P_f	10.60	6.60	-0.30	0.13
Cd_f	7.24	5.11	-0.24	0.12
Zn_f	4.91	3.09	-0.21	0.06
OC_f	3.55	1.91	0.18	0.06
OC	1.48	0.60	-0.12	0.03
Zn_f	0.71	0.95	0.07	0.05
Sum	**99.72**	**10.32**		
dust ($R^2 = 0.58 \pm 0.07$)				
Al_f	20.31	9.35	-0.44	0.10
Ca_f	19.32	8.24	0.42	0.12
Si_f	15.61	6.86	-0.38	0.09
Se_f	7.92	4.86	0.27	0.09
Fe_f	2.13	1.21	-0.14	0.05
Cr_f	1.82	2.35	-0.12	0.07
P_f	1.49	1.13	0.10	0.06
Cr	0.99	1.22	0.08	0.06
Sum	**72.57**	**10.16**		
pulp/paper production ($R^2 = 0.52 \pm 0.15$)				
Na_f	41.34	19.24	-0.63	0.15
K_f	12.99	11.12	-0.31	0.18
P_f	8.42	6.76	-0.26	0.13
Na	5.76	10.16	0.19	0.14
K	0.86	1.19	0.07	0.06
Sum	**69.35**	**25.16**		

Sum is the averaged sum of fractions of the total uncertainty explained by linear regression, and includes all contributors

variable*	UC (%) mean	UC (%) STD	SRC mean	SRC STD
coal combustion ($R^2 = 0.60 \pm 0.04$)				
Ca_f	48.53	11.65	-0.69	0.08
Se_f	12.84	5.72	-0.35	0.09
P_f	10.33	5.99	-0.30	0.12
Al_f	4.23	4.87	-0.17	0.12
OC_f	2.97	3.08	-0.15	0.08
Mn_f	2.86	2.10	-0.16	0.06
EC	0.96	0.81	0.08	0.05
Mg	0.82	0.71	0.08	0.04
Sum	**84.73**	**10.41**		
mineral production ($R^2 = 0.43 \pm 0.11$)				
Al_f	12.29	7.94	0.33	0.12
Ca_f	11.96	7.76	-0.33	0.11
Na_f	3.98	4.40	0.16	0.12
Pb_f	2.76	2.30	-0.15	0.07
Si_f	2.29	2.53	-0.13	0.07
P_f	2.14	2.15	0.13	0.07
Cd_f	2.00	1.34	-0.13	0.05
As_f	1.80	1.33	0.12	0.06
Co_f	1.76	2.06	-0.11	0.08
Cr_f	0.74	0.66	-0.08	0.04
Sum	**43.25**	**12.07**		
oil combustion ($R^2 = 0.65 \pm 0.11$)				
Ni	25.65	15.22	0.48	25.65
Ni_f	9.76	8.52	-0.28	9.76
Pb_f	6.22	5.07	-0.23	6.22
Al_f	5.68	5.09	0.21	5.68
P_f	3.69	3.56	-0.17	3.69
Cu_f	2.97	2.77	0.15	2.97
Ca_f	2.56	2.62	0.13	2.56
V	2.37	3.75	0.12	2.37
Si_f	2.32	3.17	0.12	2.32
Fe_f	2.29	1.92	-0.14	2.29
Pb	1.77	1.41	0.12	1.77
Mn_f	1.67	1.21	0.12	1.67
Pb	1.63	1.89	0.11	1.63
V_f	1.35	2.29	-0.09	1.35
Zn_f	1.24	2.20	-0.07	1.24
Cu	1.16	0.59	-0.10	1.16
Sum	**75.06**	**13.80**		
metal production (R^2=0.81±0.05)				
Pb_f	23.51	12.11	-0.47	0.12
Ca_f	22.58	14.29	0.44	0.19
Zn_f	9.12	4.59	-0.29	0.07
Cu_f	6.78	5.00	-0.22	0.14
Pb	5.90	5.72	0.22	0.10
As_f	4.83	5.67	-0.19	0.12
As	4.24	4.36	0.19	0.09
Cu	3.71	2.63	0.18	0.07
Zn	3.23	1.78	0.17	0.05
Fe_f	2.96	3.04	-0.14	0.09
Al_f	2.42	2.49	0.13	0.08
Ni	0.80	1.30	-0.07	0.06
Sum	**91.94**	**7.46**		

CHAPTER 6

CONCLUSIONS AND FUTURE RESEARCH

$PM_{2.5}$ affects the environment in different ways. Adverse human health effects and visibility impairment associated with $PM_{2.5}$ are main driving forces for both scientific researches and regulations. As March, 2006, more than 200 counties are designated as non-attainment areas in terms of $PM_{2.5}$ and 47 counties in the Southeast. State agencies with $PM_{2.5}$ non-attainment counties must develop their own plans that demonstrate how they will achieve attainment status. State agencies also have to address emission sources of visibility impairment and develop strategies to improve visibility. It is essential to understand of $PM_{2.5}$ and sources in order to develop effective control strategies of $PM_{2.5}$. Air quality impacts of primary $PM_{2.5}$ emission sources can be estimated by source apportionment techniques such as source-oriented and receptor-oriented models.

This thesis describes fundamental and applied studies related with receptor-oriented models for better understanding of $PM_{2.5}$ and sources in the southeastern U.S. Although source apportionment studies have been conducted to understand air quality impacts of $PM_{2.5}$ emission sources in the Southeast, little information is available regarding to regional perspective of $PM_{2.5}$ source impacts in the region. A regional source apportionment study (Chapter 3) using CMB receptor model shows that secondary origin particles are major components of ambient $PM_{2.5}$ in the Southeast. Motor vehicles and biomass burning (*i.e.*, wild fires, prescribed burning, and residential wood burning *etc*) are main primary emission sources apportioned to ambient $PM_{2.5}$ in the region and followed by dust and other combustion sources. It was also found that secondary particles

were distributed more regionally, while primary source impacts were distributed more locally. This suggests that regional efforts have to be applied effective to reduce secondary origin particles, while more localized efforts have to be applied to reduce impacts of primary emission sources.

The source apportionment results from Chapter 3 can be used for PM health studies to understand associations between sources and adverse health effects and for policy analysis and decision making to develop implementation plans of $PM_{2.5}$. It is necessary to understand uncertainties in the source apportionment results since they can play a significant role in PM health studies and policy decision making. Knowledge of uncertainties can help policy makers prioritize which $PM_{2.5}$ source should be further studied and controlled. An uncertainty estimating study (Chapter 5) suggests that measurement errors in source profile data contribute more to uncertainties in estimates source contributions than those in ambient measurement data.

The CMB receptor model utilizes ambient measurement and source profile data to estimate air quality impacts of emission sources to ambient $PM_{2.5}$ concentrations. Previous studies (Christensen and Gunst, 2004; Watson et al., 1984) and Chapter 5 in this thesis show that source contributions and uncertainties estimated by the CMB receptor model are largely influenced by source profiles and their uncertainties. Therefore, it is important to use more accurate and representative source profiles of primary emission sources at a specific region in the CMB receptor model in order to obtain more accurate air quality impacts of primary emission sources. Results in the Chapter 3 indicate that biomass burning including prescribed burning is an important emission source of $PM_{2.5}$ in the Southeast. However, there is little emission characterization data of actual prescribed

burning. Particulate emissions from actual prescribed burning in two Georgian forest areas were characterized to develop a real-world prescribed burning source profile. It was found that particulate emissions from actual prescribed burning are organic matter dominant emissions showing OC (60% of $PM_{2.5}$ mass) and followed by EC (4%) and K (0.57%). The application of a combined source profile (residential wood burning and prescribed burning) in the CMB receptor model indicates that biomass burning source impacts are estimated 21% less but relatively higher uncertainties than just using residential wood burning. More detailed organic compound speciation shows that cholesterol, an important fingerprint of meat cooking source, was found in emissions from actual prescribed burning, suggesting combustion of soil organisms or animal litter during the understory prescribed burning. Cholesterol has been used as a main tracer of meat cooking in the CMB receptor model by using molecular markers. However, a previous study has suggested that there may be other sources emitting cholesterol due to highly overestimated meat cooking (Sheesley *et al.*, 2004). It is suggested that prescribed burning can be an important cholesterol source where are impacted by emissions from prescribed burning.

This thesis describes regional perspective of $PM_{2.5}$ source impacts in the Southeast by using the CMB receptor model and addresses related issues such as uncertainties of the estimated source contributions and emission characteristics (i.e., source profiles). The following are detailed conclusions of each chapter and recommendations for future research.

Gaseous and particulate emissions from prescribed burning in Georgia

Direct measurements of gaseous and particulate emissions at prescribed burning sites in Georgia provide detailed chemical characteristics of $PM_{2.5}$ and VOC from active prescribed burning. The measurements allowed the determination of emission factors for the flaming and smoldering stages of prescribed burns. VOC emission factors from smoldering were distinctly higher than those from flaming except for ethene, ethyne, and organic nitrate compounds. Important precursors of secondary organic aerosol, such as aromatic compounds and terpenes, are much higher from active prescribed burning than from fireplace wood and laboratory open burning studies. Although levoglucosan is found as the major particulate organic compound emitted from prescribed burning as in previous biomass burning studies, cholesterol, an important fingerprint for meat cooking, was observed in this study of active prescribed burning. This indicates that there is a significant release of cholesterol from the soil and organisms during active open burning. A CMB source apportionment using a newly developed prescribed burning source profile shows increased prescribed burning impacts during and immediately after burns. A CMB sensitivity test using previous different prescribed burning source profiles indicates that prescribed burning impacts are on average 27%, lower when the source profile from our *in situ* study is used.

Source apportionment of $PM_{2.5}$ in the southeastern U.S.

$PM_{2.5}$ chemical composition data from the U.S. EPA STN program provides an opportunity to address $PM_{2.5}$ source impacts in the southeast from a regional prespective. Secondary particles, such as NH_4HSO_4, $(NH_4)_2SO_4$, NH_4NO_3, and SOC, formed by

atmospheric photochemical reactions contribute to the majority (>50%) of ambient $PM_{2.5}$ with strong seasonality. Source apportionment results indicate that motor vehicle and biomass burning are the two main primary sources in the southeast showing more motor vehicle source impacts in populated urban areas and more biomass burning source impacts in less urbanized areas. Spatial distributions of primary source impacts show that each primary source has distinctively different spatial source impacts. Results also find emission impacts from ship activities along the coast. Spatiotemporal correlations indicate that secondary particles are more regionally distributed, and primary source impacts are more local. In order to reduce primary source impacts, the results imply that targeted control strategies should be developed for specific regions based on the sources identified and the relative costs of emission reductions.

Source apportionment of $PM_{2.5}$ in Atlanta: a case study for spatial representativeness at an urban scale

Source apportionment results from receptor models, such as CMB, can be used for epidemiologic studies by associating source impacts with adverse health effects. However, the spatial representativeness of the source apportionment results at a single monitoring site needs to be investigated to better assess their application in PM health studies since health outcome data often are taken over an entire city or metropolitan area. Source apportionment results from four Atlanta monitoring sites indicate that secondary particles have good spatial representativeness for Atlanta, while the degree of spatial representativeness of primary sources varies. Biomass burning, dust, and motor vehicle source impacts were found to be spatially relatively uniform, whereas both coal and oil

combustion sources are not. When source apportionment results of both coal and oil combustion at a single monitoring site are used for PM health studies, they may introduce errors or uncertainties in results.

Estimating uncertainties and uncertainty contributors of CMB PM2.5 source apportionment results.

Uncertainties in CMB source apportionment results can be used in PM health studies, policy analysis and decision making. Monte Carlo analysis with Latin hypercube sampling (MC-LHS) was performed for a better understanding of uncertainties in source apportionment results by propagating uncertainties in ambient measurement and source profile data in a probabilistic framework. It was found that the most influential uncertainty contributors vary among the sources. Uncertainties in source profile data contribute more to the final uncertainties in source apportionment results than from those in ambient measurement data. Mineral production source has the largest relative uncertainties, which is larger than twice its source impacts. The results from this study suggest that non-linear interactions and collinearities among source profiles also affect the final uncertainties although their influence is typically less than uncertainties in source profile data.

Future Research

Emission characterization of active prescribed burnings was investigated in Chapter 2. Although the study provided useful information for better understanding of air quality impacts of prescribed burning, more research is still needed to be done in order to

get more representative emission data for the southeastern U.S. There are several different forest types in the southeast, which includes loblolly pine forests investigated in Chapter 1. Each forest type occupied by different tree species has not only different fuels but also very different fuel loadings for prescribed burning (Ottmar, 2001). There has been improvement in fuel loading estimations and classifications (Ottmar and Vihnanek, 2001; Sandberg *et al.*, 2001). Thus, more emission characteristic data for different forest types combined with better fuel information can provide more insight about air quality impacts of prescribed burning in the southeast and elsewhere.

CMB receptor modeling was applied for source apportionment of $PM_{2.5}$ in the southeastern U.S. This study provides regional spatial distributions of $PM_{2.5}$ source impacts. However, there are incongruities in spatial distributions of some primary source impacts when they are compared to those of the national emission inventory. It is needed to address why there are discrepancies between both data. Since CMB modeling can not directly link source impacts to emission sources, potential source contribution function (PSCF) analysis (Hopke *et al.*, 1995) can be performed to find possible source areas based on CMB source apportionment results. Comparing the results with the emission inventory data may help identify the reasons of the incongruities in order to compromise both emission inventory and source apportionment data.

Source apportionment results can be used for PM epidemiologic studies which attempt to associate PM sources with adverse health outcomes. However, there are uncertainty issues of source apportionment results that need to be addressed before their further application. One uncertainty issue is representativeness of source apportionment results at a single monitoring site for an entire city when the source apportionment results

are incorporated with aggregated health outcomes for an entire city. The other issue is uncertainty of source apportionment results due to measurement errors in ambient measurement and source profile data. Chapter 4 investigated the representativeness of source apportionment results for Atlanta. Although it gives insights about which calculated source impacts are more spatially representative, this analysis should be extended so that more concrete conclusions may be developed.

In Chapter 5, Monte Carlo analysis was applied to investigate uncertainties of source apportionment results by propagating the measurement errors in the model. The results indicate that measurement errors in source profile data contribute more to the total uncertainties of source apportionment results rather than those in ambient measurement data in general. Therefore, more accurate source profile data are of primary importance to reduce source apportionment uncertainties. Sensitive analytic methods such as inductively coupled plasma mass spectrometry (ICP-MS) can be used to create more accurate source profile and ambient measurement data. Accurate CMB source apportionment also depends on how well source profiles used in CMB represent sources impacting a particular receptor site. There are several recent emission characterization studies of biomass burnings in the southeastern U.S. (Fine *et al.*, 2002; Hays *et al.*, 2002; Lee *et al.*, 2005). However, there is a lack of emission information for point sources such as industrial facilities in the southeastern U.S. Thus, having representative emission source profiles of industrial emission sources in the southeast can decrease uncertainties in CMB source apportionment. Practically, it may not be possible to get updated emission source profiles for all emission sources in the near future. A possible alternative way to get around this problem may be to use ICFA (Christensen *et al.*, 2006) or CMB-LGO

(Marmur *et al.*, 2005). ICFA treats source profiles differently by applying different degrees of constraints depending on their credibility. It puts loosened constrains onto less accurate source profiles, such as industrial source profiles, and *vice versa*. CMB-LGO incorporates source indicative gas-to- particle ratios as model constraints to optimize source profiles. Distinctly different ratios among emission sources reduce collinearities among source profiles to improve the performance of the traditional CMB model.

This thesis examines the emission characterization of prescribed burning and air quality impacts of $PM_{2.5}$ emission sources in the southeast U.S, and addresses uncertainty issues in CMB source apportionment results due to spatial representativeness and measurement uncertainties. More emission characterization studies of prescribed burning should be done for different forest types in Georgia in order to obtain better representative emission characteristics. Spatial variability of source impacts needs to be conducted with enough data sets for better application for further health studies. It is desired to update emission characteristics of primary emission sources not only to improve accuracy of source apportionment by reducing uncertainties in source profiles, but also to provide better emission data for air quality models.

APPENDIX A

Table A.1. Average and standard deviation (STD) of normalized POC emissions from prescribed burning in mg per g OC.

	AVERAGE	STD
Alkanes		
Tetracosane	0.1388	0.0705
Pentacosane	0.2501	0.1276
Hexacosane	0.2282	0.1250
Heptacosane	0.2499	0.1639
Octacosane	0.1155	0.0538
Nonacosane	0.8068	0.3847
iso-nonacosane	DL	DL
anteiso-triacontane	DL	DL
Triacontane	0.1939	0.0937
Hentriacontane	0.2884	0.1375
Dotriacontane	DL	DL
Tritriacontane	0.0900	0.0723
Tetratriacontane	DL	DL
Pentatriacontane	DL	DL
Hexatriacontane	DL	DL
Tetratetracontane	DL	DL
iso-hentriacontane	DL	DL
anteiso-dotriacontane	DL	DL
iso-tritriacontane	DL	DL
Alkenoic Acids		
9-hexadecenoic acid	0.5076	0.3254
9-octadecenoic acid (oleic acid)	2.4382	1.1394
9,12-octadecadienoic acid	2.2530	1.2726
Alkanoic Acid		
tetradecanoic acid	2.0066	0.9764
pentadecanoic Acid	0.6372	0.3281
hexadecanoic acid	6.7301	2.9428
heptadecanoic acid	0.2481	0.1184
octadecanoic acid	2.2421	1.0502
nonadecanoic acid	0.4882	0.2505
eicosanoic acid	1.1948	0.5701
heneicosanoic acid	0.2886	0.1278
docosanoic acid	1.7855	0.8199
tricosanoic acid	0.6541	0.2863
tetracosanoic acid	4.9520	2.2088
pentacosanoic acid	0.3832	0.1679
hexacosanoic acid	3.6715	1.6200
heptacosanoic acid	0.1411	0.0652
octacosanoic acid	0.9882	0.4472
nonacosanoic acid	0.1684	0.0868
triacontanoic acid	0.8029	0.4244
pinonic acid	DL	DL
Alkanedioic Acids		
butanedioic acid	0.3964	0.2064
pentanedioic acid	0.0813	0.0429
hexanedioic acid	0.0265	0.0196
heptanedioic acid	0.0300	0.0240
octanedioic acid	0.0595	0.0409
nonanedioic acid	0.2586	0.1358
decanedioic acid	0.0679	0.0416

Table A.1. Continued

	AVERAGE	STD
PAHs		
Fluoranthene	0.0895	0.0390
Acephenanthrylene	0.0280	0.0140
Pyrene	0.1068	0.0450
benz[a]anthracene	0.0800	0.0329
chrysene/triphenylene	0.0978	0.0411
Coronene	0.0074	0.0044
benzo [b]fluoranthene	0.0505	0.0210
benzo[k]fluoranthene	0.0407	0.0167
benzo[j]fluroanthene	0.0128	0.0067
benzo[a]pyrene	0.0298	0.0124
benzo[e]pyrene	0.0499	0.0208
Perylene	0.0039	0.0022
indeno[c,d]pyrene	0.0737	0.0342
dibenz[a,h]anthracene	0.0017	0.0013
benzo[ghi]perylene	0.0358	0.0149
cyclopenta[c,d]pyrene	0.2888	0.1381
1-methylchrysene	0.0279	0.0159
benzo[ghi]fluoranthene	0.0972	0.0778
Retene	0.3490	0.1645
9,10 anthraquinone	DL	DL
1h-phenalen-1-one	DL	DL
9-fluorenone	DL	DL
benz[a]anthracene-7,12-dione	DL	DL
benz[d,e]anthracene-7-one	DL	DL
1,8-naphthalic anhydride	DL	DL
Phthalates		
bis[2-ethylhexyl]phthalate	0.0895	0.0390
butyl benzyl phthalate	DL	DL
diethyl phthalate	0.0355	0.0322
dimethyl phthalate	0.0142	0.0095
dibutyl phthalate	0.1031	0.0671
dioctyl phthalate	DL	DL
Aromatic Carboxylic Acids		
1,2-benzenedicarboxylic acid	0.0147	0.0088
1,3-benzenedicarboxylic acid	DL	DL
1,4-benzenedicarboxylic acid	0.0090	0.0071
1,2,4-benzenetricarboxylic acid	DL	DL
1,3,5 or 1,2,3 benzenetricarboxylic acid	DL	DL
1,2,4,5-benzenetetracarboxylic acid	DL	DL
1,2,3,5 or 1,2,3,4 benzenetetracarboxylic acid	DL	DL
4-methyl-1,2-benzenedicarboxylic acid	DL	DL
Resin Acids		
dehydroabietic acid	33.3164	14.3022
isopimaric acid	2.9594	1.2311
pimaric acid	2.4659	1.0099
Others		
Levoglucoscan	94.7506	40.2568
Cholesterol	0.8071	0.3511
Stigmasterol	1.0115	0.4408
Squalene	2.6824	1.2024

* DL: below detection limit
§ steranes and hopanes (16 species) are below detection limit.

Table A.2. Emission ratios relative to CO_2 (± standard error, and coefficient of determination R^2) of gaseous emissions from least squares linear fittings between mixing ratios of individual VOC and CO_2 measured in 10 flaming and 12 smoldering emission samples, respectively.

	Flaming (10)			Smoldering (12)		
	ΔX/ΔCO2	± uncertainty	R^2	ΔX/ΔCO2	± uncertainty	R^2
CO, ppmv/ppmv	0.0709	± 0.0205	0.89	0.2337	± 0.0133	0.99
CH_4, ppmv/ppmv	0.0030	± 0.0016	0.69	0.0107	± 0.0016	0.96
chloroform, pptv/ppmv	0.0016	± 0.0128	0.01	0.0000	± 0.0026	0.00
dichloromethane, pptv/ppmv	-0.1606	± 0.5010	0.06	-0.0669	± 0.3050	0.02
trichloroethylene, pptv/ppmv	0.0001	± 0.0039	0.00	0.0190	± 0.0029	0.96
tetrachloroethylene, pptv/ppmv	0.0074	± 0.0416	0.02	0.0039	± 0.0030	0.47
methyl chloride, pptv/ppmv	8.6976	± 3.7600	0.78	32.6700	± 3.0600	0.98
methyl bromide, pptv/ppmv	0.2959	± 0.1540	0.71	2.0833	± 0.2140	0.98
methyl nitrate, pptv/ppmv	0.8219	± 0.3510	0.79	0.0113	± 0.0113	0.33
ethylnitrate, pptv/ppmv	0.0579	± 0.0253	0.78	0.0044	± 0.0011	0.89
i-propylnitrate, pptv/ppmv	0.1025	± 0.0464	0.76	0.0352	± 0.0031	0.98
n-propylnitrate, pptv/ppmv	0.0075	± 0.0068	0.45	0.0004	± 0.0003	0.49
2-butylnitrate, pptv/ppmv	0.0531	± 0.0207	0.81	0.0095	± 0.0028	0.86
ethane, ppbv/ppmv	0.2621	± 0.1320	0.72	0.9095	± 0.1010	0.98
propane, ppbv/ppmv	0.0525	± 0.0284	0.69	0.2445	± 0.0275	0.98
i-butane, ppbv/ppmv	0.0029	± 0.0019	0.62	0.0177	± 0.0019	0.98
n-butane, ppbv/ppmv	0.0091	± 0.0053	0.66	0.0651	± 0.0071	0.98
i-pentane, ppbv/ppmv	0.0007	± 0.0015	0.13	0.0022	± 0.0002	0.98
n-pantane, ppbv/ppmv	0.0034	± 0.0020	0.66	0.0255	± 0.0028	0.98
2-methylpentane, ppbv/ppmv	0.0007	± 0.0003	0.74	0.0051	± 0.0006	0.98
3-methylpentane, ppbv/ppmv	0.0002	± 0.0001	0.60	0.0011	± 0.0001	0.98
n-hexane, ppbv/ppmv	0.0023	± 0.0013	0.67	0.0162	± 0.0018	0.98
n-heptane, ppbv/ppmv	0.0018	± 0.0009	0.72	0.0118	± 0.0013	0.98
n-octane, ppbv/ppmv	0.0012	± 0.0007	0.69	0.0091	± 0.0010	0.97
ethene, ppbv/ppmv	1.2414	± 0.5550	0.77	0.8568	± 0.1680	0.93
ethyne, ppbv/ppmv	0.3888	± 0.1780	0.76	0.0969	± 0.0566	0.59
propene, ppbv/ppmv	0.2447	± 0.0960	0.81	0.3982	± 0.0426	0.98
1-butene, ppbv/ppmv	0.0374	± 0.0152	0.80	0.0621	± 0.0053	0.99
i-butene, ppbv/ppmv	0.0240	± 0.0108	0.77	0.0890	± 0.0086	0.98
trans-2-butene, ppbv/ppmv	0.0083	± 0.0040	0.74	0.0299	± 0.0031	0.98
cis-2-butene, ppbv/ppmv	0.0063	± 0.0034	0.69	0.0220	± 0.0025	0.97
1,3-butadiene, ppbv/ppmv	0.0232	± 0.0178	0.53	0.0280	± 0.0092	0.82
benzene, ppbv/ppmv	0.0952	± 0.0325	0.85	0.1885	± 0.0247	0.97
toluene, ppbv/ppmv	0.0431	± 0.0151	0.84	0.1044	± 0.0219	0.92
ethylbenzene, ppbv/ppmv	0.0053	± 0.0021	0.80	0.0133	± 0.0033	0.89
m-xylene, ppbv/ppmv	0.0090	± 0.0044	0.74	0.0362	± 0.0083	0.90
p-xylene, ppbv/ppmv	0.0042	± 0.0021	0.74	0.0080	± 0.0031	0.77
o-xylene, ppbv/ppmv	0.0035	± 0.0017	0.74	0.0127	± 0.0019	0.96
isopropylbenzene, ppbv/ppmv	0.0006	± 0.0003	0.73	0.0021	± 0.0005	0.89
propylbenzene, ppbv/ppmv	0.0008	± 0.0005	0.57	0.0047	± 0.0013	0.87
3-ethlytoluene, ppbv/ppmv	0.0022	± 0.0014	0.62	0.0052	± 0.0038	0.48
4-ethyltoluene, ppbv/ppmv	0.0015	± 0.0009	0.64	0.0101	± 0.0033	0.83
2-ethyltoluene, ppbv/ppmv	0.0007	± 0.0005	0.60	0.0031	± 0.0004	0.97
isoprene, ppbv/ppmv	0.0010	± 0.0106	0.01	0.0250	± 0.0102	0.75
α-pinene, ppbv/ppmv	0.0012	± 0.0052	0.03	0.0202	± 0.0254	0.24
β-pinene, ppbv/ppmv	0.0017	± 0.0019	0.35	0.0123	± 0.0029	0.90

Table A.3.a. Emission Factors of gas phase emissions from flaming and smoldering stages in g or mg per kg biomass burned.

	Flaming Stages		Smoldering Stages	
	AVERAGE	STD	AVERAGE	STD
CO, g/kg	63.65	18.61	149.28	53.97
CO_2, g/kg	1436.76	30.82	1247.68	105.76
CH_4, g/kg	1.63	0.81	6.49	4.91
NH_3, g/kg	0.1505	0.2894	0.4982	0.7748
SO_2, g/kg	0.0312	0.0601	0.1035	0.1609
HONO, g/kg	0.0786	0.1512	0.2602	0.4047
HNO_3, g/kg	0.0026	0.0049	0.0085	0.0132
HCl, g/kg	0.0031	0.0059	0.0102	0.0158
acetic acid, g/kg	0.2928	0.5631	0.9695	1.5075
formic acid, g/kg	0.1558	0.2996	0.5158	0.8020
oxalic acid, g/kg	0.0373	0.0718	0.1235	0.1921
chloroform, mg/kg	0.0249	0.0367	0.0794	0.1788
dichloromethane, mg/kg	0.0877	0.1862	1.8782	3.1042
trichloroethylene, mg/kg	0.0154	0.0322	0.0146	0.0350
tetrachloroethylene, mg/kg	0.0930	0.1833	0.0365	0.0721
methyl chloride, mg/kg	11.2191	4.7485	23.8814	9.7904
methyl bromide, mg/kg	0.7599	0.5661	1.6765	1.5210
methyl nitrate, mg/kg	0.7330	0.7270	0.1743	0.1335
ethylnitrate, mg/kg	0.0752	0.0704	0.0316	0.0351
i-propylnitrate, mg/kg	0.1408	0.1230	0.1464	0.1605
n-propylnitrate, mg/kg	0.0178	0.0186	0.0081	0.0131
2-butylnitrate, mg/kg	0.0840	0.0743	0.1246	0.2148
ethane, g/kg	0.2179	0.1008	0.7387	0.5714
propane, g/kg	0.0635	0.0316	0.2476	0.2139
i-butane, g/kg	0.0047	0.0025	0.0143	0.0120
n-butane, g/kg	0.0146	0.0081	0.0397	0.0341
i-pentane, g/kg	0.0039	0.0038	0.0043	0.0057
n-pantane, g/kg	0.0067	0.0036	0.0178	0.0155
2-methylpentane, g/kg	0.0016	0.0010	0.0034	0.0037
3-methylpentane, g/kg	0.0005	0.0004	0.0009	0.0011
n-hexane, g/kg	0.0049	0.0027	0.0103	0.0095
n-heptane, g/kg	0.0042	0.0022	0.0088	0.0082
n-octane, g/kg	0.0031	0.0018	0.0069	0.0071
ethene, g/kg	0.8405	0.3461	1.3573	0.6210
ethyne, g/kg	0.2986	0.1348	0.3277	0.1785
propene, g/kg	0.2664	0.0985	0.5841	0.2951
1-butene, g/kg	0.0554	0.0219	0.1125	0.0462
i-butene, g/kg	0.0363	0.0155	0.0947	0.0477
trans-2-butene, g/kg	0.0134	0.0061	0.0401	0.0257
cis-2-butene, g/kg	0.0099	0.0050	0.0311	0.0211
1,3-butadiene, g/kg	0.0537	0.0324	0.1205	0.0619
benzene, g/kg	0.2115	0.0731	0.4226	0.2446
toluene, g/kg	0.1074	0.0371	0.3582	0.3458
ethylbenzene, g/kg	0.0142	0.0057	0.0505	0.0532
m-xylene, g/kg	0.0231	0.0112	0.1278	0.1330
p-xylene, g/kg	0.0112	0.0051	0.0452	0.0481
o-xylene, g/kg	0.0091	0.0043	0.0325	0.0262
isopropylbenzene, g/kg	0.0019	0.0009	0.0107	0.0104
propylbenzene, g/kg	0.0023	0.0016	0.0270	0.0365
3-ethlytoluene, g/kg	0.0066	0.0040	0.0655	0.0866
4-ethyltoluene, g/kg	0.0045	0.0033	0.0790	0.1196
2-ethyltoluene, g/kg	0.0020	0.0013	0.0075	0.0061
isoprene, g/kg	0.0236	0.0286	0.1433	0.1114
α-pinene, g/kg	0.0338	0.0306	0.5108	0.5966
β-pinene, g/kg	0.0098	0.0064	0.0882	0.0951

Table A.3.b. Emission Factors of particle phase emissions from flaming and smoldering stages in g or mg per kg biomass burned.

	Flaming Stages		Smoldering Stages	
	AVERAGE	STD	AVERAGE	STD
PM2.5, g/kg	0.6621	0.2479	1.1453	0.4288
OC, g/kg	0.3989	0.1932	0.6900	0.3343
EC, g/kg	0.0259	0.0123	0.0449	0.0212
acetate, g/kg	0.0036	0.0017	0.0063	0.0030
formate, g/kg	0.0030	0.0013	0.0051	0.0023
nitrate, g/kg	0.0029	0.0023	0.0050	0.0039
Cl^-, g/kg	0.0035	0.0023	0.0060	0.0040
K^+, g/kg	0.0043	0.0033	0.0074	0.0057
sulfate, g/kg	0.0016	0.0010	0.0028	0.0017
ammonium, g/kg	0.0007	0.0008	0.0012	0.0013
oxalate, g/kg	0.0005	0.0002	0.0008	0.0003
Cl, g/kg	0.0028	0.0018	0.0048	0.0032
K, g/ kg	0.0038	0.0028	0.0065	0.0049
Na^+, g/kg	0.0001	0.0001	0.0002	0.0001
Na, mg/kg	0.0003	0.0002	0.0005	0.0003
Mg, mg/kg	0.0010	0.0018	0.0017	0.0032
Al, mg/kg	0.1514	0.2876	0.2619	0.4974
Si, mg/kg	0.1229	0.1768	0.2126	0.3058
P, mg/kg	0.0064	0.0102	0.0111	0.0177
S, mg/kg	0.7108	0.3769	1.2295	0.6520
Ca, mg/kg	0.0039	0.0073	0.0068	0.0126
Ti, mg/kg	0.0025	0.0043	0.0044	0.0075
Mn, mg/kg	0.0075	0.0071	0.0129	0.0122
Fe, mg/kg	0.0541	0.0929	0.0936	0.1607
Cu, mg/kg	0.0065	0.0073	0.0112	0.0127
Zn, mg/kg	0.1058	0.0709	0.1831	0.1226
As, mg/kg	0.0013	0.0020	0.0022	0.0035
Se, mg/kg	0.0008	0.0011	0.0014	0.0020
Br, mg/kg	0.0931	0.0695	0.1610	0.1202
Rb, mg/kg	0.0278	0.0215	0.0480	0.0372
Sr, mg/kg	0.0011	0.0023	0.0018	0.0039
Pb, mg/kg	0.0010	0.0017	0.0017	0.0030

***** Emission factors were calculated by using the same value for both flaming and smoldering for SO_2, NH_3, HONO, HNO_3, HCl, acetic acid, formic acid, oxalic acid, and particulate components since there was no separate measurement between flaming and smoldering for those species.

APPENDIX B

Table B.1. Ambient PM2.5 composition in Atlanta, GA

Species	Mean STD	(Min – Max)
Sb	0.00436 ± 0.00439	(0.00005 - 0.03170)
As	0.00125 ± 0.00098	(0.00002 - 0.00539)
Al	0.02102 ± 0.03556	(0.00046 - 0.35400)
Ba	0.01297 ± 0.01085	(0.00002 - 0.05390)
Br	0.00318 ± 0.00168	(0.00023 - 0.00928)
Cd	0.00191 ± 0.00134	(0.00004 - 0.01160)
Ca	0.03139 ± 0.01658	(0.00348 - 0.08360)
Cr	0.00064 ± 0.00080	(0.00005 - 0.01070)
Co	0.00030 ± 0.00017	(0.00001 - 0.00157)
Cu	0.00400 ± 0.00382	(0.00023 - 0.02250)
Fe	0.07296 ± 0.04343	(0.01160 - 0.26200)
Pb	0.00242 ± 0.00183	(0.00010 - 0.01360)
Mn	0.00125 ± 0.00092	(0.00005 - 0.00481)
Ni	0.00038 ± 0.00031	(0.00002 - 0.00296)
Mg	0.00790 ± 0.01831	(0.00006 - 0.16000)
La	0.00366 ± 0.00532	(0.00013 - 0.03210)
P	0.00226 ± 0.00346	(0.00005 - 0.02880)
Se	0.00125 ± 0.00078	(0.00005 - 0.00499)
Ti	0.00521 ± 0.00345	(0.00023 - 0.02120)
V	0.00086 ± 0.00065	(0.00005 - 0.00443)
Si	0.09311 ± 0.07676	(0.00316 - 0.56200)
Zn	0.00847 ± 0.00829	(0.00023 - 0.10200)
K	0.05848 ± 0.03902	(0.00698 - 0.35700)
Na	0.04084 ± 0.05082	(0.00080 - 0.30700)
NH_4^+	1.40 ± 0.78	(0.16 - 4.80)
OC	2.61 ± 1.84	(0.13 - 11.31)
NO_3^-	0.86 ± 0.77	(0.14 - 5.00)
EC	0.90 ± 0.59	(0.06 - 3.46)
SO_4^{2-}	4.70 ± 2.91	(0.91 - 17.00)
$PM_{2.5}$	15.72 ± 6.73	(5.11 - 37.80)

Table B.2. Primary emission source profile data used in this study

	Biomass burning[a]		Motor vehicle[b]		Dust[c]		Pulp/paper production[d]	
species	f	σ_f	f	σ_f	f	σ_f	f	σ_f
Sb	0.00000	0.00010	0.00063	0.00211	0.00000	0.00010	0.00004	0.00022
As	0.00000	0.00010	0.00000	0.00027	0.00000	0.00010	0.00001	0.00003
Al	0.00000	0.00010	0.00131	0.00120	0.09280	0.02970	0.00090	0.00161
Ba	0.00000	0.00010	0.00000	0.00750	0.00000	0.00010	0.00016	0.00042
Br	0.00002	0.00000	0.00000	0.00011	0.00036	0.00027	0.00010	0.00004
Cd	0.00000	0.00010	0.00043	0.00115	0.00000	0.00010	0.00003	0.00007
Ca	0.00020	0.00001	0.00121	0.00065	0.03150	0.01090	0.00424	0.00100
Cr	0.00000	0.00010	0.00007	0.00033	0.00270	0.00025	0.00002	0.00004
Co	0.00000	0.00010	0.00007	0.00008	0.00000	0.00010	0.00000	0.00010
Cu	0.00000	0.00010	0.00007	0.00011	0.00000	0.00026	0.00003	0.00006
Fe	0.00000	0.00010	0.00067	0.00011	0.03140	0.01010	0.00075	0.00100
Pb	0.00004	0.000003	0.00007	0.00038	0.00000	0.00010	0.00004	0.00013
Mn	0.00000	0.00010	0.00007	0.00020	0.00080	0.00035	0.00034	0.00025
Ni	0.00000	0.00010	0.00000	0.00011	0.00000	0.00023	0.00007	0.00018
Mg	0.00000	0.00010	0.00000	0.00008	0.00000	0.00010	0.00091	0.00184
La	0.00000	0.00010	0.00089	0.00990	0.00000	0.00010	0.00027	0.00061
P	0.00000	0.00010	0.00096	0.00049	0.00123	0.00104	0.00026	0.00100
Se	0.00000	0.00010	0.00003	0.00011	0.00010	0.00018	0.00001	0.00001
Ti	0.00000	0.00010	0.00003	0.00276	0.00444	0.00147	0.00003	0.00002
V	0.00000	0.00010	0.00000	0.00092	0.00030	0.00022	0.00009	0.00003
Si	0.00046	0.00004	0.00521	0.00042	0.19700	0.06200	0.00182	0.00167
Zn	0.00035	0.00001	0.00104	0.00009	0.00090	0.00037	0.00017	0.00007
K	0.00699	0.00008	0.00011	0.00077	0.00494	0.00174	0.04799	0.03548
Na	0.00000	0.00010	0.00000	0.00008	0.00000	0.00010	0.10775	0.05139
NH_4^+	0.00086	0.00012	0.01136	0.00087	0.00000	0.00010	0.00000	0.00010
OC	0.88299	0.05983	0.26557	0.01412	0.00000	0.00010	0.29735	0.07373
NO_3^-	0.00345	0.00035	0.00299	0.00300	0.00000	0.00010	0.00374	0.00190
EC	0.09564	0.01011	0.24943	0.01952	0.00000	0.00010	0.02634	0.01824
SO_4^{2-}	0.00406	0.00038	0.01026	0.00198	0.00000	0.00010	0.20396	0.05818
species	Coal combustion[e]		Mineral production[d]		Oil combustion[d]		Metal production[d]	
Sb	0.00011	0.00049	0.00021	0.00070	0.00066	0.00023	0.03749	0.00834
As	0.00002	0.00055	0.00008	0.00009	0.00004	0.00001	0.05028	0.00707
Al	0.05027	0.03261	0.02111	0.00415	0.00655	0.00075	0.02354	0.01027
Ba	0.01011	0.01010	0.00061	0.00204	0.00158	0.00007	0.00071	0.00095
Br	0.00028	0.00057	0.00012	0.00005	0.00008	0.00008	0.00072	0.00034
Cd	0.00003	0.00027	0.00015	0.00031	0.00000	0.00010	0.01444	0.00348
Ca	0.15708	0.10526	0.09860	0.01812	0.02750	0.00900	0.01215	0.01475
Cr	0.00024	0.00019	0.00126	0.00011	0.00022	0.00004	0.00314	0.00204
Co	0.00004	0.00065	0.00175	0.00096	0.00093	0.00012	0.00003	0.00010
Cu	0.00085	0.00075	0.00062	0.00022	0.00104	0.00041	0.03931	0.00594
Fe	0.03428	0.02019	0.00779	0.00225	0.01550	0.00300	0.05170	0.00886
Pb	0.00052	0.00090	0.00242	0.00086	0.01400	0.00400	0.08497	0.01367
Mn	0.00109	0.00106	0.00071	0.00014	0.00029	0.00006	0.01203	0.00249
Ni	0.00019	0.00017	0.00061	0.00029	0.01700	0.00350	0.00243	0.00024
Mg	0.00801	0.00859	0.00328	0.00377	0.00000	0.00010	0.00346	0.00606
La	0.00004	0.00269	0.00002	0.00007	0.00027	0.00003	0.00000	0.00010
P	0.00276	0.00455	0.00045	0.00030	0.01250	0.00250	0.00185	0.00036
Se	0.00548	0.00833	0.00057	0.00001	0.00002	0.00001	0.00058	0.00004
Ti	0.00807	0.00516	0.00134	0.00019	0.00085	0.00035	0.00082	0.00077
V	0.00075	0.00081	0.00004	0.00002	0.01500	0.00300	0.00055	0.00007
Si	0.10147	0.06807	0.08834	0.03146	0.02250	0.00500	0.04432	0.00772
Zn	0.00294	0.00333	0.00127	0.00018	0.00965	0.00295	0.05962	0.00597
K	0.00493	0.00256	0.01306	0.00587	0.00185	0.00040	0.02542	0.00562
Na	0.00862	0.01778	0.01466	0.00412	0.02850	0.00750	0.00897	0.00348
NH_4^+	0.01697	0.02128	0.00000	0.00010	0.00000	0.00010	0.00000	0.00010
OC	0.25786	0.25766	0.05255	0.02273	0.02100	0.00500	0.02400	0.00733
NO_3^-	0.00651	0.01092	0.00271	0.00637	0.00000	0.00010	0.00254	0.00524
EC	0.01313	0.02225	0.01467	0.03922	0.03960	0.00835	0.00171	0.00127
SO_4^{2-}	0.27273	0.22563	0.14061	0.08087	0.42500	0.05000	0.05734	0.01345

REFERENCES

Altshuller, A.P. Natural volatile organic substances and their effect on air quality in the United States, *Atmos. Environ.* 1983, 17, 2131-2165.

Barnard, W.; Sabo, E. *Review of 1999 NEI and recommendations for developing the 2002 VISTAS inventory for regional haze modeling*, North Carolina DENR, Asheville, NC, 2003.

Battye, W.; Battye, R. *Development of Emissions Inventory Methods for Wildland Fire*, final report, EC/R Inc., NC, 2002.

Baumann, K.; Ift, F.; Zhao, J.Z.; Chameides, W.L. Discrete measurements of reactive gases and fine particle mass and composition during the 1999 Atlanta supersite experiment. *J. Geophys. Res.* 2003, 108.

Bell, M.L.; McDermott, A.; Zeger, S.L.; Samet, J.M.; Dominici, F. Ozone and short-term mortality in 95 U.S. urban communities, 1987-2000. *J. Am. Med. Assoc.* 2004, 292, 2372-2378.

Birch, M.E.; Cary, R.A. Elemental carbon-based method for monitoring occupational exposures to particulate diesel exhaust. *Aerosol Sci. Technol.* 1996, 25, 221-241.

Bongsan, B.; Lambert, G.; Boissard, C.C. Light hydrocarbon emissions from African savanna burnings in *Global Biomass Burning: Atmospheric, Climatic, and Biospheric Implications*, edited by J.S. Levine, 155-161, MIT press, Cambridge, Massachusetts, 1991.

Boylan, J.W.; Odman, M.T.; Wilkinson, J.G.; Russell, A.G.; Doty, K.G;, Norris, W.B.; McNider, R.T. Development of a comprehensive, multiscale "one-atmosphere" modeling system: Application to the Southern Appalachian Mountains. *Atmos. Environ.* 2002, 36, 3721-3734.

Boylan, J.W.; Odman, M.T.; Wilkinson, J.G.; Russell, A.G. Integrated assessment modeling of atmospheric pollutants in the Southern Appalachian Mountains. Part II: fine particulate matter and visibility. *J. Air & Waste Manage. Assoc.* 2006, 56, 12-22

Burnett, R.T.; Dales, R.; Krewski, D.; Vincent, R.; Dann, T.; Brook, J.R. Associations between ambient particulate sulfate and admissions to Ontario hospitals for cardiac and respiratory disease. *Am. J. Epidemiol.* 1995, 142, 15-22.

Butler, A.; Andrew, M.S.; Russell, A.G. Daily sampling of PM2.5 in Atlanta, Results of the first year of the Assessment of Spatial Aerosol Composition in Atlanta study. *J. Geophy. Res.* 2003, 108 (D7), 8415.

Cabada, J.C.; Pandis, S.N.; Robinson, A.L. Sources of atmospheric carbonaceous particulate matter in Pittsburgh, Pennsylvania; *J. Air & Waste Manage Assoc.* 2002, 52, 732-741.

Cabada, J.C.; Pandis, S.N.; Subramanian, R.; Robinson, A.L.; Polidori, A.; Turpin, B.J. Estimating the secondary organic aerosol contribution to PM2.5 using the EC tracer method; *Aerosol Sci. Technol.* 2004, 38 (supplement 1), 140-155.

Castro, L.M.; Pio, C.A.; Harrison, R.M.; Smith, D.J.T. Carbonaceous aerosol in urban and rural European atmospheres: estimation of secondary organic carbon concentrations; *Atmos. Environ.* 1999, 33, 2771-2781.

Charlson, R.J.; Schwartz, S.E.; Hales, J.M.; Cess, R.D.; Coakley, J.A.; Hansen, J.E.; Hofmann, D.J. Climate forcing by anthropogenic aerosols; *Science* 1992, 255, 423-430.

Chow, J.C.; Watson, J.G.; Kuhns, H.; Etyemezian, V.; Lowenthal, D.H., Crow, D., Kohl, S.D.; Engelbrecht, J.P.; Green, M.C. Source profiles for industrial, mobile, and area sources in the Big Bend Regional Aerosol Visibility and Observational study; *Chemosphere* 2004, 54, 185-208.

Chow, J.C.; Watson, J.G.; Pritchett, L.C.; Pierson, W.R.; Frazier, C.A.; Purcell, R.G. The DRI thermal/optical reflectance carbon analysis system: Description, evaluation and applications in U.S. air quality studies; *Atmos. Environ.* 1993, 27A, 1185-1201.

Chow, J.C.; Watson, J.G.; Richards, L.W.; Haase, D.L.; McDade, C.; Dietrich, D.L.; Moon, D.; Sloane, C.S. (1991). *The 1989-90 Phoenix PM10 Study, Volume II: Source apportionment.* Report No. DRI8931.6F2. Prepared for Arizona

Department of Environmental Quality, Phoenix, AZ, by Desert Research Institute, Reno, NV.

Christensen, W.F. and Gunst R. F. Measurement error models in chemical mass balance analysis of air quality data; *Atmos. Environ.* 2004, 38, 733-744.

Christensen, W.F.; Schauer, J.J.; Lingwall, J.W. Iterated confirmatory factor analysis for pollution source apportionment; *Environmetrics* 2006, 17, 663-681.

Chu, S-H. Stable estimation of primary OC/EC ratios in the EC tracer method; *Atmos. Environ.* 2005, 39, 1383-1392.

Claeys, M., B. Graham, G. Vas, W. Wang, R. Vermeylen, V. Pashynska, J. Cafmeyer, P. Guyon, M.O., Andreae, P. Artaxo, W. Maenhaut; Formation of secondary organic aerosols through photooxidation of isoprene; *Science* 2004, 303, 1173-1176.

Colman, J.J.; Swanson, A.L.; Meinardi, S.; Sive, B.C.; Blake, D.R.; Rowland, F.S. Description of the analysis of a wide range of volatile organic compounds in whole air samples collected during PEM-Tropics A and B. *Analytical Chemistry* 2001, 73, 3723-3731.

Cooper, J.A. *Determination of source contributions to fine and coarse suspended particulate levels in Petersville, Alabama.* Report to Tennessee Valley Authority by NEA, Inc., 1981.

Corbett, J.J; Fischbeck, P. Emissions from ships; *Science* 1997, 278, 823-824.

Cullen, A.C. and Frey, H.C. Probabilistic Techniques in Exposure Assessment: A Handbook for Dealing with Variability and Uncertainty in Models and Inputs. Plenum Press, New York, 1998.

Dockery, D.W.; Pope, C.A.; Xu, X.P.; Spengler, J.D.; Ware, J.H.; Fay, M.E.; Ferris, B.G.; Speizer, F.E. An Association between Air-pollution and Mortality in 6 United States Cities; *New Engl. J. Med.* 1993, 329, 1753-1759.

Dockery, D.W.; Cunningham, J., Damokosh, A.I.; Neas, L.M.; Spengler, J.D.; Koutrakis, P.; Ware, J.H.; Raizenne, M.; Speizer, F.E. Health effects of acid aerosols on North American children: respiratory symptoms. *Environ. Health Perspect.* 1996, 104. 500-505.

ENVIRON international corporation 2006. *User's Guide Comprehensive Air Quality Model with Extenions version 4.30*.

Environmental Systems Research Institute, Inc. (ESRI) 2004. *Using ArcGIS Spatial Analyst.* ESRI, Inc., Redlands, CA.

Fine, P.M.; Cass, G.R.; Simoneit, B.R.T. Chemical characterization of fine particle emissions from the fireplace combustion of woods grown in the southern Unites States. *Eviron. Sci. Technol.* 2002, 36, 1442-1451.

Fowler, C.T. Human health impacts of forest fires in the Southern United States: a literature review. *Journal of Ecological Anthropology* 2003, 7, 39-59.

Friedlander, S.K. Chemical element balances and identification of air pollution sources. *Eviron. Sci. Technol.* 1973, 7, 234-240.

Fujita, E.M.; Watson, J.G.; Chow, J.C.; Lu, Z. Validation of the chemical mass balance receptor model applied to hydrocarbon source apportionment in the Southern California Air Quality Study. *Environ. Sci. Technol.* 1994, 28, 1633-1649.

Glasius, M. Lahaniati, M., Calogirou, A., Bella, D.D., Jensen, N.R., Hjorth, J., Kotzias, D., Larsen, B.R. Carboxylic acids in secondary aerosols from oxidation of cyclic monoterpenes by ozone; *Environ. Sci. Technol.* 2000, 34, 1001-1010.

Gray, H.A.; Cass, G.R.; Huntzicker, J.J.; Heyerdahl, E.K.; Rau, J.A. Characteristics of Atmospheric Organic and Elemental Carbon Particle Concentrations in Los Angeles; *Environ. Sci. Technol.* 1986, 20, 580-589.

Gundel, L.A.; Lane, D.A. Direct determination of semi-volatile organic compounds with sorbent-coated diffusion denuders. *J. Aerosol Sci.* 1998, 29, s341-s342.

Gundel, L.A.; Lee, V.C.; Mahanama, K.R.R.; Stevens, R.K.; Daisey, J.M. Direct determination of the phase distributions of semivolatile polycyclic aromatic-hydrocarbons using annular denuders. *Atmos. Environ.* 1995, 1719-1733.

Hardy, C.C.; Hermann, S.M.; Mutch, R.E. Overview. In *Smoke management guide for prescribed and wildland fire*; C.C. Hardy *et al.*, Eds.; NFES 1279, National Wildfire Coordination Group, Boise, ID, 2001.

Harley, R.A.; Hannigan, M.P.; Cass, G.R. Respeciation of organic gas emissions and the detection of excess unburned gasoline in the atmosphere. *Environ. Sci. Technol.* 1992, 26, 2395-2408.

Hays, M.D.; Geron, C.D.; Linna, K.J.; Smith, N.D. Speciation of gas-phase and fine particle emissions from burning of foliar fuels. *Environ. Sci. Technol.* 2002, 36, 2281-2295.

Henry, R.C.; Kim, B.M. Extension of self-modeling curve resolution to mixtures of more than three components: Part 1. Finding the basic feasible region. *Chemometrics and Intelligent Laboratory Systems*, 8, 205-216, 1990.

Hopke, P.K.; Barrie, L.A.; Li, S.-M.; Cheng, M.-D.; Li, C.; Xie, Y. Possible sources and preferred pathways for biogenic and non-sea-salt sulfur for the high Arctic. *J. Geophys. Res.* 1995, 100, 16595-16603.

Hoffmann, T.; Odum, J.R., Bowman, F., Collins, D., Klockow, D., Flagan, R.C., Seinfeld, J.H. Formation of organic aerosol from the oxidation of biogenic hydrocarbons; *Atmos. Environ.* 1997, 26, 189-222.

Houck, J.E.; Chow, J.C.; Watson, J.G.; Simons, C.A.; Pritchett, L.C.; Goulet, J.M.; Frazier, C.A. (1989). *Determination of particle size distribution and chemical composition of particulate matter from selected sources in California: Volume III.* Report No. A6-175-32. Prepared for California Air Resources Board, Sacramento, CA, by OMNI Environmental Services Inc., Beaverton, OR, and Desert Research Institute, Reno, NV.

Ito, K.; Xue, N.; Thurston, G. Spatial variation of PM2.5 chemical species and source-apportioned mass concentrations in New York City; *Atmos. Environ.* 2004, 38, 5269-5282.

Jang, M. and R.M. Kamens Atmospheric secondary aerosol formation by heterogeneous reactions of aldehydes in the presence of a sulfuric acid catalyst; *Environ. Sci. Technol.* 2001, 35,4758-4766.

Jang, M. and R.M. Kamens Newly characterized products and composition of secondary aerosols from the reaction of α-pinene with ozone; *Atmos. Environ.* 1999, 33, 459-474.

Javitz, H.S.; Watson, J.G.; Robinson, N. Performance of the chemical mass balance model with simulated local-scale aerosols; *Atmos. Environ.* 1988, 22, 2309-2322.

Johnson, P.R.S.; Graham, J.J.; Analysis of primary fine particle National Ambient Air Quality Standard metrics; *J. of Air & Waste Manage. Assoc.* 2006, 56, 206-218.

Kim, B.M.; Henry, R.C. Extension of self-modeling curve resolution to mixtures of more than three components: Part 2. Finding the complete solution. *Chemometrics and Intelligent Laboratory Systems*, 49, 67-77, 1999.

Kim, B.M.; Henry, R.C. Extension of self-modeling curve resolution to mixtures of more than three components: Part 3. Atmospheric aerosol data simulation studies. *Chemometrics and Intelligent Laboratory Systems*, 52, 145-154, 2000.

Kim, E.; Hopke, P.K. Source identification of Atlanta aerosol by positive matrix factorization. *J. Air & Waste Mannage. Assoc.*, 53, 731-739, 2003.

Kim, E.; Hopke, P.K.; Edgerton, E.S. Improving source identification of Atlanta aerosol using temperature resolved carbon fractions in positive matrix factorization. *Atmos. Environ.*, 38, 3349-3362, 2004.

Kim, E.; Hopke, P.K. Improving source apportionment of fine particles in the eastern United States utilizing temperature-resolved carbon fractions. *J. Air & Waste Mannage. Assoc.*, 55, 1456-1463, 2005a.

Kim, E.; Hopke, P.K; Pinto, J.P.; Wilson, W.E. Spatial variability of fine particle mass, components, and source contributions during the regional air pollution study in St. Louis. *Environ. Sci. Technol.* 2005b, 39, 4172-4179.

Laden, F.; Neas, L.M.; Dockery, D.W.; Schwartz, J. Association of fine particulate matter from different sources with daily mortality in Six U.S. Cities; *Environ. Health Perspect.*, 108, 941-947, 2000.

Lane, D.A., *Advances in Environmental, Industrial and Process Control Technologies, vol. 2, Gas and Particle Phase Measurements of Atmospheric Organic Compounds*, 402pp., Gordon and Breach, Amsterdam, 1999.

Lee, S.; Baumann, K.; Schauer, J.J.; Sheesley, R.J.; Naeher, L.P.; Meinardi, S.; Blake, D.R.; Edgerton, E.S.; Russell, A.G.; Clements, M. Gaseous and particulate emissions from prescribed burning in Georgia; *Environ. Sci. Technol.* 2005, 39, 9049-9056.

Lee, S.; Baumann, K; Russell, A.G. Source apportionment of fine particulate matter in the Southeastern United States; *J. Air & Waste Manage. Assoc.* 2006, (in preparation).

Liu, W.; Wang, Y.; Russell, A.G.; Edgerton, E.S. Atmospheric aerosol over two urban-rural pairs in the southeastern United States: Chemical composition and possible sources. *Atmos. Environ.*, 39, 4453-4470, 2005.

Malm, W.C. 1999, *Introduction to Visibility*, Cooperative Institute for Research in the Atmosphere, NPS Visibility Program, Colorado State University, Fort Collins, CO.

Manchester-Neesvig, J.B.; Schauer, J.J.; Cass, G.R. The distribution of particle-phase organic compounds in the atmosphere and their use for source apportionment during the southern California children's health study. *J. Air & Waste Manage Assoc.* 2003, 53, 1065-1079.

Mar, T.F.; Norris, G.A.; Koenig, J.Q.; Larson, T.V. Associations between Air Pollution and Mortality in Phoenix, 1995-1997; *Environ. Health Perspect.* 2000, 108, 347-353.

Marmur, A.; Unal, A.; Mulholland, J.A.; Russell, A.G. Optimization-based source apportionment of PM2.5 incorporating gas-to-particle ratios. *Environ. Sci. Technol.*, 39, 3245-3254, 2005.

Marmur, A.; Park, S.-K.; Mulholland, J.A.; Tolbert, P.E.; Russell, A.G. Source apportionment of PM2.5 in the southeastern United States using receptor and emissions-based models: Conceptual differences and implications for time-series health studies. *Atmos. Environ.*, 40, 2533-2551, 2006.

Metzger, K.B.; Tolbert, P.E.; Klein, M.; Peel, J.L.; Flanders, W.D.; Todd, K.; Mulholland, J.A.; Ryan, P.B.; Frumkin, H. Ambient air pollution and cardiovascular emgergency department visits. *Epidemiology* 2004, 15, 46-56.

Miller, M.S.; Friedlander, S.K.; Hidy, G.M. A chemical element balance for the Pasadena Aerosol. *J. Colloid and Interface Science* 1972, 39, 165-176.

Morgan, M. and Henrion, M. Uncertainty: *A Guide to Dealing with Uncertainty in Quantitative Risk and Policy Analysis*. Cambridge University Press, Cambridge, 1990.

Noziere, B., Barnes, I., Becker, K.H. Product study and mechanisms of the reactions of α-pinene and pinonaldehyde with OH radicals; *J. Geophys. Res.* 1999, 104, 23645-23656.

Odum, J.R., Hoffmann, T., Bowman, F., Collins, D. Flagan, R.C., Seinfeld, J.H. Gas/particle partitioning and secondary organic aerosol yields; *Environ. Sci. Technol.* 1996, 30, 2580-2585.

Odum, J.R., Jungkamp, T.P.W., Seinfeld, J.H. The atmospheric aerosol-forming potential of whole gasoline vapor; *Science* 1997, 276, 96-99.

Ottmar, R.D.; Vihnanek, R.E. Photo series for major natural fuel types of the United States-phase II. Abstract. Presented at the joint fire science program principle investigators meeting; 2000; Reno, Nevada.

Ottmar, R.D. Smoke source characteristics. In *Smoke management guide for prescribed and wildland fire*; C.C. Hardy *et al.*, Eds.; NFES 1279, National Wildfire Coordination Group, Boise, ID, 2001.

Paatero, P. Least squares formulation of robust non-negative factor analysis. *Chemometrics and Intelligent Laboratory Systems*, 37, 23-35, 1997.

Paatero, P. The multilinear engine-a table-driven least squares program for solving multilinear problems, including the n-way parallel factor analysis model. *J. Computational and Graphical Statistics*, 8, 854-888, 1999.

Park, S.-K.; Marmur, A.; Ke, L; Yan, B.; Russell, A.G.; Zheng, M. Comparison between chemical mass balance receptor and CMAQ model PM2.5 source apportionment. *Environ. Sci. Technol.* 2005 (submitted).

Park, S.-K.; Cobb, C.E.; Wade, K.; Mulholland, J.; Hu, Y.; Russell, A.G. Uncertainty in air quality model evaluation for particulate matter due to spatial variation in pollutant concentrations. *Atmos. Environ.* 2006 (submitted).

Peel, J.L.; Tolbert, P.E.; Klein, M.; Metzger, K.B.; Flanders, W.D.; Todd, K.; Mulholland, J.A.; Ryan, P.B.; Frumkin, H. Ambient air pollution and respiratory emergency department visits. *Epidemiology* 2005, 16, 164-174.

Perrino, C.; Gheradi, M. Optimization of the coating layer for the measurement of ammonia by diffusion denuders. *Atmos. Environ.* 1999, 4579-4587.

Pinto, J.P.; Pleasant, M.; Kellogg, R.; Torok, S.; Stiles, D.; Willis, R.D.; Koutrakis, P.; Allen, G.A. Chemical characterization of the ambient aerosol in Philadelphia. Presented at: particulate matter: health and regulatory issues: an Air & Waste Management Association international specialty conference; April 1995, Pittsburgh, PA.

Pope, C.A.; Kanner, R.E.; Acute effects of PM10 pollution on pulmonary function of smokers with mild to moderate chronic obstructive pulmonary disease. *Am. Rev. Respir. Dis.* 1993, 147, 1336-1340.

Pope, C.A.; Thun, M.J.; Namboodiri, M.M.; Dockery, D.W.; Evans, J.S.; Speizer, F.E.; Heath, C.W. Particulate air-pollution as a predictor of mortality in a prospective-study of U.S. adults; *Am. J. Respir. Crit. Care Med.* 1995, 151, 669-674.

Pope, C.A.; Kalkstein, L.S.; Synoptic weather modeling and estimates of the exposure-response relationship between daily mortality and particulate air pollution. *Environ. Health Prespect.* 1996, 104, 414-420.

Pope, C.A.; Burnett, R.T.; Thun, M.J.; Calle, E.E.; Krewski, D.; Ito, K.; Thurston, G.D. Lung cancer, cardiopulmonary mortality, and long-term exposure to fine particulate air pollution. *J. Am. Med. Assoc.* 2002, 287, 1132-1141.

Puglisi, E; Nicelli, M; Capri, E; Trevisan, M; Del Re, A. A. M. Cholesterol, β-sitosterol,ergosterol, and coprostanol in agricultural soils. *J. Environ. Qual.* 2003, 32, 466-471.

Radke, L.F.; Hegg, D.A.; Lyons, J.H., Brock, C.A.; Hobbs, P.V., *Airborne measurements on smokes from biomass burning, in Aerosols and Climate*, edited by P.V. Hobbs and M.P. McCormick, pp. 411-422, A. Deepak, Hampton, VA, 1998.

Ramaswamy, V.; O. Boucher, J. Haigh, D. Hauglustaine, J. Haywood, G. Myhre, T. Nakajima, G.Y. Shi, S. Solomon, 2001: *Radiative Forcing of Climate Change. In: Climate Change 2001: The Scientific Basis. Contribution of Working Group I to the Third Assessment Report of the Intergovernmental Panel on Climate Change* [R. Betts, R. Charlson, C. Chuang, J.S. Daniel, A. Del Genio, R. van Dorland, J. Feichter, J.uglestvedt, P.M. de F. Forster, S.J. Ghan, A. Jones, J.T. Kiehl, D. Koch, C. Land, J. Lean, U. Lohmann, K. Minschwaner, J.E. Penner, D.L. Roberts, H. Rodhe, G.J. Roelofs, L.D. Rotstayn, T.L. Schneider, U. Schumann, S.E. Schwartz, M.D. Schwarzkopf, K.P. Shine, S. Smith, D.S. Stevenson, F. Stordal, I. Tegen, Y. Zhang, and F. Joos, J. Srinivasan (eds.)]. Cambridge University Press, Cambridge, United Kingdom and New York, NY, USA, 881p.

Rogge, W.F.; Hildemann, L.M.; Mazurek, M.A.; Cass, G.R. Sources of fine organic aerosol. 1. charbroilers and meat cooking operations. *Environ. Sci. Technol.* 1991, 25, 1112-1125.

Rogge, W.F.; Hildemann, L.M.; Mazurek, M.A.; Cass, G.R.; Simoneit, B.R.T. Sources of fine organic aerosol. 2. Noncatalyst and catalyst-equipped automobiles and heavy duty diesel trucks. *Environ. Sci. Technol.* 1993a, 27, 636-651.

Rogge, W.F.; Hildemann, L.M.; Mazurek, M.A.; Cass, G.R.; Simoneit, B.R.T. Sources of fine organic aerosol. 3. Road dust, tire debris, and organometallic brake lining dust: Roads as sources and sinks. *Environ. Sci. Technol.* 1993b, 27, 1892-1904.

Rogge, W.F.; Hildemann, L.M.; Mazurek, M.A.; Cass, G.R.; Simoneit, B.R.T. Sources of fine organic aerosol. 4. particulate abrasion products from leaf surfaces of urban plants. *Environ. Sci. Technol.* 1993c, 27, 2700-2711.

Rogge, W.F.; Hildemann, L.M.; Mazurek, M.A.; Cass, G.R.; Simoneit, B.R.T. Sources of fine organic aerosol. 5. Natural gas home appliances. *Environ. Sci. Technol.* 1993d, 27, 2736-2744.

Rogge, W.F.; Hildemann, L.M.; Mazurek, M.A.; Cass, G.R.; Simoneit, B.R.T. Sources of fine organic aerosol. 6. Cigarette smoke in the urban atmosphere. *Environ. Sci. Technol.* 1994, 28, 1375-1388.

Russell, A.G. Particulate matter modeling and source apportionment. An international specialty conference of AAAR, Atlanta, GA, February, 2004.

Samet, J.M.; Dominici, F.; Curreiro, F.C.; Coursac, I.; Zeger, S.L. Fine particulate air pollution and mortality in 20 U.S. cities, 1987-1994. *New Engl. J. Med.* 2000, 343, 1742-1749.

Sandberg, D.V.; Ottmar, R.D.; Peterson, J.L.; Core, J. 2002 *Wildland fire in ecosystems: effects of fire on air*, General Technical Report RMRS-GTR-42-5, USDA, Forest Service, Rocky Mountain Research Station. 79 p.

Sapkota, A.; Symons, J.M.; Kleissl, J.; Wang, L.; Parlange, M.B.; Ondov, J.; Breysse, P.N.; Diette, G.B.; Eggleston, P.A.; Buckley, T.J. Impact of the 2002 Canadian forest fires on particulate matter air quality in Baltimore city. *Environ. Sci. Technol.*, 2005, 39, 24-32.

Sarnat, J.A.; Klein, M.; Tolber, P.E.; Marmur, A.; Russell, A.G.; Kim, E.; Hopke, P.K.; Examining the cardiovascular health effects of Atlanta aerosol using three source apportionment techniques. In: Proceedings of 7th International Aerosol Conference, St. Paul, MN, 2006.

Schauer, J.J.; Rogge, W.F.; Hildemann, L.M.; Mazurek, M.A.; Cass, G.R.; Simoneit, B.R.T. Source apportionment of airborne particulate matter using organic compounds as tracers. *Atmos. Environ.* 1996, 30, 3837-3855.

Schauer, J.J; Kleeman, M.J.; Simoneit, B.R.T. Measurement of emissions from air pollution sources. 2. C_1 through C_{30} organic compounds from medium duty diesel trucks. *Environ. Sci. Technol.* 1999a, 33, 1578-1587.

Schauer, J.J; Kleeman, M.J.; Simoneit, B.R.T. Measurement of emissions from air pollution sources. 1. C_1 through C_{29} organic compounds from meat charbroiling. *Environ. Sci. Technol.* 1999b, 33, 1566-1577.

Schauer, J.J.; Cass, G.R. Source apportionment of wintertime gas-phase and particle-phase air pollutants using organic compounds as tracers. *Environ. Sci. Technol.* 2000, 34, 1821-1832.

Schauer, J.J.; Kleeman, M.J.; Cass, G.R; Simoneit, B.R.T. Measurement of emissions from air pollution sources. 3. C_1-C_{29} organic compounds from fireplace combustion of wood. *Environ. Sci. Technol.* 2001, 35, 1716-1728.

Schauer, J.J; Kleeman, M.J.; Simoneit, B.R.T. Measurement of emissions from air pollution sources. 5. C_1-C_{32} organic compounds from gasoline-powered motor vehicles. *Environ. Sci. Technol.* 2002, 36, 1169-1180.

Schauer, J.J.; Mader, B.T.; DeMinter, J.T.; Heidemann, G.; Bae, M.S.; Seinfeld, J.H.; Flagan, R.C.; Cary, R.A.; Smith, D.; Huebert, B.J.; Bertram, T.; Howell, S.; Quinn, P.; Bates, T.; Turpin, B.; Lim, H.J.; Yu, J. ACE-Asia intercomparison of a thermal-optical method for the determination of particle-phase organic and elemental carbon. *Environ. Sci. Technol.* 2003, 37, 993-1001.

Schwartz, J. Particulate air pollution and chronic respiratory disease. *Environ. Res.* 1993, 62, 7-13.

Schwartz J.; Dockery, D.W.; Neas, L.M.; Wypij, D.; Ware, J.H.; Spengler, J.D.; Koutrakis, P.; Speizer, F.E.; Ferris, B.G. Acute effects of summer air-pollution on respiratory symptom reporting in children; *Am. J. Respir. Crit. Care Med.* 1994, 150, 1234-1242.

Schwartz, J.; Dockery D.W.; Neas, L.M. Is daily mortality associated specifically with fine particles? *J. Air & Waste Manage. Assoc.* 1996, 46, 927-939.

Shareef, G.S. Engineering Judgment, Radian Corporation, September, 1987.

Sheesley, R.J.; Schauer, J.J. *et al.* Proceedings of the AWMA Annual Meeting, 2000, Salt Lake City, Utah.

Sheesley, R.J.; Schauer, J.J.; Bean, E.; Kenski, D. Trends in secondary organic aerosol at a remote site in Michigan's upper peninsula. *Environ. Sci. Technol.* 2004, 38, 6491-6500.

Simoneit, B.R.T.; Rogge, W.F.; Mazurek, M.A.; Standley, L.J.; Hildemann, L.M.; Cass, G.R. Lignin pyrolysis products, Lignans, and resin acids as specific tracers of plant classes in emissions from biomass combustion. *Environ. Sci. Technol.* 1993, 27, 2533-2541.

Sinha, P.; Hobbs, P.V.; Yokelson, R.J.; Blake, D.R.; Gao, S.; Kirchstetter, T.W. Emissions from miombo woodland and dambo grassland savanna fires. *J. Geophys. Res.* 2004, 109, D11305.

Skjølsvik, K.O.; Andersen, A.B.; Corbett, J.J.; Skjelvik, J.M (2000). *Study of Greenhouse Gas Emissions from Ships (MEPC 45/8 Report to International Maritime Organization on the outcome of the IMO Study on Greenhouse Gas Emissions from Ships)*. Trondheim, Norway, MARINTEK Sintef Group, Carnegie Mellon University, Center for Economic Analysis, and Det Norke Veritas.

Stern, J.E.; Flagan, R.C.; Grosjean, D.; Seinfeld, J.H. Aerosol Formation and Growth in Atmospheric Aromatic Hydrocarbon Photooxidation; *Environ. Sci. Technol.* 1987, 21, 1224-1231.

Strader, R.; Lurmann, F.; Pandis, S.N. Evaluation of secondary organic aerosol formation in winter; *Atmos. Environ.* 1999, 33, 4849-4863.

Thurston, G.D.; Ito, K.; Hayes, C.G.; Bates, D.V.; Lippmann, M. Respiratory hospital admissions and summertime haze air pollution in Toronto, Ontario: Consideration of the role of acid aerosols; *Environ. Res.* 1994, 65, 271-290.

Tolbert, P.E.; Klein, M.; Metzger, K.B.; Peel, J.; Flanders, W.D.; Todd, K.; Mulholland, J.A.; Ryan, P.B.; Frumkin, H. Interim results of the study of particulates and health in Atlanta (SOPHIA). *J. Expos. Anal. Environ. Epidemiol.* 2000, 10, 446-460.

Tsai, F.C.; Apte, M.G.; Daisey, J.M. An exploratory analysis of the relationship between mortality and the chemical composition of airborne particulate matter. *Inhalation Toxicology* 2000, 12(supplement 2), 121-135.

Turpin, B.J.; Huntzicker, J.J. Secondary formation of organic aerosol in the Los Angeles basin: A descriptive analysis of organic and elemental carbon concentrations; *Atmos. Environ.* 1991, 25, 207-215.

Turpin, B.J.; Huntzicker, J.J. Identification of secondary organic aerosol episodes and quantitation of primary and secondary organic aerosol concentrations during SCAQS; *Atmos. Environ.* 1995, 29, 3527-3544.

Turpin, B.J. and H.J. Lim, Species contributions to $PM_{2.5}$ mass concentrations: revisiting common assumptions for estimating organic mass, *Aerosol Sci. Technol.* 35, 602-610, 2001.

Turpin, B.J.; Lim, H.-J. Species contributions to PM2.5 mass concentrations: Revisiting common assumptions for estimating organic mass. *Aerosol. Sci. Technol.* 2001, 35, 602-610.

U.S. EPA, 1999: *Particulate Matter Speciation guidance*; U.S. EPA; Office of Air Quality Planning and Standards, Research Triangle Park, NC.

U.S. EPA, 1997: Federal Register 40 CFR part 50. *National Ambient Air Quality Standards for Particulate Matter; Final Rule*.

U.S. EPA, 2002: *EPA Acid Rain Program 2001 Annual Progress Report*, Clean Air Markets Program, Office of Air and Radiation, Washington, DC.

U.S. EPA, *The Particle Pollution Report; Current understanding of air quality and emissions through 2003*, Office of Air Quality Planning and Standards, Research Triangle Park, NC.

U.S. EPA, 2004: *Air Quality Criteria for Particulate Matter*, Office of Research and Development, Research Triangle Park, NC.

U.S. EPA, 2006: Federal Register 40 CFR part 50. *National Ambient Air Quality Standards for Particulate Matter; Proposed Rule*.

Wade, K.S; Mulholland, J.A.; Marmur, A.; Russell, A.G.; Hartsell, B.; Edgerton, E.; Klein, M.; Waller, L.; Peel, J.L.; Tolber, P.E. Assessment of the temporal variation of ambient air pollution in Atlanta, Georgia. *J. Air & Waste Manage Assoc.* 2006, 56, 876-888.

Wangberg, I., Barnes, I., Becker, K.H. Product and mechanistic study of the reaction of NO_3 radicals with α-pinene; *Environ. Sci. Technol.* 1997, 31, 2130-2135.

Watson, J.G; Cooper, J.A.; Huntzicker, J.J. The effective variance weighting for least squares calculations applied to the mass balance receptor model; *Atmos. Environ.* 1984, 18, 1347-1355.

Watson, J.G.; Chow, J.C.; Richards, L.W.; Anderson, S.R.; Houck, J.E.; Dietrich, D.L. (1988). *The 1987-88 Metro Denver Brown Cloud Air Pollution Study, Volume II: Measurements.* Report No. 8810.1F2. Prepared for 1987-88 Metro Denver Brown Cloud Study, Inc.; Greater Denver Chamber of Commerce, Denver, CO, by Desert Research Institute, Reno, NV.

Watson, J.G.; Chow, J.C.; Houck, J.E. PM2.5 chemical source profiles for vehicle exhaust, vegetative burning, geological material, and coal burning in Northwestern Colorado during 1995; *Chemosphere* 2001, 43, 1141-1151.

Watson, J.G.; Robinson, N.F.; Chow, J.C.; Fujita, E.M.; Lowenthal, D.H.; *CMB8 User's Manual Draft*; U.S. Environmental Protection Agency: Washington, DC, 2001.

Watson, J.G. Visibility: *Science* and Regulation; *J. Air & Waste Manage. Assoc.* 2002, 52, 628-713.

Winchester, J.W.; Nifong, G.D. Water pollution in Lake Michigan by trace elements from pollution aerosol fallout. Water, Air, & Pollution 1971, 1, 50-64.

Wotawa, G.; Trainer M. The influence of Canadian forest fires on pollutant concentrations in the Unites States. *Science*, 2000, 288, 324-328.

Yu, J., Cocker, D.R., Griffin, R.J., Flagan, R.C., Seinfeld, J.H. Gas-phase ozone oxidation of monoterpenes: gaseous and particulate products; *J. Atmos. Chem.* 1999, 34, 207-258.

Zheng, M.; Cass, G.R.; Schauer, J.J.; Edgerton, E.S. Source apportionment of PM2.5 in the southeastern Unites States using solvent-extractable organic compounds as tracers. *Environ. Sci. Technol.* 2002, 36,2361-2371.

Zheng, M.; Ke, L.; Edgerton, E.S.; Schauer, J.J.; Dong, M.; Russell, A.G. Spatial distribution of carbonaceous aerosol in the southeastern United States using molecular markers and carbon isotope data. *J. Geophys. Res.*, 111, D10S06, 2006.

Zielinska, B.; McDonald, J.D.; Hayes, T.; Chow, J.C.; Fujita, E.M.; Watson, J.G. (1998). *Northern Front Range Air Quality Study Final Report. Volume B.: Source Measurements*. Prepared for Colorado State University, Cooperative Institute for Research in the Atmosphere, Fort Collins, CO, by Desert Research Institute, Reno, NV.

VITA

SANGIL LEE

Sangil Lee was born in Kimcheon, Korea, in October 1974. He received his B.E. in Environmental Engineering from ChunNam National University, Korea. He started his graduate studies at Georgia Institute of Technology's School of Civil and Environmental Engineering in 2000. He studied about particle formation with Professor Rodney Weber for his M.S. EnvE and then began his Ph.D. studies with Dr Karsten Baumann researching characteristics of particulate matter. He finished his Ph.D. studies under the advisement of Professor Armistead Russell. Sangil has worked on characterization of ambient and emission particulate matter involving in several projects. He has also studied about source apportionment of particulate matter for understanding of air quality impacts of primary emission sources.